THE ELECTRICAL PROPERTIES OF FROG HEART

A thesis submitted for the degree of Ph.D.

by

CHRISTOPHER HENRY FRY, B.Sc.

Department of Physiology, School of Biological Sciences, University of Leicester

February 1976

This is to certify that the thesis I have submitted in fulfilment of the requirements governing candidates for the degree of Doctor of Philosophy in the University of Leicester, entitled "The Electrical Properties of Frog Heart", is the result of work done mainly by me during the period of registration for the above degree.

C. Fry

(C.H. FRY)

Contents

Acknowledgements

I am indebted to the Medical Research Council for financial support. It is my pleasure to thank Dr R.A. Chapman for his guidance, friendship and patience throughout the period of this study, without whom none of this work would have come to fruition.

I would also like to thank the academic and technical staff of the Physiology Department, University of Leicester for their co-operation and also Dr Claude Léoty, University of Poitiers, and Dr John McGuigan, University of Bern, for their help in reading the manuscript and making many useful suggestions.

I would also like to thank my parents for their continual encouragement throughout this period of study. Lastly, may I thank Sue Preedy and Rita Häsler for typing parts of the introduction for me.

βρεκεκεκὲξ κοὰξ κοὰξ.
λιμναῖα κρηνῶν τέκνα.
ξύναυλον ὕμνων βοὰν
φθεγξωμεθ'. εὔγηρυν ἐμὰν ἀοιδὰν.
κοὰξ κοὰξ.
ἥν ἀμφὶ Νυσήιον
Διὸς Διώνυσον ἐν
Λίμναις ἰαχήσαμεν.
ἡνίχ' ὁ κραιπαλόκωμος
τοῖς ἱεροῖσι Χύτροισι
χωρεῖ κατ' ἐμὸν τέμενος λαῶν ὄχλος.
βρεκεκεκὲξ κοὰξ κοὰξ.

'Ο! ΒΑΤΡΑΧΟΙ 209–220

ARISTOPHANES

Symbols and definitions

The following symbols and definitions are used to describe the core conductor model and its modifications

V = voltage (volt)

J = current (ampere)

R = resistance (ohm)

Z = impedance (ohm)

G = conductance (mho)

Y = admittance (mho)

V_o = potential of external fluid, with respect to a distant point (volt)

V_i = potential of internal fluid, with respect to a distant point (volt)

V_m = transmembrane potential (volt), = $V_o - V_i$

i_o = longitudinal current flowing through the external fluid (ampere)

i_i = longitudinal current flowing through the internal fluid (ampere)

I = total current flowing through the fibre and external fluid (ampere)

i_m = current through the membrane at any point (ampere cm^{-1})

r_o = resistance per unit length of external fluid (ohm cm^{-1})

r_i = resistance per unit length of intracellular medium (ohm cm^{-1})

r_c = resistance per unit length of cytoplasm (ohm cm^{-1})

r_m = resistance x unit length of surface membrane (ohm cm)

r_d = resistance x unit length of membrane forming low resistance connexions between cells (presumed to be desmosomal area)(ohm cm^{-1})

R_i = specific resistivity of intracellular pathway (ohm cm)

R_f = total specific resistance to flow of current along the intracellular pathway (equivalent to Ri - Ri is a theoretical parameter, Rf is an experimentally determined quantity) (ohm cm)

R_c = specific resistivity of cytoplasm (ohm cm)

R_m = resistance x unit area of the surface membrane (ohm cm^2)

R_d = resistance x unit area of desmosomal area (ohm cm^2)

Σ/σ = conductivity of internal medium at planes perpendicular and parallel to the axis of the trabecula, respectively (mho cm^{-1}) In spherically symmetrical case $\Sigma = \sigma$

R_{inp} = input resistance $= \left(\frac{V}{I}\right)_{x=o}$ (ohm)

x = one dimensional distance from spatial frame of reference (e.g. point of stimulation) (cm)

r = distance from point current case (spherical situation) (cm)

t = time from temporal frame of reference (e.g. time of stimulation of a d.c. pulse) (sec)

λ = space constant (cm)

$X = x/\lambda$

c_m = capacity per unit length of surface membrane (farad cm^{-1})

c_d = capacity per unit length of desmosomal area (farad cm^{-1})

C_m = capacity per unit area of surface membrane (farad cm^{-2})

C_d = capacity per unit area of desmosomal area (farad cm^{-2})

τ_m = time constant of surface membrane (sec)

$T = t/\tau_m$

τ_d = time constant of desmosomal area (sec)

θ = conduction velocity (cm sec^{-1})

$\tau_{a.p.}$=time constant from the foot of the action potential (= 1/k)(sec)

a = cell radius (cm)

s = space between adjacent membranes at the desmosome (cm)

f = frequency of sine wave (cycles sec^{-1}, Hz)

ω = radian frequency ($= 2\pi f$)

m = constants relating d.c. and a.c. analyses of the cable model

n = (defined on p 12)

γ = propagation constant

The following experimental definitions are also used (definition is also found in the text the first time the symbols appear)

R_{EL} = microelectrode resistance (ohm)

R_{ext}= resistivity of calibrating solutions in the determination of the cytoplasmic resistivity (ohm cm)

R_p = polarisation resistance of platinum black electrodes (ohm)

R_s = sample resistance in longitudinal impedance arrangement (ohm)

C_p = polarisation capacitance of platinum black electrodes (farad)

C_s = sample capacitance in longitudinal impedance arrangement (farad)

C_x = interelectrode capacitance in longitudinal impedance arrangement (farad)

$Q = \omega C/G$

Mathematical descriptions

sinh = hyperbolic sine of $x = \frac{1}{2}(e^{x} - e^{-x})$

cosh = hyperbolic cosine of $x = \frac{1}{2}(e^{x} + e^{-x})$

erf = error function $\quad \operatorname{erf} x = \frac{2}{\sqrt{\pi}} \int_{o}^{x} e^{-t^2}\, dt$

∇ = divergance (div) of a vector

grad = gradient of a vector

$\underline{i}$ = current vector

$\underline{E}$ = voltage vector

j = complex operator $(=\sqrt{-1})$

I_o = modified Bessel function of the first kind of order zero

I_ν = generalised modified Bessel function of the first kind of order ν

K_o = modified Bessel function of the second kind of order zero

K_ν = generalised modified Bessel function of the second kind of order ν

Other symbols, illustrating theoretical concepts, are defined as they appear in the text.

INTRODUCTION

The Development and Description of the Linear Core Conductor Model

Although it was Galvani who first described the existence of animal electricity, it was not until the experiments of Mateucci (1862) and Hermann (1879) that the true explanation for the electrotonic (a word coined by Du Bois Raymond) spread of current was explained. Hermann placed a wire in a saline-filled tube and recorded the potential at different distances from a source of stimulation. He interpreted his results in that the polarisation resistance between the fluid and wire was the cause of the current spread and such a model was designated the linear core conductor model.

The temporal changes of potential necessitated the introduction of an impedance element into the model. This impedance was designated as a capacitance in the membrane and was analogized to the capacitance observed in polarisable electrodes (e.g. Phillipson, 1921; Cole, 1932), although this analogy was entirely empirical and "was purely an admission of ignorance", (Curtis and Cole, 1938).

The model could now be described as a resistive core with an imperfect insulation - the value of which was frequency dependent - allowing leakage of current to earth. The equations describing this system were analogous to several physical systems, e.g. the flow of heat in one dimension and, more interestingly, the submarine cable (Thompson, 1855). It was due to the analogy with the latter system that core conductor theory became commonly called cable theory.

The physical system can be described first, as some interesting consequences arise which are of use in the biological model.

Consider a length of cable with an earth return; it will have an impedance of Z dx along a length, dx, of cable and a shunt admittance of Y dx for the same length, so that voltage, V, and current, J, changes become:

$$-dV = J\,Z\,dx \qquad 1)$$

$$-dJ = V\,Y\,dx \qquad 2)$$

thus: $$\frac{d}{dx}\left(\frac{1}{Z}\,\frac{dV}{dx}\right) - Y\,V = 0 \qquad 3)$$

this is the equation arrived at by Jeans (1911), for which he gave as a solution

$$V = A\cosh (Z\,Y)^{\frac{1}{2}}x + B\sinh (Z\,Y)^{\frac{1}{2}}x \qquad 4)$$

on the assumption that Z and Y do not change along the length of the cable. To evaluate the values of A and B, for the condition of a leaky cable, A = -B so that equation 4) becomes

$$V = A\cosh (Z\,Y)^{\frac{1}{2}}x - A\sinh (Z\,Y)^{\frac{1}{2}}x \qquad 5)$$

The definition of the exponential function in hyperbolic terms is

$$e^{-x} = \cosh x - \sinh x \qquad 6)$$

so that eq. 5) reduces to the well-known form

$$V = A\exp -(Z\,Y)^{\frac{1}{2}}x. \qquad 7a)$$

Furthermore, if Z is equivalent to the internal resistance, r_i, and 1/Y equivalent to the membrane resistance, r_m, then $(Z\,Y)^{\frac{1}{2}}$ equals $(r_i/r_m)^{\frac{1}{2}}$, so the eq. 7a) can be rewritten as

$$V = A.\exp -(x/\lambda) \qquad 7b)$$

where the constant λ is equal to $(r_m/r_i)^{\frac{1}{2}}$.

It may however prove useful to expand eq. 3) more fully and study it in more detail (McLachlan, 1963).

If Z and Y are respectively designated as $Z_1 x^{\alpha}$ and $Y_1 x^{\beta}$ so that Z_1 and Y_1 are now non-dimensional and constant, as also are α and β, then eq. 3) becomes

$$\frac{d^2V}{dx^2} - \frac{\alpha}{x}\frac{dV}{dx} - k_1^2 x^{\gamma} V = 0 \qquad 8)$$

where $\gamma = (\alpha + \beta)$ and $k_1 = (Y_1 Z_1)^{\frac{1}{2}}$.

Solution of eq. 8) gives:

$$V = x^{\nu/q} A_1 I_{\nu} (kx^{1/q}) + B_1 K_{\nu} (kx^{1/q}) \qquad 9)$$

where $\nu = (\alpha + 1)/(\alpha + \beta + 2)$

$q = 2/(\alpha + \beta + 2)$

$k = (Y_1 Z_1)^{\frac{1}{2}}/(\alpha + \beta + 2)$

and I_{ν} and K_{ν} are modified Bessel functions of the first and second kind respectively, of order ν.

If $\alpha = \beta = 0$ so that Z and Y do not depend on the position in the cable - the condition assumed by Jeans (1911) - then eq. 9) yields eq. 4).

However, in the case where $\alpha = -1$ and $\beta = 1$ so that $Z = Z_1/x$ and $Y = Y_1 x$, the situation is the so-called Heaviside-Bessel cable but can also be thought of as a two-dimensional system. Solution of eq. 9) in this case gives:

$$V = A I_0 (kx) + B K_0 (kx) \qquad 10)$$

This is the solution arrived at by George (1961), Tanaka and Sasaki (1966) and Shiba (1971) for plane networks and used by Woodbury and Crill (1961) to describe potential distribution in a two-dimensional preparation of rat atrial muscle. Thus, in the situations of eqs. 7)

and 10), biological and physical cable theories produce identical results.

The mathematical evaluation of the biological system proceeded along similar lines to that of the physical system of Thompson (1855). Beginning with Hermann's kernleiter model for electrotonic spread, there was a controversy as to whether electrotonus was propagated instantaneously or proceeded with a finite velocity. Hermann (1905), in replacing his kernleiter by a combination of lossy condensers connected by non-inductive resistors, derived the differential equation for a continuous linear capacity conductor, giving an equation (eq. 3) analogous to the physical model. The consequence of this was that an application of an electrotonic potential at one end of the model would allow this potential to appear at all points on the model but that steepness of rise would decrease with increasing distances along the model. The experimental evidence to support this was poor however, due to the inadequacy of the galvanometers to follow such quick responses. Thus, although Weiss and Gildemeister (1903) found an infinite velocity, Tschirjew (1879) found the opposite result and it was not until the work of Bogue and Rosenburg (1934), working with electronic amplifiers and oscillographs, that it was conclusively shown that the electrotonus travels with an infinite velocity. It was not until the work of Hodgkin and Rushton (1946) that the model was rigorously applied to nerve fibres providing a spatial and temporal solution for the potential in the fibre in a convenient and utilizable form. The solution of the equation can thus be approached in the manner of Hodgkin and Rushton.

The cable is assumed to be infinite in extent so that no problems of terminating impedances need to be considered. It is assumed that the membrane impedance, Z, is merely represented by a capacitance with shunting resistance and that the intracellular and extracellular media are purely conducting and that there is no reactive component, so that the phase angle is zero. The battery, E, which represents the resting potential, and is assumed constant, can be set to zero as its actual magnitude is unimportant, only voltage changes being sought. Thus, the transient solution is only a component of the total solution which is obtained from the superposition theorem by setting $E = 0$.

If the intracellular and extracellular media are purely homogeneous and isotropic, then the Poisson equation is obeyed everywhere in these media, i.e.

$$\nabla^2 V = \xi / \varepsilon_o \qquad 11)$$

where ξ is the charge density per unit volume and ε_o is the permittivity of free space.

Thus, the core conductor model can be described with the additional assumption that the membrane is so thin that it carries no longitudinal current.

As pointed out by Hellerstein (1968), the relaxation time for charge concentration is less than 10^{-11} secs. so that no charge density will build up and Laplace's equation is obeyed everywhere inside and outside the membrane, so that in spherical coordinates

$$\nabla^2 V_i (r, \phi, \psi) = 0 \quad r \leq a$$
$$\nabla^2 V_o (r, \phi, \psi) = 0 \quad r \geq a \qquad 12)$$

where a = cell radius, and the subscripts o and i refer to outside and inside the cell respectively.

By application of Kirchoff's laws to the core-conductor model, the following cable equations can be obtained

$$\frac{\delta i_i}{\delta x} = -i_m \qquad 13)$$

$$i_i = -i_o \qquad 14)$$

$$\frac{\delta V_o}{\delta x} = -i_o r_o \qquad 15)$$

$$\frac{\delta V_i}{\delta x} = -i_i r_i \qquad 16)$$

The currents i_o and i_i are presumed to flow parallel to the axis of the model (i_m is the membrane current). In effect, equations 13) and 16) are restatements of equations 1) and 2).

It can be shown from these equations (Hodgkin and Rushton, 1946), that

$$-\lambda^2 \frac{\delta^2 V_m}{\delta x^2} + \tau_m \frac{\delta V_m}{\delta t} + V_m = r_i \lambda^2 \frac{\delta I}{\delta x} \qquad 17)$$

where I is the total current flowing -i.e. $i_o + i_i$. As $\delta I/\delta x$ vanishes except at the electrode, then outside the electrode region.

$$-\lambda^2 \frac{\delta^2 V_m}{\delta x^2} + \tau_m \frac{\delta V_m}{\delta t} + V_m = 0 \qquad 18)$$

In these equations λ is defined as $\sqrt{\frac{r_m}{r_i + r_o}}$ and $\tau_m = c_m r_m$

When the fibre, to which the model is being applied, is submerged in a large volume of fluid, as is the case for intracellular recording, r_o can be considered to be zero so that $\lambda = (r_m/r_i)^{\frac{1}{2}}$: this is the same constant as occurred in equation 7b). Under such conditions V_o can be regarded as zero.

With the boundary conditions that V_m (the transmembrane voltage $= V_o - V_i$) = 0 everywhere in the time domain $-\infty < t < o$, $V_m = o$ when $x \pm \infty$, V_m and the current flowing through the axis cylinder are a continuous function of x, then solution of equation 18) for the case of a step of current at t = 0 gives:

$$(V_m)_{x,t} = \frac{r_i \lambda I}{4} \left\{ e^{-X}\left[1 - \text{erf}\ (X/2\sqrt{T}-\sqrt{T})\right] - e^{X}\left[1 - \text{erf}\ (X/2\sqrt{T}+\sqrt{T})\right] \right\} \quad 19)$$

where $X = x/\lambda$ and $T = t/\tau_m$.

For the case when $t = \infty$, i.e. the steady-state solution, eq. 19) is simplified to

$$V_m = \frac{I \lambda r_i}{2} \cdot e^{-X} \quad 20)$$

which is in the same form as eq. 7b). Thus, if cable theory is to describe the system under test, there should be a linear relationship between the distance from the stimulating point and the logarithm of the recorded steady-state voltage. Similarly for the case of recording at the stimulation point, at X = 0, then

$$V_m = V_m(\text{max})\ \text{erf}\ (\sqrt{T}). \quad 21)$$

Thus, the time constant of the membrane, τ_m, can be estimated as the time needed for the potential to reach 84% (erf 1) of the steady state voltage. For transients recorded away from the stimulation point, the time constant will have to be calculated from eq. 19).

The most stringent test for the applicability of cable theory to a particular preparation is to see whether the recorded voltage transient fits exactly a plot of eq. 19) for a given distance X from the stimulating electrode and at different times, T. - This will be attempted in the results section.

Thus far, a cable infinite in extent has been considered so that the effect of a terminating impedance has not been of consequence. The latter situation is however more real so it will be seen how much a finite length affects the spatial and temporal distribution of potential.

There are two possible limiting conditions for the termination of a cylindrical cell. It can have an open end in which it is presumed that the resistance at the end of the fibre is zero, so that all of the current passes into the external medium and none through the membrane. Alternatively, the end could be sealed so that the cable is terminated by an infinite impedance so that all of the current passes through the membrane.

The open-end situation is described as for a fibre of length l

$$(V_m)_x = (V_m)_{x=0} \frac{\sinh(l-x)/\lambda}{\sinh l/\lambda} \qquad 22)$$

and for the closed end

$$(V_m)_x = (V_m)_{x=0} \frac{\cosh(l-x)/\lambda}{\cosh l/\lambda} \qquad 23)$$

Fig. 1 shows how greatly these potential distributions differ from the infinite example. Curves 1 and 2 are for a fibre of electrical length l/λ equal to unity and curves 3 and 4 for $l/\lambda = 2$. As can be seen, serious deviation only occurs near the ends of the cable so that if the length of the fibre is about 5 times the space constant (i.e. $l/\lambda = 5$) as is the usual situation in the experiments to be described, the deviation from the exponential term within the first three space constants of length - about 1mm. - will be negligible and masked by experimental error.

Figure 1 A semilogarithmic plot of the potential distribution in a cable under a variety of conditions. Curves 1 and 3 are for cables with a sealed end of electrical length ($1/\lambda$) equal to one and two respectively. Curves 2 and 4 are for open-ended cables of electrical lengths one and two respectively. Curve 5 is for an infinite cable of space constant λ.

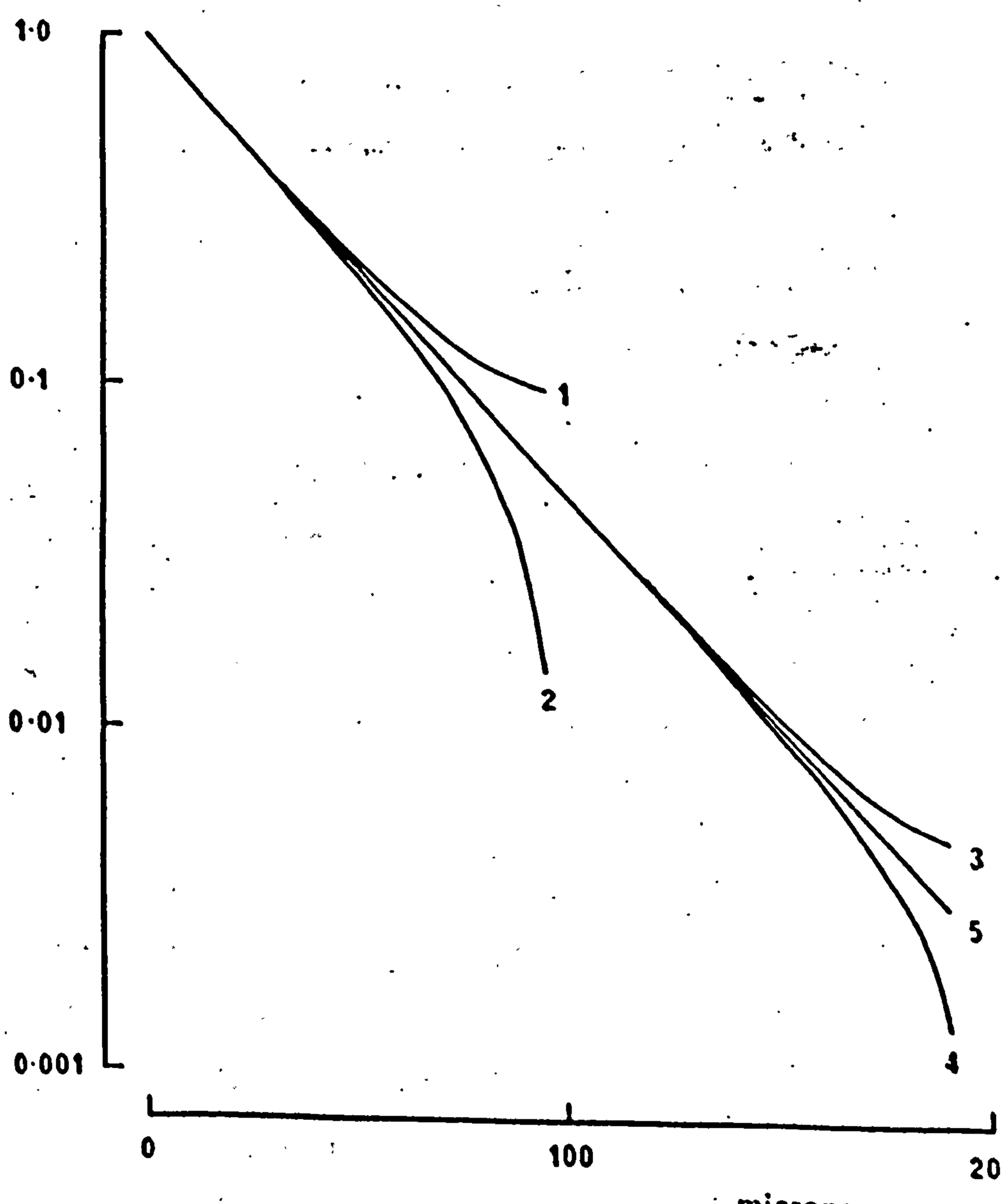
1·0
0·1
0·01
0·001
1
2
3
4
5
0
100
200
microns

The time constant of the membrane would also be expected to be altered by imposing a limitation on the fibre length. Rall (1969a) calculated the time constants with a variety of finite fibre terminations but the terms involved rather cumbersome integrals which poorly converged when numerically evaluated. Norman (1972) obtained similar results with a Laplace transform technique. Finite cables (with a sealed end) had a slower rate of rise than for an infinite cable, but it is doubtful whether such changes could be experimentally differentiated.

Thus far, solution of the cable equations has been for a step of current suddenly applied at t = 0 and maintained for a specific duration. The core-conductor model will also be expected to respond to a sinusoidally varying input, of which the output would be expected to be a function of the frequency of the input voltage due to the reactance of the membrane.

Tasaki and Hagiwara (1957) solved the cable equations for sinusoidally varying stimulating current by modifying cable eq. 16) to

$$\left[\frac{\partial V_m(x,t)}{\partial x}\right]_{x=0} = r_i I \cos(2\pi f t) \qquad 24)$$

where f is the frequency of the input voltage.

Solution of eq. 18) now gives

$$V_m(x,t) = \frac{I \lambda r_i}{2\sqrt[4]{1+(2\pi f \tau_m)^2}} e^{-mx/\lambda} \cdot \cos\left(2\pi f t - \frac{nx}{\lambda} - \tan^{-1}\cdot\frac{n}{m}\right) \qquad 25)$$

where $m = \frac{\sqrt{1+\sqrt{1+(2\pi f \tau_m)^2}}}{\sqrt{2}}$, $n = \frac{\sqrt{-1+\sqrt{1+(2\pi f \tau_m)^2}}}{\sqrt{2}}$.

It can be seen that setting f = 0, as for a d.c. pulse, eq. 25) reduces to eq. 20).

The approximation that $2\pi f \tau_m > 1$ was added in order to linearise the equations and thus concerning only the magnitude part of eq. 25) and not the phase term, eq. 25) becomes

$$V_m(x,t) \qquad \frac{I\sqrt{r_i}}{2\sqrt{2\pi f c_m}} \cdot \exp - x\sqrt{\pi f c_m r_i} \qquad 26)$$

of which rearrangement yields an equation for a straight line - i.e. $y = mx + c$.

$$\lg \frac{V_m(x,t)\sqrt{f}}{I} = - x\sqrt{f}\sqrt{\pi c_m r_i} + \lg \frac{\sqrt{r_i}}{2\sqrt{2\pi c_m}} . \qquad 27)$$

Thus a plot of $\lg \frac{V_m\sqrt{f}}{I}$ versus $\sqrt{f}$ will give a straight line plot of slope $x\sqrt{\pi c_m r_i}$ so that it will be possible to estimate the membrane capacity or the internal resistance if the other is known.

Having considered the basic equations of electrotonus, the next procedure is to mention those describing the propagation of an action potential. The means of propagation of an action potential in an excitable tissue is by the flow of local circuits from the active to the inactive region. Thus, in the time before the threshold level for regenerative action is reached, the potential variation will be determined by the cable properties of the membrane. The problem is again identical to that evaluated by Thompson (1855) in which he calculated that the retardation of a transmitted signal was not so

great as to make transmission from one side of the Atlantic ocean to the other unfeasible. The only approximation we must make is that the rate of change of currents is not so great as to make the 'induction phenomena' significant (Jeans, 1911) so the equations cannot be applied to t = 0 when the currents are varying infinitely quickly.

Thus, the trans-membrane potential can be mathematically described by the one-dimensional wave equation

$$\nabla^2 V_m = \frac{\delta^2 V_m}{\delta x^2} = \frac{1}{\theta^2} \frac{\delta^2 V_m}{\delta t^2} \qquad 28)$$

Substitution into eq. 18) gives

$$\frac{\lambda^2}{\theta^2} \frac{\delta^2 V_m}{\delta t^2} - \tau_m \frac{\delta V_m}{\delta t} - V_m = 0 \qquad 29)$$

Eq. 29) is now a linear second order differential equation with constant coefficients and can be solved by the usual procedures. The general solution as worked out by Cole and Curtis (1938) and Rosenbleuth, Wiener, Pitts and Garcia Ramos (1948)

$$V_m(t) = A \exp \frac{(\theta\tau_m + \sqrt{\theta^2\tau_m^2 + 4\lambda^2})\,\theta t}{2\lambda^2}$$

$$+ B \exp \frac{(\theta\tau_m - \sqrt{\theta^2\tau_m^2 + 4\lambda^2})\,\theta t}{2\lambda^2} . \qquad 30)$$

With the condition that $V_m(t) = 0$ for $-\infty < t < 0$, then B = 0 so that

$$V_m(t) = A \exp \frac{(\theta\tau_m + \sqrt{\theta^2 \tau_m^2 + 4\lambda^2})\theta t}{2\lambda^2} \qquad 31a)$$

or $$V_m(t) = A \exp kt. \qquad 31b)$$

Thus, the passive 'foot' of an action potential before the threshold level for regenerative action is reached describes an exponential pathway with a time constant of $1/k$ ($= \tau_{a.p.}$ - the time constant of the foot of the action potential).

Thus, an experimental measurement of $\tau_{a.p.}$ will allow an estimate of the membrane capacity to be made as

$$\frac{1}{\tau_{a.p.}} = k = \frac{(\theta\tau_m + \sqrt{\theta^2 \tau_m^2 + 4\lambda^2})\theta}{2\lambda^2}. \qquad 32)$$

The further approximation has been made - valid in the cases of skeletal muscles and nerves, such as the squid axon - that $\theta\tau_m \gg 2\lambda$, so that the second term under the square root sign can be neglected; thus using the relations that

$$\lambda = \sqrt{r_m/r_i}$$

$$\tau_m = c_m r_m$$

$$R_i = r_i \pi a^2 \quad (\text{ohm.cm}) \qquad 33)$$

$$R_m = r_m . 2\pi a \quad (\text{ohm cm}^2)$$

$$C_m = c_m/2\pi a \quad (\text{farad cm}^{-2})$$

where a = fibre radius then

$$C_m = \frac{a}{2R_i \theta^2 \tau_{a.p.}}. \qquad 34)$$

In the case of frog cardiac muscle, the approximation that $\theta\tau_m \gg 2\lambda$ is not valid mainly due to the low value of the conduction velocity, θ, so that the whole of eq. 32) must be used. Rearrangement gives a value for the specific membrane capacitance of

$$C_m = \frac{a}{2R_i\theta^2\tau_{a.p.}} \cdot \left(1 + \frac{\tau_{a.p.}}{\tau_m}\right)^{-1} \qquad 35)$$

which will reduce the value of the membrane capacity compared to that derived by the approximate eq. 34).

The equation is also based on the assumption that the external resistance is negligible compared to the internal resistance which is justifiable when the preparation is surrounded by a large volume of physiological saline. Thus, several groups of workers (Kamiyama and Matsuda, 1966; Fozzard, 1966; Sakamoto, 1969; Sakamoto and Goto, 1970), calculating the membrane constants of mammalian ventricular and Purkinje tissue, have used eq. 34). Weidmann(1970), also working with mammalian ventricular preparations, performed his experiments under silicone oil so that the effect of the extracellular resistance was now no longer negligible and, following a suggestion by Prof. Hodgkin, modified eq. 34) to

$$C_m = \frac{a}{2R_i\theta^2\tau_{a.p.}} \cdot \frac{r_i}{r_i + r_o} \qquad 36)$$

Bonke (1973) has used eq. 35) in calculation of the membrane parameters of rabbit atrial fibres although he gives an equation of the form

$$C_m = \frac{(1+F)ka}{2R_i\theta^2} \qquad 37)$$

where k is $1/\tau_{a.p.}$ and F is a correction factor. In this form, F will have to be a negative number as the full form of the equation (eq. 35) will give a smaller value for the membrane capacity than the approximate eq. 34).

The Applicability of One-Dimensional Cable Theory to Three-Dimensional Problems

One-dimensional cable theory is based on the assumption that one end of the model is uniformly stimulated in a plane perpendicular to the axis of the cable. This was the situation attempted by Kamiyama and Matsuda (1966) in cardiac muscle and which has been used by several other workers including some of the work that will be described here. Thus, if this condition is not fulfilled, one-dimensional cable theory will not hold exactly so we shall see how far practice and hopefulness diverge under certain other conditions.

Eisenberg and Johnson (1970) have calculated the deviation from one-dimensional cable theory if a point source of current - i.e. a microelectrode - is used under different conditions of electrode placement. This is of considerable interest as much work has been done on current spread in a cardiac syncitium using such a source of current (e.g. Woodbury and Crill, 1961; Tanaka and Sasaki, 1966), and also many voltage-clamp studies have been made (notably by Noble and his co-workers with Purkinje fibres) with a microelectrode feeding current into the system in the feedback network - which theoretically should hold the potential steady in a given region of the fibre.

Eisenberg and Johnson (1970) consider two cases when the conditions for one-dimensional cable theory are not present - namely when current leaves the point source and when it turns to leave the fibre via the limiting membrane, so that in both cases, there will be radial as well as longitudinal flow of current. The former situation will be important at small distances from the point source but, owing to the nature of potential distribution under these circumstances, potential distribution will be essentially exponential at greater distances. The latter situation will depend on the membrane properties. If the membrane resistance is so low that most of the current has left within a length equal to the fibre diameter, then the currents cannot be considered to be longitudinal at all. The larger the space constant - i.e. the larger the membrane resistance - the more currents will flow in a longitudinal direction. In most resting fibres, the space constant is usually many times larger than the fibre diameter but caution must be exercised in examining data from fibres in an active state when the membrane resistance is greatly reduced.

The problem had been previously dealt with by a number of authors - Clark and Plonsey (1966), Hellerstein (1968) and Rall (1969a,b). Some estimation was made by Clark and Plonsey (1966) and Rall (1969b) of the error introduced when current flow was not entirely longitudinal - assumed by the cable equations 15) and 16). Clark and Plonsey (1966) showed that the total internal and external longitudinal currents were compounded of two terms, (shown here as I^i and I^o respectively) i.e.

$$I_1^o(x) = I_1^o(x) + I_2^o(x)$$
$$I_1^i(x) = I_1^i(x) + I_2^i(x) \qquad 38)$$

$I_1^o(x)$ and $I_1^i(x)$ were proportional to the voltage gradient whilst I_2^o and I_2^i were integral terms which represent the electrical field at the membrane which will be influenced by the current turning from the fibre to pass through the membrane. Evaluation of the integrals showed that whereas I_2^i was not significant as compared to I_1^i, I_2^o was significantly comparable to I_1^o.

Thus, it was concluded that if only internal parameters were considered and the external resistance could be short-circuited, the cable equations could be justifiably used. Using such approximations, Hellerstein (1968) showed it was possible to calculate the cable eq.. 19) (Hodgkin and Rushton, 1946) from Laplace's equation in cylindrical coordinates.

Rall (1969b) considered the potential distribution in space and time of the cylindrical form

$$V_{n,m}(r,\theta,x,t) = F_{n,m}(r)\, G_n(\theta)\, H_m(x)\, Q_{n,m}(t) \qquad 39)$$

and considered that the one-dimensional cable equations were a good approximation when the radius was small compared to the measured space constant, $r_o = 0$, and there was no angular dependence between the current cource and the recording device. He showed that the effect of making r_o as large as $2r_i$ only made a 1% difference in the space constant - a more optimistic view than that of Clark and Plonsey (1966).

Measurement of the Cellular Parameters

Having mathematically described some of the electrical properties of the cell, it will best be seen how some of them were experimentally determined. Early work on the measurement of the membrane and intracellular parameters was carried out mainly using alternating current frequency techniques. This had the advantage that whole tissue samples could be used - as verified by Cole (1932) who showed that whole tissue could be represented by a simple electrical analogue of lumped impedances. Thus, the experimental problems were mainly confined to technical details of instrumentation.

Suspensions of cells and whole organs or muscle were first used. The cellular suspensions were either red blood cells or eggs from various echinoderm genera. Their use had the advantage that Poisson (1826) and Maxwell (1872) had previously calculated the theoretical relation between the resistances of the suspension, the suspending and suspended phases and the volume concentration of the spheres. Fricke (1923, 1924, 1925) extended the theoretical consideration to non-spheroidal particles and, from impedance measurements, found that his suspensions of red blood cells had a static capacity - i.e. independent of frequency between 1 kHz and 4.5 MHz - which was probably due to the membrane of the corpuscles. The value of this capacity was 0.81 $\mu F\ cm^{-2}$ (Fricke, 1926; Fricke and Morse, 1926).

However, these results were apparently at variance with those obtained by Phillipson (1921). Cole (1928) and others found using echinoderm eggs and various tissue samples that the capacity was frequency-dependant and similar to the polarisation capacity found at the surface of contact between metal electrodes and electrolytes.

The analogy was further strengthened as it was observed in animal tissues at least, that the measured cellular capacity and the polarisation capacity (Neumann, 1899) both varied inversely with the square root of the frequency.

The apparent paradox was solved for it had been assumed in the work of Cole (1928) that the reactance of the membrane was a pure capacitance and that the series resistance could be ignored. If this was now taken into account, the membrane capacity would become very much less frequency-dependent. On replotting the results on a complex plane plot, Cole (1932) found that the phase angle was considerably less than 90° for most biological tissues - the closest to a phase angle of 90° was the plot for red blood cells. (A phase angle of 90° represents a pure capacity - with phase angles of a smaller value, there is a series resistance with the capacity representing a dielectric loss which may be proportional to the permeability to ions).

The problem was resolved by improved measurement techniques which enabled the resistive and capacitative components to be determined separately instead of the bulk measurement of impedance. Thus, in a series of studies, Cole (Cole, 1935; Cole and Cole, 1936a,b) found a static membrane capacity for echinoderm eggs of the genera Hipponoë, Asterias and Arbacia, although there was some evidence of a low-frequency-dependent capacitance which could have been due to a surface conductance. The values of 0·87 $\mu F\ cm^{-2}$, 1·10 $\mu F\ cm^{-2}$ and 0·73 $\mu F\ cm^{-2}$ respectively for the static membrane capacities agreed closely with the value given by Fricke (1926).

These measurements also gave estimates for the specific resistance of the cellular contents which were taken from the impedance measurements at infinite frequencies when the capacitative elements would be expected to offer zero impedance. Höber (1910, 1912) first made such measurements, concluding that the interior of red blood corpuscles had a conductivity between a 0.1 and 0.4 per cent NaCl solution. Fricke, with his improved measurement techniques, calculated that the specific resistance of the interior of red blood cells was about 3.5 times that of serum (equivalent to a 0.17 per cent NaCl solution). The values from nucleated echinoderm eggs were more variable. Cole (1928) originally obtained a value of 3.6 times that of sea water - about 90 Ω cm . - but his later experiments with Hipponoë eggs gave a much larger value of 203 Ω cm , and 120 to 225 Ω cm for Arbacia and Asterias eggs (Cole, 1935; Cole and Cole, 1936a,b). These values seemed to necessitate the presence of a large amount of undissociated material to maintain osmotic equilibrium with the surrounding sea water. It is probable that the later results were more correct as there was difficulty in determining the exact high frequency transect of the resistance axis - indicating zero reactance - especially in the earlier experiments.

Such techniques were soon applied to excitable cells, most notably the large plant cells Nitella and Valonia. Some work was attempted with nerve fibres such as the frog sciatic nerve and the non-medullated fibres from Limulus optic nerve, but little information could be obtained due to the multifibre nature of these

nerves (Cole and Curtis, 1936). A tentative figure of 0.6 $\mu F\ cm^{-2}$ was obtained for the sciatic nerve membranes using a statistical distribution of fibre diameters and membrane capacities. The introduction by J.Z. Young (1936) of the squid giant axon however enabled measurement to be taken on a single irritable cell so that the theory calculated by Cole and Curtis (1936) for transverse and axial impedances could be tested. Transverse impedance measurements of Curtis and Cole (1938) gave a membrane capacity of about 1.1 $\mu F\ cm^{-2}$ at 1 kHz with a phase angle of 76^{o}. Thus, even in single cells, there was evidence of a polarisation-type impedance, so the phenomenon was concluded to be a property of the membrane itself.

The experiments thus far had given little information as to the nature of the membrane resistance and although Curtis and Cole (1938) gave a lower limit of 3 $\Omega\ cm^2$, they hinted that it might be greater than 1000 $\Omega\ cm^2$ - as was the case with Nitella, which was shown to have a value of $10^5\ \Omega\ cm^2$ (Blinks, 1930). Measurement of the impedance of the axon during activity (Cole and Curtis, 1939) showed that there was a transient decrease in impedance during the passage of an action potential, which was attributed to a decrease in the membrane resistance to about 25 $\Omega\ cm^2$. With a high membrane resistance, such impedance measurement would be expected to give little information because, at low frequencies, most of the current would pass through the extracellular fluid whilst, at high frequencies, current penetrating the cell would do so via the low impedance of the membrane capacity so that the membrane resistance would again be short circuited. If the external resistance could be made very high, then d.c. pulses should give some information as the membrane capacity's impedance should be infinitely high. This was the rationale behind the experiments of Cole and

Hodgkin (1939). Electrodes were placed with their faces in the longitudinal axis of the axon. Placing the interpolar region under oil greatly reduced the extracellular conductance so that current had to flow over the membrane resistance and along the axon interior. Changing the interpolar region would allow an estimate of the internal resistance to be made so that the membrane resistance could be measured. A value of 700 $\Omega\,cm^2$ was obtained for the membrane resistance, although they thought that a value of 1000 $\Omega\,cm^2$ was more justifiable as axons showing such values tended to be more healthy. A value of 29 Ω cm - 1.4 times that of sea water - was obtained for the internal resistivity which was significantly smaller than that obtained by Curtis and Cole (1938) of 1.5 to 6.9 times tha of sea water with transverse alternating currents.

With this method, Cole and Baker (1941) measured the axial impedance of a squid axon which would offer more information about the membrane and, to their surprise, found an inductance of 0.2 henrys cm^{-2} in series with the membrane resistance of 400 $\Omega\,cm^2$. The site of this inductance was difficult to visualise but other reports of such an inductance had appeared (e.g. Arvanitaki, 1939). This apparent inductance was ascribed to the delayed potassium conductance change following a change in membrane potential (e.g. Hodgkin and Huxley, 1952d; Cole, 1968). Following a change in membrane potential (dV_m) the redistribution of potassium ions will lag behind such a change in V_m. The behaviour of I_K will then be indistinguishable from current flowing through a series inductance and resistance if dV_m is small compared to $(V_m - E_K)$.

A complete theoretical and analytical analysis of the cable parameters was carried out by Hodgkin and Rushton (1946). The cable equations were evaluated into a utilizable form and the experimental results were found to correspond closely to the theoretical values. Application of the methods to skeletal muscle (Katz, 1948) showed that bundles of several muscle fibres also follow the cable equations reasonably well.

The Ultrastructure of Frog Ventricular Muscle

The irritable tissues that had been studied thus far - nerve fibres (Hodgkin and Rushton, 1946), skeletal muscle fibres (Katz, 1948) and Purkinje fibres (Weidmann, 1952) - had a simple cylindrical structure and thus the core-conductor model could be visualised to hold. The use of cardiac and smooth muscle preparations has the disadvantage that they are made up of a network of interconnecting fibres giving a syncitial arrangement. Thus, it would be expected that current flow in such tissues would be more complex.

Studies of the structure of frog ventricular myocardium and its relevance to excitation-contraction coupling have been carried out by a number of authors (e.g. Staley and Benson, 1968; Sommer and Johnson, 1969) so that description here can be confined to those details relevant to the interpretation of the electrical measurements that are to be described.

Each cardiac cell can be considered to be tubular in shape with a number of side branches producing a syncitial structure when observed under the light microscope. The diameter of each cell has been measured by a number of authors to be about 4-5μ (e.g. Sommer and Johnson, 1969; S. Page and Niedergerke, 1972). The length of frog

cardiac cells however is subject to a greater range of observed values. Frog atrial cells teased free in EDTA-containing (i.e. Ca^{2+}-free) solutions were described as long tapering cells, 175-200μ in length, more closely resembling smooth muscle cells, than mammalian cardiac cells (Barr, Dewey and Berger, 1965). On the other hand Fabiato and Fabiato (1972) using a mixture of proteolytic enzymes in an attempt to isolate individual cells reported long strands with a diameter of 3μ extending 100μ or more without branching - corresponding, they claimed, to a chain of cells. They also observed that 10% of single isolated cells were tubular and striated with a length of some 15μ.

The question of cell connexions in the frog ventricular syncitium also appears to be different from that observed in mammalian cardiac muscle. Cellular connexions in mammalian cardiac muscle are characterised by clearly defined intercalated disks which occur at the ends of individual cardiac cells. Certain regions of such disks consist of specialized areas where the cell membranes of opposed cells seem to fuse - the nexus - and this is supposed to be the location of low resistance connexions between cells. In frog ventricular tissue the intercalated disk is not so clearly defined, consisting of a number of small step-like disks rather than a continuous feature traversing the whole diameter of the cell, as in the mammalian tissue. This is why light microscopists denied the existence of intercalated disks in frog cardiac tissue (e.g. Marceau, 1904). Also no true nexuses have been observed in the amphibian tissue and in the abscence of any other observed structure it has been presumed that low resistance connexions between cells lie at the desmosomes (Staley and Benson, 1968; Sommer and Johnson, 1969). That such low resistance pathways are necessary have been shown by the elegant experiments of Barr,

Dewey and Berger (1965) in which they showed that a monophasic action potential could be recorded between two ends of muscle in a sucrose-gap arrangement - the sucrose-gap being greater than the cell length - if the external shunt resistance was made low enough. The desmosomes are similar structures to intercalated disks, except that whereas the disks lie perpendicular to the myofibril axis the desmosomes lie parallel to the axis. Indeed Grimley and Edwards (1960) suppose that the two structures have a common origin in a modification of the Z-line structure. Measurements made by Fawcett and Selby (1958) on turtle atrium (a tissue admitted by Grimley and Edwards (1960) and Nayler and Merrillees (1964) to be very similar to frog tissue) show that the gap between opposing cell membranes at the desmosomes is some 150-200 Å, whilst elsewhere it is in the region of 0.1 microns (1000 Å) - see also Nayler and Merrillees (1964). Thus, if the desmosomes and simple intercalated disks are regions of low resistance between cells such electrical coupling can occur over the entire cell surface. Thus, no study of their specific electrical properties can be made until a study of their area, relative to the entire surface membrane, has been made. It must be mentioned that the desmosomes are at least regions of cell adhesion, because when cells are shrunken by hypertonic solutions these regions often remain attached together (De Mello, Motta and Chapeau, 1969).

The other feature of importance is the lack of a tubular system in frog ventricle. This structure, conspicuous in skeletal and some mammalian ventricular muscle, allows electrical activity to reach the centre of the fibre, so reducing the diffusion distance for the

activator chemical to reach the myofibrils to a minimum, and thus allow the whole fibre to contract synchronously. In the frog ventricle however, the average cell diameter is about 5μ (Staley and Benson, 1968; Page and Niedergerke, 1972) as compared to about 100μ for skeletal fibres and 10 - 15μ for mammalian ventricular fibres, so that problems of diffusion distances are not limiting. Matching this lack of a T-system, the sarcoplasmic reticulum is very poorly organised and composed of small membrane bound vesicles which occasionally are seen to form networks (Staley and Benson, 1968; Sommer and Johnson, 1969). Page and Niedergerke (1972) calculated that the sarcoplasmic reticulum comprises 0·5% of the myofibrillar volume as compared to 7·3% of the myofibrillar volume in rat ventricle (Page, McCallister and Power, 1971).

The lack of a T-system thus greatly simplifies the calculation of the area of surface membrane as each cell can be regarded as a simple cylinder of circular cross-section. It has been observed by Lorber and Bertaud (1971) that the surface of frog atrial cells is covered by pinocytotic vesicles but they can give no estimate of how much they would increase the surface area, if indeed these membranes would be of any electrophysiological importance.

<u>The Passive Electrical Properties of Cardiac Muscle</u>

The publication of the cable equations in a usable form (Hodgkin and Rushton, 1946) and the introduction of glass microelectrodes small enough to penetrate a muscle cell (Ling and Gerard, 1949) enabled cardiac muscle to be studied in more detail, so that the individual

cellular parameters could be studied. Previous work had been mainly in the fields of electrocardiography and impedance studies (Rapport and Ray, 1927; Rosenbleuth and del Pozo, 1943), but little information could be gained on individual cells due to the complex geometry of the system, although Kahn (1941) did measure the time course of an electrotonic pulse in frog ventricle, finding two time constants in the region of 3·0 and 5·0 msecs.

The first records of an intracellular action potential using the Ling and Gerard microelectrodes were made by Coraboeuf and Weidmann (1949) on Purkinje fibres obtaining a mean resting potential of 71mV, but they observed no overshoot to the action potential. Woodbury, Woodbury and Hecht (1950) and Woodbury, Hecht and Christopherson(1951) recorded intracellularly from frog ventricle, finding a resting potential of some 60mV and an action potential of 80mV height. These authors mentioned that several factors would reduce the absolute values - i.e. leakage caused by puncture of the cells and the presence of a tip potential - but the values were greater than those obtained from extracellular recordings.

Later measurements by Draper and Weidmann (1951) on the same Purkinje preparation as used previously gave a value for the resting potential of 90mV and for the action potential of 120mV. Thus, with this preparation Weidmann (1952) made the first complete study of the cellular properties of cardiac muscle with a two-microelectrode technique - one for injecting square pulses of current into the fibre and the other to record the pulse at varying interelectrode distances. The values obtained are shown in table 1 along with values

from other cardiac preparations and various excitable tissues. The advantages of the Purkinje preparation were that the large cells - approximately 70 microns in diameter - and its non-contractility made penetration by two microelectrodes easy and that even with a point source of current, one-dimensional cable theory could explain the potential distribution within the fibre, in the limits of experimental error. However, with true cardiac muscle preparations (the Purkinje preparations are highly specialised conducting strands within the mammalian heart and can be considered as semi-nervous in properties), these advantages did not exist and, as shown by Woodbury and Crill (1961) and Tanaka and Sasaki (1966), a point source of current did not produce a one-dimensional distribution of current. Woodbury and Crill described the current spread as a two-dimensional flow with a preferential pathway in the longitudinal axis of the trabecula, using a pinned-out rat auricle so that the 'thickness' of the preparation was negligible compared to the other two dimensions. Tanaka and Sasaki found that their results approximately fitted their two-dimensional lattice model, but stressed that a three-dimensional model would have been more appropriate.

Previous studies by Trautwein, Kuffler and Edwards (1956), using thin strips of frog auricle and external electrodes, found a value for the space constant and the membrane time constant from a limited number of experiments. In an attempt to characterise frog ventricular cells, van der Kloot and Dane (1964), using an intracellular stimulating electrode, quoted a similar value for the membrane time constant - see table 1 - a value very much larger than those obtained by Woodbury and Crill (1961).

Table 1 Cellular Parameters of Excitable Tissues

Tissue	θ (m sec^{-1})	$\tau_{a.p.}$ (msec)	τ_m (msec)	λ (mm)	R_i (Ω cm)	R_m ($k\Omega cm^2$)	C_m ($\mu F\ cm^{-2}$)	Reference
Crustacean axon			2.3	1.61	60.5	2.29	1.33^{+}	Hodgkin and Rushton (1946)
Crustacean axon	4.5					3.5-6.8		Katz (1948) ; Chapman (1966)
Frog skeletal (sartorius) muscle			9	0.65	176	1.50	6^{+}	Katz (1948)
Frog skeletal (toe) muscle	1.6		18.5	1.11	255	4.30	4.4^{+}	Katz (1948)
Frog - slow muscle			351	0.96	250*	1.12	3.24^{+}	Stefani and Steinbach (1968)
Guinea-pig smooth muscle (rectum)	0.044	8.77	83.7	0.81	300* 125*	19.70 8.20	4.25^{x}-1.6^{+} 10.2^{x} -3.68^{+}	Kuriyama and Mekata (1971)
Guinea-pig smooth muscle (taenia coli)	0.046 -0.088	6.6	106.7	1.45		30 -50	2-3^{x}	Abe and Tomita (1963)
Purkinje fibres (kid)			19.5	1.90	105	1.94	12.4^{+}	Weidmann (1952)
Purkinje fibres (sheep)	2.7	0.14	21.6	2.0	116	1.71	12.8^{+} 2.4^{x}	Fozzard (1966)

Table 1 Continued

Tissue	θ (m sec^{-1})	$\tau_{a.p.}$ (msec)	τ_m (msec)	λ (mm)	R_i (Ω cm)	R_m (kΩ cm^2)	C_m (μF cm^{-2})	Reference
Purkinje fibres (dog)	2.01	0.11	15.0	1.25	100*	8.93	1.68x	Sakamoto and Goto (1970)
Atrial fibres (frog)			6.3	0.33				Trautwein, Kuffler and Edwards (1956)
Atrial fibres (dog)	0.40	0.68	14.6	1.24	100*	5.59	2.61x	Sakamoto and Goto (1970)
Atrial fibres (rabbit)	0.533	0.217	2.66	0.66	500*		1.27x	Bonke (1973)
Ventricle fibres (frog)	0.103	2.9	3.2	0.35*	460	2.60	1.2+	van der Kloot and Dane (1964)
Ventricle fibres (dog)			2.0	1.35				Kamiyama and Matsuda (1966)
Ventricle fibres (dog)	0.68	1.1	3.3	1.20	100*	3.50	0.76x	Sakamoto (1969)
Ventricle fibres (dog)	0.78	0.88	3.2	1.18	100*	5.33	0.60x	Sakamoto and Goto (1970)
Ventricle fibres (calf and sheep)	0.75	0.38	4.4	0.96	470	9.10	0.59+ 0.81x	Weidmann (1970)
Neonatal cells (rat)			1.7	0.36	500	1.30	1.3+	Jongsma and van Rijn (1972)

*Assumed values; +C_m calculated from $_m/R_m$; xC_m calculated from the foot of the action potential

The necessary conditions for the proper one-dimensional cable analysis of cardiac muscle had been already established, in theory at least, by the sucrose gap technique of Stämpfli (1954) and a modification of this was used by Kamiyama and Matsuda (1966), in which two chambers separated by a partition were electrically connected only via the intracellular pathway of a trabecula which passed through a just adequate gap in the partition. Stimulation at the partition by large external electrodes produced equal currents around the surface of the trabecula, and hopefully throughout the cross-section also, at the point where the muscle penetrated the partition which should decrease in a one-dimensional manner away from the partition. Use of this method on cardiac (Sakamoto, 1969; Sakamoto and Goto, 1970) and smooth muscle (Abe and Tomita, 1968) preparations thus enabled the membrane characteristics to be evaluated.

Weidmann (1970), using end stimulation of a ventricular bundle, characterised the membrane constants and also measured the internal resistivity of the cells, finding the value to be significantly higher than that of Purkinje fibres and also higher than the value determined from radioactive potassium diffusion data (Weidmann, 1966). He explained the latter phenomenon in that potassium movements within the cell could be assisted by convection and that only the intercalated disks would provide a significant barrier. The difference between the Purkinje fibre value and that obtained from ventricle could have been due to the myofibrils and mitochondria taking up a larger part of the intercellular volume and the greater resistance and/or number of intercalated disks.

A summary of the electrical constants obtained from various nerve and muscle preparations is seen in table 1.

The problem of intercellular junctions providing a barrier to current flow in the intracellular pathway only arises in smooth and cardiac muscle preparations, as the skeletal fibres run the whole length of the muscle. Thus, it was of interest to see whether such junctions - which can be lumped under the convenient title of intercalated disks in cardiac muscle - formed a significant barrier to current flow. The work of Sperelakis and his co-workers (e.g. Hoshiko, Sperelakis and Berne, 1959; Tarr and Sperelakis, 1964; Sperelakis, 1969) on frog and mammalian heart indicated that the intercalated disks had a high electrical resistance and proposed that transmission between cells was by chemical means.

However, other work (Weidmann, 1966; Heppner and Plonsey, 1970; Woodbury and Crill, 1970) - both theoretical and experimental - yielded a much lower value for this resistance, about 3 Ω cm^2 (in mammalian heart) and suggested that transmission was electrical. This view supported the microscopic observations of Dewey and Barr (1964) who found, in mammalian preparations, regions of fused membrane between opposing cells which could offer a low-resistance pathway. One of the purposes of this work is to see whether the frog intercalated disk offers a high or low resistance to current flow.

Voltage-Clamp Studies

In their classical series of experiments, Hodgkin and Huxley & Katz (Hodgkin, Huxley & Katz, 1952; Hodgkin & Huxley, 1952a-d) dissected the action potential into its component parts by their voltage-clamp studies. Basically the technique tries to

maintain a constant membrane potential difference over the region of interest during an active process by means of a feedback process. The dynamic characteristics of the currents needed to achieve this will be a measure of the membrane currents flowing.

There are a number of basic conditions which must be achieved, however, for the recorded currents to be a true measure of the membrane currents: that 1) the recorded potential is the true membrane potential, 2) spatial control exists - i.e. the membrane is 'clamped' to the same potential at all points, 3) temporal control exists - i.e. the membrane is 'clamped' at all times and 4) the passive properties of the preparations do not change during the course of the experiment.

Hodgkin, Huxley & Katz (1952) realized these requirements by using an internal electrode which passed along the longitudinal axis of the axon. The measured potential was not the true membrane potential but included the potential over the resistance of the cytoplasm from the electrode to the membrane; however, this resistance was very small compared to the membrane resistance. Spatial control could be achieved everywhere in the test region and temporal control depended only on the speed of response of the feedback amplifier - control only being lost during the initial rapid charging of the membrane capacitance. The last condition could be seen if any of the current changes varied with time.

With cardiac muscle, the same approach to the problem obviously could not be taken, due to its complex multicellular nature. As no precedure has yet been developed which allows the study of single cardiac cells - except some work on artificially grown cells (cf. Lieberman et al., 1973) - then the preparations used have been multicellular trabeculae which contain anything up to one to two thousand cells in cross-section. Thus, the membrane potential of both superficial and intratrabecular cells will have to be equally clamped. This is not an easy problem as the deeper cells in cardiac preparations are connected to the exterior of the trabecula by narrow clefts which would be expected to form a resistance to current flow which is in series to the membrane - for this reason, it has been dubbed with the obvious title, the series resistance. Thus, deeper cells will not be clamped to the same potential as superficial cells.

A less serious problem is that the total membrane area cannot be accurately known so that currents in terms of amps cm^{-2} cannot be calculated and the description of currents will have to be more qualitative. The other structural problem is that of intercellular connexions along the length of the preparation, which will introduce a delay in the transmission of a signal. Thus, if there is any flow of current at all in the preparation needed to clamp all the cells this will not be achieved instantaneously throughout all the cells, so that temporal control is not even theoretically possible. However, it remains for us to see how serious these limitations are on the interpretation of voltage-clamp data.

Two techniques have been used to voltage-clamp cardiac muscle using 1) two microelectrodes or 2) a single- or double-sucrose gap.

The two-microelectrode technique has been applied mainly to the large-celled Purkinje preparations from mammalian heart (e.g. Deck, Kern and Trautwein, 1964; McAllister and Noble, 1966). With this method, one microelectrode is used for recording potential changes and the other for passing clamping current. The main problem is of adequate spatial voltage control. If we calculate the potential distribution according to one-dimensional cable theory - which, as Weidmann (1952) has shown, applies to a first approximation to this preparation with a point source of current - reference to table 2 shows how the potential distribution varies with distance under optimal conditions, i.e. the current electrode in the middle of the preparation and the ends perfectly sealed (cf. Deck, Kern and Trautwein, 1964). For lengths of about 1mm, voltage control is fairly good along the length of the preparation. It must, of course, be recognised that if the termini are not perfectly sealed, then current leakage will occur and so the potential distribution will be worse.

The three-dimensional aspects of a point source of current were studied by Eisenberg and his co-workers (Eisenberg and Engel, 1970; Eisenberg and Johnson, 1970; Engel, Barcilon and Eisenberg, 1972). Eisenberg and Johnson (1970) showed that when the space constant is very much larger than the fibre radius, the correction for radial flow of current is quite small - about 4% for λ/a (a is the fibre radius) equal to 10 - but becomes larger as the ratio decreases. The latter condition will be reached when the membrane conductance rises as in the upstroke of an action potential, so that voltage control can be expected to be lost to an even greater extent than if one-dimensional cable theory merely existed. Thus, it seems that under optimal

conditions, spatial control can be fairly good under steady-state conditions or during slowly varying currents, as studied by Noble and his co-workers (McAllister and Noble, 1966; Noble and Tsien 1968, 1969,a,b; Hauswirth, Noble and Tsien, 1972,a,b).

Two experimental approaches were taken to study the faster inward currents without the interference of lack of spatial control and the initial capacitative transients. Dudel et al. (1966) used ramp-clamping pulses to avoid the capacitative transients, however, the effects of potential and time on membrane currents were not so discernible so that the time dependence of specific components of current had to be evaluated by measuring the current at several different ramp gradients. However, it was difficult to assess the degree of inhomogeneity at each ramp gradient, so that only qualitative data could be obtained. Dudel and Rüdel (1970) attempted to separate the inward currents from the capacitative transients by cooling the preparation and so slowing the ionic currents, and observed that the inward current could be resolved into two components.

Apart from the technical difficulties of inserting several microelectrodes into a ventricular or auricular trabecula, the deviation from one-dimensional cable theory would be even more serious in these preparations with a point source of current, so that spatial control could never be reached (Woodbury and Crill, 1961). The method of the sucrose-gap technique introduced by Stämpfli (1954) is thus useful in that it produces a planar source of current at right angles to the axis of the trabecula so that flow of current is reduced to one dimension.

Table 2 The Maximum Estimated Voltage Homogeneity in Voltage Clamped Preparations Assuming a Closed-end Situation

Method	Tissue	Preparation length	Space constant	Maximum Homogeneity
2 microelectrodes	Purkinje fibres	1 mm	1·9 mm	87·6%
		2 mm		62·2%
Single sucrose-gap	Mammalian ventricle	1 mm	0·96 mm	62·8%
Single sucrose-gap	Frog ventricle	0·3 mm	0·33 mm	69·0%
		0·5 mm		41·6%
Double sucrose-gap	Frog auricle	0·1 mm	0·3 mm	94·7%
		0·2 mm		81·3%

The preparation lengths are typical values of lengths used with the particular method and preparation. The space constant values are taken from Weidmann (1952, 1970) for Purkinje fibres and mammalian ventricle. The frog ventricle value is taken from the results presented here; the value for frog auricle is an estimated value. Note: the calculations apply only to a small (i.e. 10 mV) step. With larger steps (i.e. 50 - 60 mV) anomalous rectification will be evident - manifesting itself by an increase in r_m after the initial inward currents, so that for measurements of currents at long times (500 msec) control will be better than tabulated above.

The principle of the method is to surround part of a trabecula with deionised sucrose so as to limit current flow to the interior of the cells. With the single-sucrose gap, changes in the intracellular potential of cells in the recording pool feed current into the preparation via the current pool so that the high resistance of the sucrose gap forces all the current into the preparation. With the double-gap arrangement, voltage is recorded over the central node and voltage pool whilst current is fed via the current pool. The current pool is often filled with KCl (e.g. Brown and Noble, 1969) which depolarises the surface membrane and so reduces the resistance to current flow into the trabecula.

The use of sucrose has two main disadvantages, a) it causes a gradual increase in the internal longitudinal resistance and so violates our fourth condition for an adequate voltage-clamp and b) it causes a hyperpolarisation of the cell membrane. The latter phenomenon has been shown by Julian, Moore and Goldman (1966) to be due to the junction potential between sucrose and Ringer, and can be reduced by the use of rubber partitions (cf. Mascher and Peper, 1969; Giebisch and Weidmann, 1971) or waterproof substances (cf. Morad and Trautwein, 1968; Rougier, Vassort, and Stämpfli, 1968) at the junctions so as to reduce the junction area.

The technique demands that the regions under study - namely the muscle membrane in the recording pool or the central node with the single- or double- sucrose gap respectively - are at the same potential along their length. This was studied by early investigators, using the single-sucrose gap (Morad and Trautwein, 1968; Beeler and Reuter, 1970a) but as yet has not been investigated in the double-gap arrangement, due

to technical hindrances. These authors found that with mammalian fibres, if the length of the muscle in the recording pool was 1mm or less, then spatial homogeneity was adequate. Morad and Trautwein (1968) also found that homogeneity was present throughout the diameter of the trabecula. Exactly similar results were found by Ehara (1971), who found that electrotonic decay was only noticeable when the muscle was longer than 1mm. Calculations show that if the muscle is regarded as a finite cable with sealed ends, using the figure of 1·2mms for the space constant of canine ventricular myocardium (Sakamoto, 1969), the decay for a 1mm length of muscle will be to 73% at its termination and to 89% for a 0·5mm length - as seen in table 2. Whether the sucrose in the adjacent gap somehow shortens the effective length of the muscle in the recording pool or any decay was lost in the experimental error is difficult to say, but it seems that extreme caution must be taken in assessing the degree of spatial homogeneity in such preparations.

With the double-sucrose-gap arrangement, much smaller regions of membrane can be isolated - Leoty and Raymond (1972) claim widths of 40 - 80 microns. This region can also be treated as a sealed-end finite cable if it is assumed that the membrane resistance in the central node is less than the internal resistance of the cells under the sucrose gap, so that all of the current will leave the central gap (Brown and Noble, 1969). With such a condition, if a space constant of 300 microns is assumed for frog auricular trabeculae, a width of 100 microns for the central gap will only show a discrepancy of 5% from one end of the preparation to the other - see table 2. The only estimation of voltage non-uniformity in the gap was made by Brown and Noble (1969)

who, using a 500 micron gap, estimated that the voltage would differ by 30% between the two ends.

The problems of temporal control were considered by Rougier, Vassort and Stämpfli (1968) in their double gap arrangement, who found an initial capacitative component merely due to passive charging of the membrane. However, Beeler and Reuter (1970a) showed that, with a small depolarising step, they merely obtained a step change in current with an exponential decay which they attributed to the presence of the series resistance. From the time constant of decay, they calculated the series resistance to have a value of about 580 Ω which was not negligible compared to the resistance of the membrane under test. Thus, the membrane capacity would be charged through different resistances throughout the preparation and so would alter the rate of charging throughout the preparation.

The final problem was that during the fast changing currents, voltage control was not possible due to the increased membrane conductance. Beeler and Reuter (1970a) merely stated that control was not possible during fast currents, whilst Nascher and Peper (1969), although recognising the problem, did not consider it serious enough to prevent them from qualitatively studying the fast currents. With the double-gap arrangement, fast inward currents were regularly studied (cf. Rougier, Vassort, Stämpfli, 1968; Rougier et al.,1969) in that they were considered to be truly sodium currents being abolished by tetrodotoxin or sodium-free solutions. Thus, in the period 1970 - 1971, it was considered that the action potential could be described by a number of ionic currents. The inward currents had been shown to be composed of a fast and slow component which were thought to control the upstroke and the duration of the plateau (Rougier, Vassort, Stämpfli, 1968;

Rougier et al.,1969; Brown and Noble, 1969; Mascher and Peper, 1969; Beeler and Reuter, 1970a-c; Ochi, 1970; Ochi and Trautwein, 1971), whilst repolarisation was due to either an increase in the outward currents, as in Purkinje fibres (Noble and Tsien, 1969) or a decrease in the inward currents (Mascher and Peper, 1969; Beeler and Reuter, 1970b; Giebisch and Weidmann, 1971).

This complacency was shattered however, by the publication of a review by Johnson and Lieberman (1971) in which they criticised the validity of the control experiments that had been performed for spatial and temporal homogeneity and put into question the very existence of some of the current components, especially the slow inward calcium or calcium-and-sodium current. They attributed its appearance to the presence of the fast inward current in a less perfectly clamped population of cells which showed more variability in its temporal behaviour, presumably a consequence of the series resistance. This possibility had been recognised by Mascher and Peper (1969) but abandoned in favour of two separate inward currents.

Indeed, Johnson and Lieberman (1971) prologized their review with their conclusion that "in the interpretation of the currents recorded during voltage-clamp experiments, one must remember that currents occuring at different times and at different potentials may be due to currents occurring at different times in different places, the potential at these places being different from that at the place one chooses to record and control it.".

Thus, although the language may have been a little harsh in places, it stimulated a considerable amount of work to study exactly what does happen to a trabecula in a sucrose-gap chamber, and it was under the

shadow of this dissention that the present experiments were carried out in attempt to examine thoroughly the properties of frog ventricular myocardium, to see whether it was a suitable material for voltage-clamp experiments.

METHODS

The Preparation

Frogs (Rana pipiens) were pithed and the hearts quickly removed. The apex of the ventricle was pinned out with fine entomological pins - ventral side uppermost - on a Petri dish, the bottom of which had been filled with Sylgard resin and the dissection carried out under Ringer. The ventral wall was cut from the atrial end to the apex and pinned out as a sheet. The valve tissue was removed as this contained pacemaker tissue also - this was recognised as two light masses at the atrial end connected by a thin sheet of connective tissue, and the whole connected to the ventricle wall by thin strands. Mechanical stimulation of this region induced rhythmic contractions which ceased when the tissue was removed. Occasionally, small unbranched trabeculae about 1mm long and 200 - 300μ in diameter could be seen running across the ventricle, i.e. parallel to the atrio-ventricular junction. But usually, preparations were taken which ran from the atrio-ventricular junction and inserted into the wall of the ventricle at the apical end. These could vary between 1 - 3mms in length and 200 - 500μ in diameter. Side connexions were often present, especially in the larger trabeculae, so that preparations were chosen which offered the least number. The chosen trabecula was ligatured at each end with fine silk thread (20μ diameter), the side connexions cut if necessary, and the preparation - as it will be called hereafter - removed from the heart and attached to the various dishes used.

With the experiments performed to measure the total intracellular resistance, strips of muscle were used. These were always taken from the right side of the pinned out heart as this region seemed to consist of a large number of parallel-orientated fibres running towards the apex.

Solutions

For a normal bathing medium, frog Ringer of the following composition was used (Chapman and Tunstall, 1971): NaCl, 117 mM; KCl, 3 mM; Na_2HPO_4, 0.8 mM; NaH_2PO_4, 0.2 mM; pH 7.3. NaCl was added as a solid, whilst the remaining chemicals were diluted from stock solutions. All chemicals were Analar grade. $CaCl_2$ was added from a 1M stock solution for volumetric analysis (B.D.H.) to give a final concentration of 0.1 to 1.0 mM. Such concentrations of calcium were used to reduce the contractility and so facilitate penetration by microelectrodes. The $CaCl_2$ was always added last to the prepared Ringer, otherwise it tended to precipitate as $Ca_3(PO_4)_2$ which was difficult to dissolve even when the chemicals had been diluted to their required value, and tended to persist as a faint cloudy colloid. Glucose was added as a solid when necessary, to give a final concentration of 10 mM.

Hypertonic Ringer solution included 400 mM glycerol thus increasing the osmolarity 2.6 times. To immobilize the preparation during the longitudinal impedance measurements during activity, Analar sucrose was added as a solid to make the Ringer two or three times hypertonic.

Tetrodotoxin (TTX) was obtained from Sankyo Ltd, Japan, in glass ampoules and diluted to a stock solution of $1.25.10^{-4}$ molar concentration.

Calculations

Calculations were performed with a Wang programmable calculator (Model 300C). Exponential plots, such as those obtained for estimation of the space constant and the time constant from the foot of the action potential, could be reduced to a straight-line relationship with a specially designed programme giving information about the slope, the intercept of the line with the ordinate and the correlation coefficient. A correlation coefficient of 0.95 or greater was a criterion for acceptance of the data for evaluation. Standard deviations of results could be calculated with a similar programme.

Error function (erf) values and Bessel function coefficients were obtained from the Handbook of Mathematical Functions (Abramovitz and Stegun, 1968). More detailed information concerning the imaginary Bessel coefficient, K_o, was obtained from the U.S. National Bureau of Standards booklet (1952).

Recording Apparatus

Intracellular recordings were made by means of glass microelectrodes filled with 3M, 1M or 0.3M KCl. The microelectrodes were pulled from 50 microlitre Pyrex pipette glass (Dade and Co. Ltd) on a vertical microelectrode puller (Narashige scientific model PE-2). The microelectrodes were filled by boiling them in the KCl solution under reduced pressure. Such 3M KCl-filled microelectrodes usually had a resistance of 10-25 MΩ.

The preamplifier was an FET-input operational amplifier (Burr-Brown 3153/25) with an input impedance of 10^{11} ohms and was set to a gain of ten throughout the experiments. The frequency response was flat to 100 kHz and 3 db down at 150 kHz. A 20 MΩ resistor

was placed in parallel with the preamplifier input so that measurements of the microelectrode resistance could be made (see the section on the measurement of cytoplasmic resistivity for details).

An input capacity due to the microelectrode wall and the shielding around the electrode leads was present. This was kept to a minimum by keeping the leads as short as practically possible and having a minimum of fluid surrounding the trabecula, as the microelectrode capacity resides in the portion surrounded by fluid (Amatniek, 1958). Neutralization of the existing capacity was important as it would introduce a time constant into the input recordings and so distort the waveform. This was achieved by applying a negative capacity to the lead shielding by means of a feedback circuit from the output of the preamplifier. Perfect equalization of the two capacities was not possible due to the phase shifting of the signal through the amplifier, which caused ringing to occur just before balance. Voltages were displayed on a Tektronix 565 oscilloscope via a 3A10 transducer amplifier or a 2A63 differential amplifier. The waveforms were then shown on a Tektronix 502A oscilloscope from which they were photographed.

Changes in the longitudinal impedance during an action potential were measured at 600 Hz with the high-pass filter of the 3A10 amplifier set at 3 db down at 100 Hz and the low-pass filter 3 db down at 3 kHz, giving a maximum bandpass at about 700 Hz. In order to reduce the bandwidth, a passive second-order band-pass filter was placed in series with the 3A10 amplifier so that the resultant waveform had a centre frequency at 790 Hz and was 3 db down at 440 Hz and 1400 Hz, with an attenuation of 0.6 db at 790 Hz.

Measurement of the Cytoplasmic Resistivity, R_c

The method involved observing the changes in microelectrode resistance, R_{EL}, when a microelectrode was placed in solutions of varying resistivities. R_{EL} was first measured with the microelectrode in the solution bathing the trabecula. The microelectrode was then inserted into a cell and R_{EL} measured again. The microelectrode was then withdrawn from the cell and re-inserted into another cell and R_{EL} measured. This procedure was performed from 6-10 times after which R_{EL} was again measured with the microelectrode in the bathing solution.

R_{EL} was measured by placing the microelectrode in parallel with a 20 MΩ resistor and applying a 100 mV peak-to-peak 1 kHz square wave to the input of the preamplifier. Figure 2A shows the situation with the microelectrode out of the bathing solution, so that all of the voltage drop is over the 20 MΩ resistor. Part B shows the microelectrode in the bathing solution so that the voltage drop is now over the parallel combination of R_{EL} and the 20 MΩ resistor. The change in voltage observed when the microelectrode is put into the bathing solution is thus a measure of R_{EL}. Part C shows the situation with the microelectrode intracellular and it will now be noted that R_{EL} is in series with the input resistance, R_{inp}, of the cell. Thus, R_{inp} must be subtracted from the observed intracellular value of R_{EL} before the true value can be obtained.

R_{inp} was measured separately by two intracellular microelectrodes, with their tips less than 10μ apart, one for passing current and the other for observing the change in membrane potential.

Figure 2 Convenient diagrammatic representations of the resistance relations of the microelectrode under different experimental situations. Part A shows the microelectrode out of the bathing solution so that all of the potential drop is over the 20 MΩ resistor. Part B shows the microelectrode in the bathing solution. Part C is the situation with the microelectrode intracellular, so that the input resistance, R_{inp}, is in series with the microelectrode resistance. The formulae at the bottom of each part are the measured resistances.

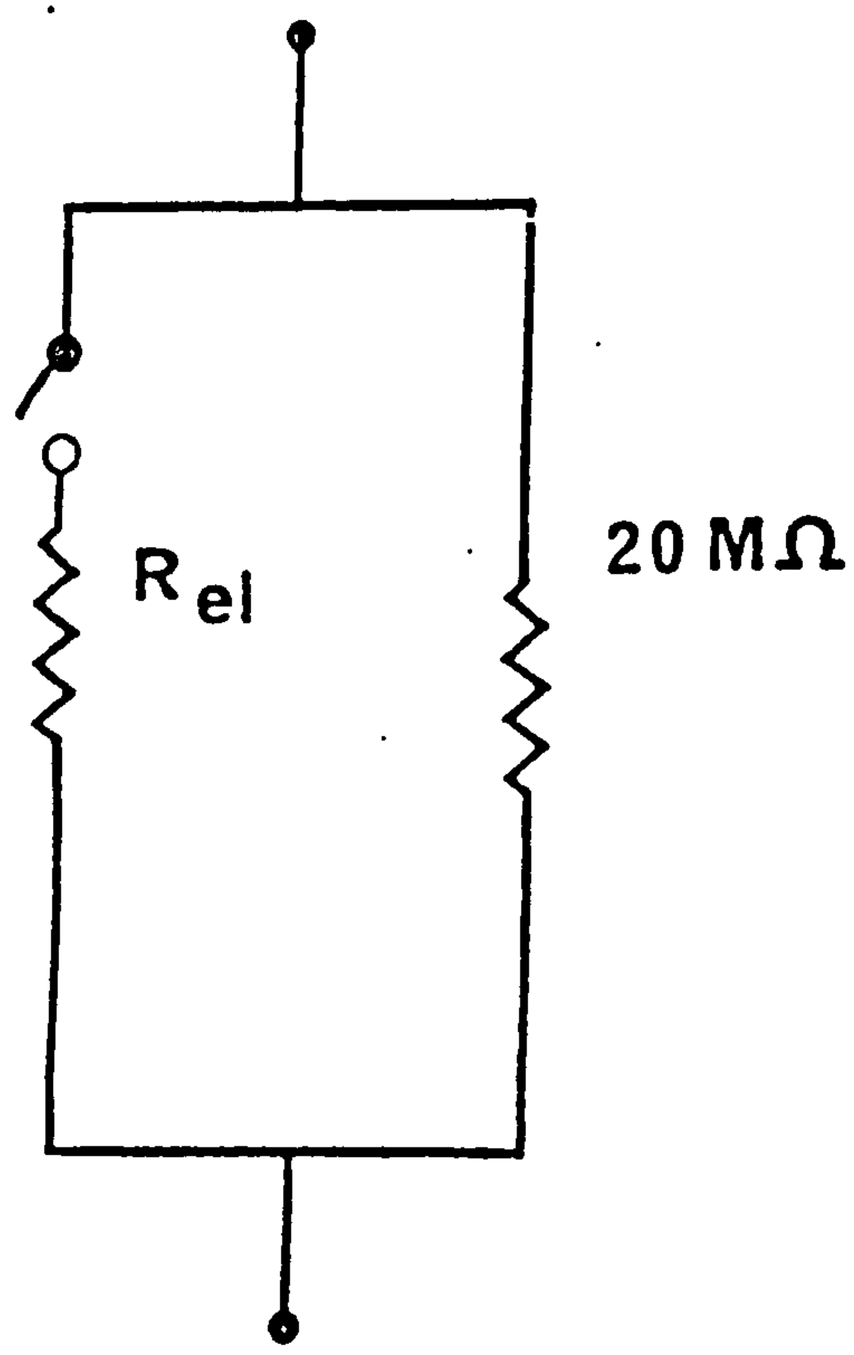

$R = 20\,M\Omega$

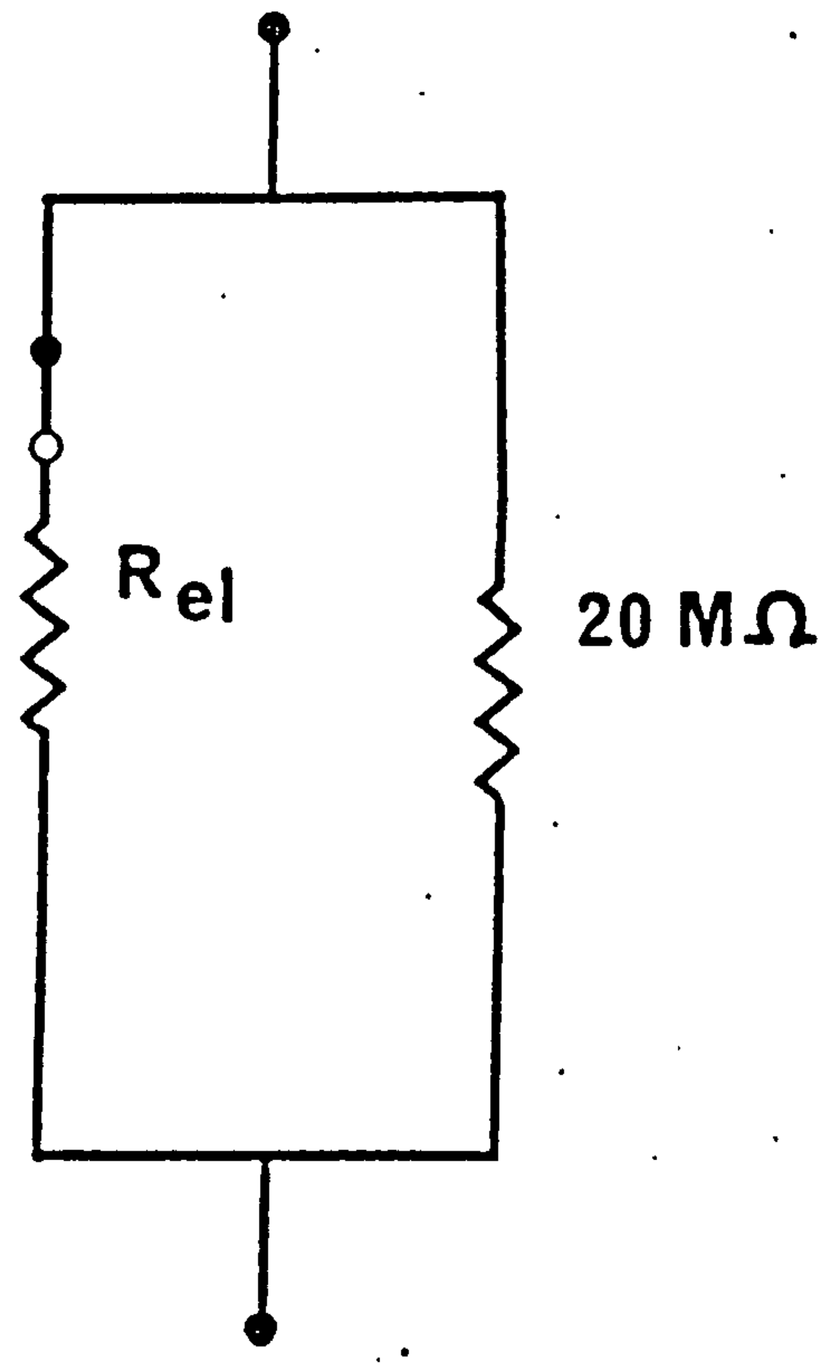

$$R' = \frac{20\,M\Omega \cdot R_{el}}{20\,M\Omega + R_{el}}$$

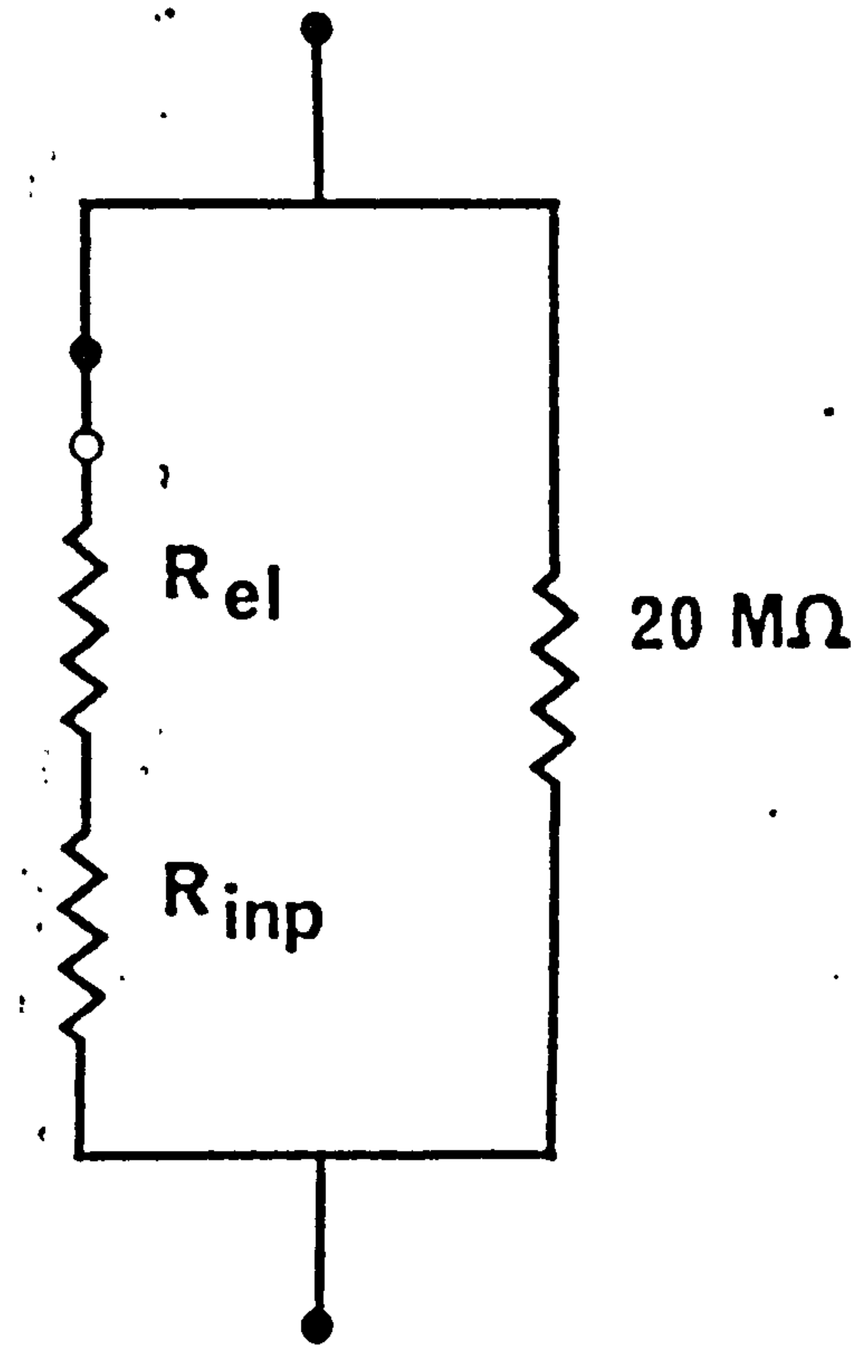

$$R'' = \frac{20\,M\Omega\,(R_{el} + R_{inp})}{20M\Omega + R_{el} + R_{inp}}$$

The amount of current passed down the microelectrode was measured by observing the voltage drop over a 2 kMΩ-550 MΩ resistor (see the section on intracellular stimulation, in the methods chapter for further details on the calculation of interelectrode distance). The value of R_{inp} was calculated from the ratio of change of membrane potential to current passed. Ideally the two microelectrodes should be a zero distance apart, but distances less than 10μ were assumed to approximate this condition. The value of R_{inp} thus calculated was used in all subsequent determinations of the cytoplasmic resistivity.

Having made measurements of R_{EL} in the bathing solution and intracellularly, the microelectrode was then calibrated in KCl solutions of known resistivity. Solutions from 10 mM to 3 M were made from Analar KCl and R_{EL} was measured when the microelectrode was placed in 10 ml of each calibrating solution. The specific resistivities of the calibrating solutions were calculated from equivalent conductivity data given by Noyes and Falk (1912). Finally the temperature of the calibrating solutions and the bathing Ringer was noted. The data given by Noyes and Falk are for temperatures of 0°C, 18°C and 25°C. When the temperature of the calibrating solutions differed from these temperatures their resistivity was calculated from an Arrhenius-type plot of $1/T^{\circ}K$ (absolute temperature) against the logarithm of the equivalent conductivity.

Thus, after subtracting R_{inp} from the intracellularly obtained value of R_{EL}, the value of the cytoplasmic resistivity could be read from the calibration curve.

Measurement of the Resistance to the Longitudinal Flow of Current, R_f

The total resistance to the flow of current in the intracellular pathway was estimated by the method described by Weidmann (1970). With this method action potentials are used as current sources and their potential heights, as recorded intracellularly and extracellularly, can be used to calculate resistances. The method requires that a portion of the trabecula be inactivated so as to exclude active processes in the region under test. The length of this portion will have to be long compared to the space constant so that action potentials, as measured at the end of the inactivated region, can be studied under conditions of zero membrane current.

Strips of frog ventricle 5-10 mm long and about 1 mm in diameter were used. The space constant was determined prior to these experiments and was found to have a value of 328 μ . In this experimental situation the extracellular resistance, r_o, was not negligible (as it was assumed to be in the determination of the space constant) so that the space constant was shorter. If the intracellular resistance, r_i, equalled r_o then the space constant would have a value of 232 μ . Thus the inactivated portion would be some 10-20 times the space constant under these conditions, so that membrane current was negligible at the end of the inactivated region.

Half of the strip was inactivated by perfusing with Ringer containing 4.10^{-8} gm ml^{-1} of tetrodotoxin, the other half being perfused with normal Ringer - the arrangement is shown in figure 3. The perfusing fluids were drawn away by a small piece of cotton

Figure 3 Diagrammatic representation of the arrangement used for measurement of the longitudinal resistance to flow of current. The central rectangle represents the muscle strip being perfused with Ringer and Ringer containing tetrodotoxin (TTX-Ringer), the arrows indicating the direction of flow of the perfusing liquids. The filled circles represent the ends of AgAgCl stimulating electrodes inserted into the perfusing streams. The significance of the microelectrodes 1, 2 and 3 is as indicated in the text.

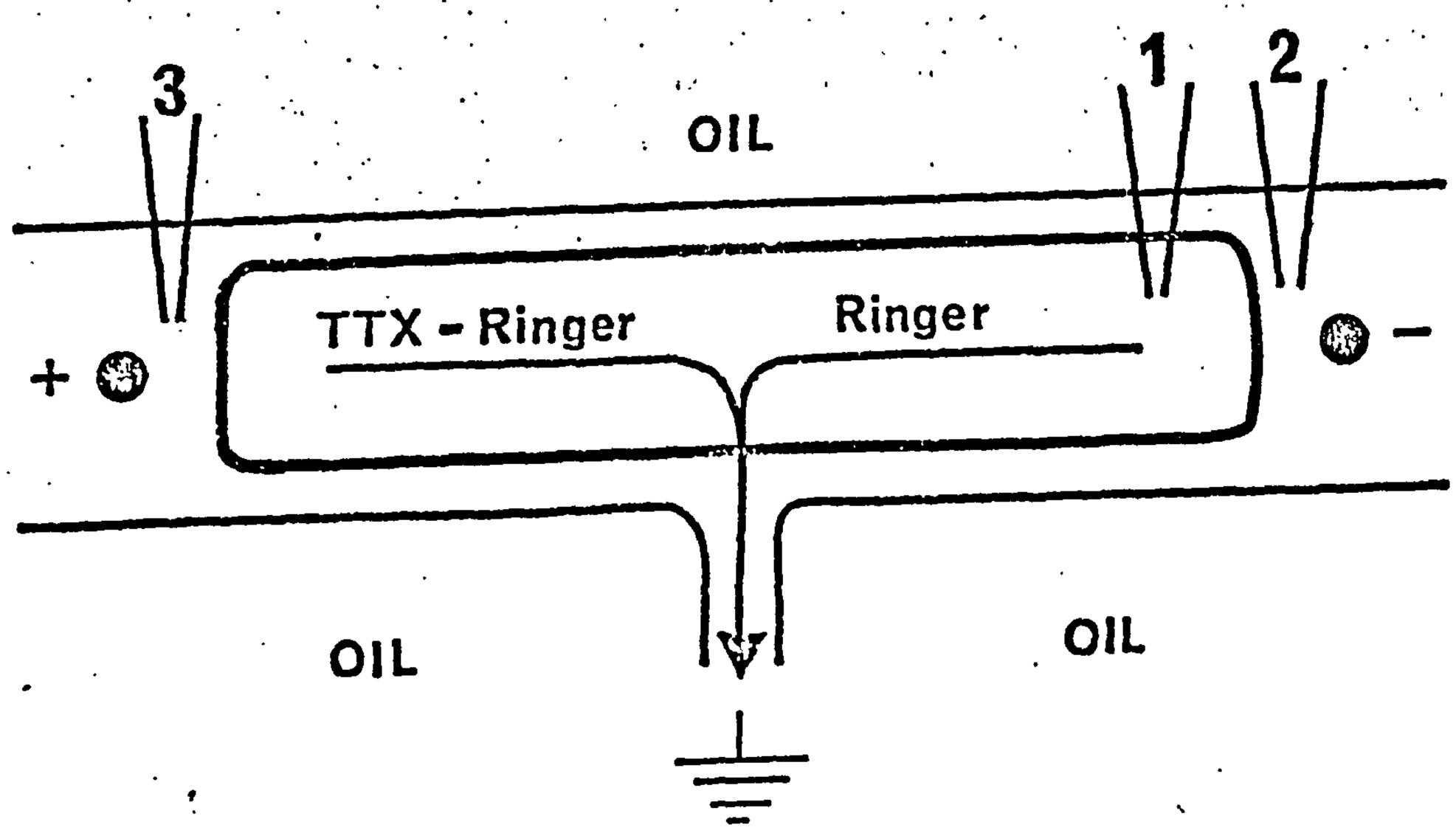
3
OIL
1
2
TTX - Ringer
Ringer
+
–
OIL
OIL

wool touching the underside of the middle of the trabecula. Stimulating AgAgCl wire electrodes were placed in the perfusing streams just before they reached the muscle so that cathodal polarization could be applied to the end of the active portion of the strip.

Action potentials were recorded between an intracellular and extracellular microelectrode at the active end of the preparation (position 1-2 of figure 3) and then an action potential was recorded with the extracellular electrode in the TTX-perfused region (position 1-3 of figure 3). An action potential propagating down the active half of the trabecula will stop at the active-inactive border. At this point it will act as a current source and with the preamplifier in the 1-3 position the pathway will be made up via the intracellular pathway. The recorded action potential will, by Ohms law, be proportional to the resistance of the pathway. With the microelectrodes in the 2-3 position the circuit will now be made up via the extracellular resistance, so that the recorded action potential height will be proportional to this resistance. Therefore, the ratio of the recorded potential values of the intracellular and extracellular action potentials will be a measure of the ratio of the corresponding resistance pathways.

Measurement of the Space Constant, λ, the Membrane Time Constant, τ_m, the Conduction Velocity, θ, and the Time Constant from the Foot of the Action Potential, $\tau_{a.p.}$.

Most of the experiments for the determination of these parameters were performed with a partition chamber similar to that described by Kamiyama and Matsuda (1966), although early experiments for the determination of θ and $\tau_{a.p.}$ were performed on trabeculae stimulated at one end.

The partition chamber consisted of two identical chambers separated by a thin rubber partition. A hole was made in the partition with a blunt microelectrode and the trabecula pulled through the hole. The partition was held under tension during this procedure so that when the trabecula was in place and the tension in the partition removed it formed a snug fit around the muscle. Separation was shown to be complete because when one chamber was perfused with a solution containing a dye no trace of the dye was seen in the other chamber. This form of separation had the advantage over the Perspex grooved partition as used by Kamiyama and Matsuda (1966) in that isolation was complete without the use of additional Vaseline, so that a minimum amount of the preparation was under the partition - the arrangement is shown in figure 4.

Polarizing current was passed between the two chambers through large AgAgCl electrodes. A large guard resistor - usually 2.7 MΩ - was placed before the anode to ensure a constant-current condition: it also providing a means of measuring the stimulating current by recording the potential drop over this resistor.

Figure 4 Diagrammatic representation of the partition method for unidirectional stimulation. The trabecula T is pulled through a hole in the rubber partition P. Current from the stimulator, S, is passed via a guard resistor to the stimulating AgAgCl electrodes. The amount of current, I, used can be measured from the voltage drop over the guard resistor. Recordings made via an intracellular and extracellular microelectrode are passed to a differential preamplifier and thence displayed on an oscilloscope.

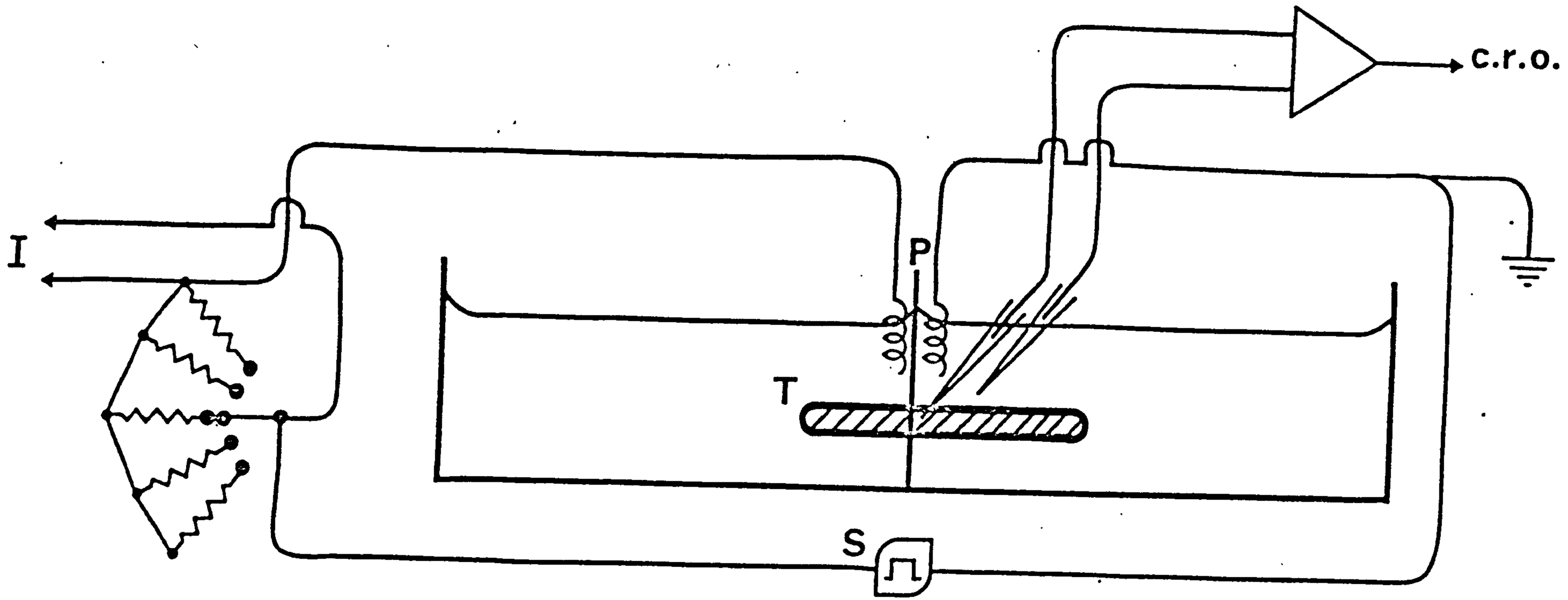
c.r.o.
I
P
T
S

For measurement of the space constant and membrane time constant, anodal subthreshold pulses were passed through the stimulating electrodes and recorded intracellularly at various distances from the partition. The first intracellular penetration was nearest the partition and the distance was measured under the binocular microscope. Subsequent movements used the micrometers on the micromanipulators to measure the distance moved by the microelectrodes. The membrane time constant was measured from the rising phases of the same electrotonic pulses as were used for measurement of the space constant.

An I.E.C. model F54/A function generator was used to pass alternating current through the AgAgCl electrodes.

The conduction velocity was measured by means of two intracellular microelectrodes a measured distance apart. The procedure is shown in figure 5. Two microelectrodes were placed in the trabecula so that identical resting potentials were recorded and a suprathreshold stimulus given. The delay in the rising phase of the action potential depended on the distance from the partition. The difference in delay was measured by the time taken to reach 50% of V_{max} of each upstroke; and the surface distance between the two microelectrodes was measured under 50-fold magnification with a binocular microscope.

These experiments were performed mainly at 16.5°C, but when the temperature deviated from this value figure 3 of Heintzen (1954), which showed a linear dependance of conduction velocity with temperature between 3°C and 27°C, was used to correct this value.

Figure 5 Measurement of the conduction velocity, θ. The record shows the rising phases of a propagated action potential by two microelectrodes a fixed distance apart. The delay, d, was measured at the point when the voltage was 50% of V_{max}. The upper horizontal line is the zero potential level - the higher line on the extreme left is the end of a calibration pulse. Experiment performed at 16.5°C in 0.1 mM Ca^{2+} Ringer.

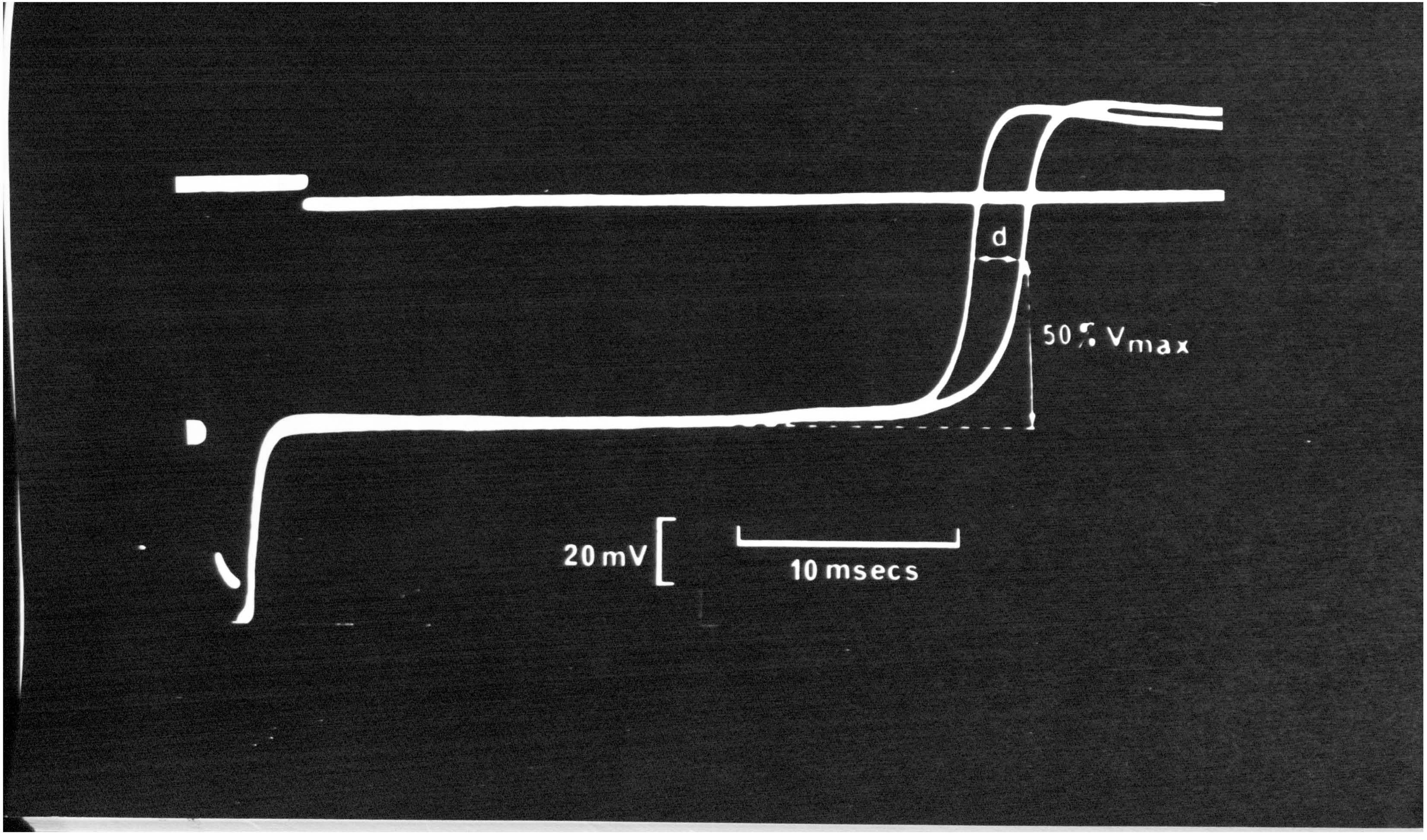
d
50% Vmax
20 mV
10 msecs

The same action potentials were used for measurement of the time constant from the foot of the action potential. The base of the action potential shows an exponentially rising phase with time before the faster regenerative. A semi-logarithmic plot of this phase was made and the time constant calculated from the slope of the resulting straight line.

Longitudinal Impedance Measurements

Measurement of the longitudinal impedance was attempted by placing a trabecula under oil, except for the two end regions, which were bathed in Ringer, where current crossed and re-crossed the cell membrane (see the theory section of the results for a fuller discussion of the various models).

The chamber was a modification of that used for measurement of the space constant. Two rubber partitions separated the dish into three chambers, the width of the middle chamber being adjusted by Perspex spacers - usually to about 5 mm. Holes were made in the rubber partition by a blunt microelectrode and the preparation was pulled through them from the central chamber, so that about 0.5-1 mm protruded into each chamber. With the preparation in place, the central chamber was drained of Ringer, the surface of the trabecula smeared with Vaseline where it entered the holes in the partitions and then filled with paraffin oil. Any leakage of Ringer into the central chamber could be recognised as the Ringer-paraffin oil interface could be observed easily, and such preparations had to be rejected. These manoeuvres should have kept the extracellular shunt between the two outer chambers to a minimum.

For impedance measurements, a platinum black electrode was placed in each outer chamber and connected to one arm of a Wien bridge (Wayne-Kerr Autobalance Universal Bridge, B642).

The manufacture of the platinum black electrodes was critical in that imperfect electrodes could have properties that masked those due to the muscle. The electrodes were made from 28 s.w.g. platinum wire, the terminal half centimetre of which was flattened out in a vice to form an electrode with dimensions 5 x 2 mm and 200 μ in thickness. The flattened portion was then thoroughly cleansed by rubbing with emery paper and immersion in concentrated nitric acid for 30 minutes. This had the dual effect of cleaning the electrode and increasing the surface area by producing surface irregularities which seemed to aid in the deposition of the platinum black. The unflattened portion of the wire was then encased in a glass micropipette and sealed with Araldite so as to reduce the capacitance between the two electrodes.

The electrodes were plated by passing current through Kohlrausch's solution (3% $PtCl_4$.HCl + 0.025% PbAcetate) using the electrode as the cathode and platinum as an anode to avoid poisoning of the solution. The best results were achieved if the electrodes were first plated quickly by passing a large d.c. current of 30 mA cm^{-2} for about five minutes, which gave a loose, irregular, coarse-grained coating. This was then scraped off with clean, blunt forceps and the plating recommenced with less current to form a smooth black coating.

For the slower plating, 1.8 mA were passed through the Kohlrausch solution for 45-60 minutes, giving a current density

of 9 mA cm^{-2} for 45-60 minutes or 24-32 coulombs cm^{-2}. This amount of current, which reduced the electrode impedance to a minimum, was arrived at by trial and error but closely agreed with the value suggested by Schwan (1963) of 10 mA cm^{-2} or 30 coulombs cm^{-2}.

An alternative way of plating was to use square pulses of current at a frequency of 1 kHz at a voltage of 100V peak-to-peak (from the calibrator of the 565 Tektronix oscilloscope) through a 5-10 kΩ resistor. This had the advantage that the plating procedure could be continuously monitored. By connecting the electrode to the oscilloscope amplifier, the effect of the electrode impedance on the square pulse could be observed. When the electrode was unplated, it had a large impedance and the square wave had a slow rise superimposed upon an instantaneous potential jump. As the impedance was reduced this time-dependant portion was reduced and plating was considered complete when the pulses were square.

The electrode impedance, in terms of a parallel resistance and capacitance, was measured both before and after plating over a range of frequencies from 400 Hz to 4 kHz, as can be seen in figure 17 in the results chapter. The resistance was not reduced by a great amount but the capacitance had to increase by at least two orders of magnitude before the electrode was considered usable (an increase in capacitance is equivalent to decrease in impedance). During the course of a week, the capacitance was observed to decrease some ten-fold so that the same electrodes were not used for longer than five days, after which the platinum black was cleaned off and the electrodes replated. When not in use, the electrodes were kept under distilled water and short-circuited.

For taking impedance measurements of the electrodes or the sample over a range of frequencies an external oscillator had to be used because the bridge operated at a fixed frequency of 1591.5 Hz. For taking readings, an input voltage of less than 0.3 volts r.m.s. was used because at frequencies less than 30 Hz or greater than 60 kHz such a voltage may have caused damage to the instrument. In practise, with the sample in place, it was difficult to balance the bridge adequately below 60 Hz. With the preparation in place readings were generally taken over the range 80 Hz to 40 kHz. For similar reasons of balance electrode polarization readings were taken over the range 400 Hz to 4 kHz. Polarization values at lower or higher frequencies were extrapolated from a conductance (or capacitance) versus $\log_{10}$frequency plot which generally described a straight line.

It should be noted that the polarization capacitance and resistance are considered to lie in series but the bridge reads the values as if they are in parallel. Thus, to obtain the true values the following relationships were used.

$$R_p = 1 / [\, G(1 + Q^2)] \qquad 40)$$

$$C_p = C (1 + 1/Q^2) \qquad 41)$$

where R_p and C_p are the polarization resistance and capacitance of the electrodes and G and C are the values obtained trom the Wien bridge - G (conductance) being the reciprocal of R (resistance). The constant Q has a value of $\omega C/G$ - where ω is the radial frequency of measurement.

With the preparation in place, drift was usually serious enough to necessitate compensation. Thus, an initial reading at the internal source frequency was taken at time zero and then after each reading at another frequency a reading at the internal source frequency was again taken, the time of each reading being noted. Thus, the true values of the conductance and capacitance could be calculated. The source of drift was difficult to ascertain but could have been due to the height of liquid in the outer chambers or heating of the preparation due to current flow. The latter may have accounted for the small steady drift but sudden changes in drift corresponded to sudden leaks of fluid from the outer chambers.

The preparation was cut from the central chamber after completion of the readings, leaving the holes in the partitions occluded. The resulting measured capacitance, C_x, was that between the two electrodes and the minute conductance due to the shunt through the paraffin oil - the latter was always negligible.

Calculation of results: To calculate the impedance of the specimen, the electrode resistance and capacitance were subtracted from the total measured values by use of the network shown below.

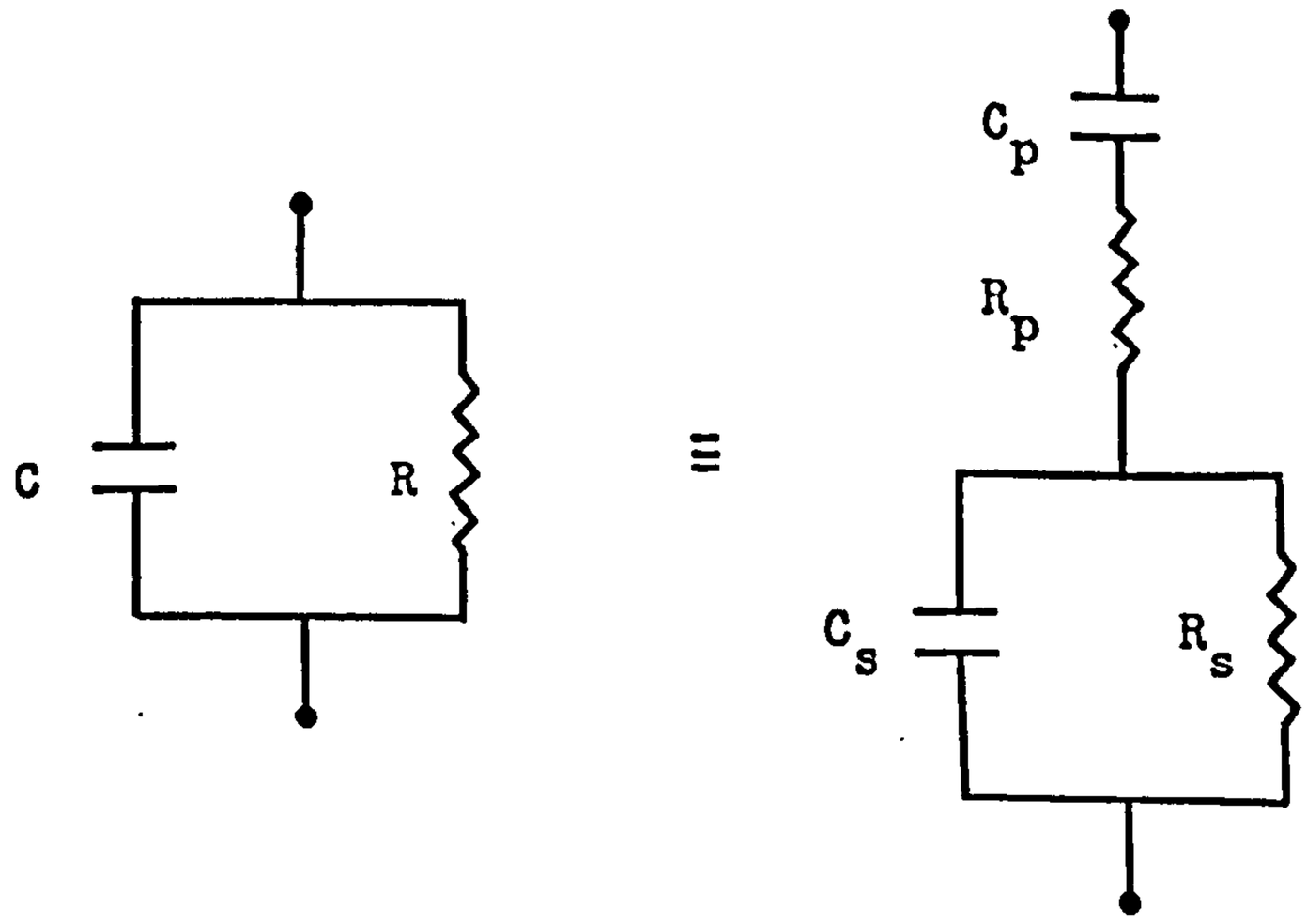

such that:

$$R = \left[1 + (R\omega C)^2\right]\left[R_p + \frac{R_s}{1+(R_s\omega C_s)^2}\right] \qquad 42)$$

and

$$\frac{1}{\omega C} = \left[1 + \frac{1}{(R\omega C)^2}\right]\left[\frac{1}{\omega C_p} + \frac{1/\omega C_s}{1+(1/R_s\omega C_s)^2}\right] \qquad 43)$$

where the subscript p refers to the polarization (electrode) values and s refers to the sample values. The unsubscripted values are those taken directly from the bridge. (The terminology of subscripts is unfortunate and misleading, especially as regards the series resistance, R_s, of voltage-clamp data, and care must be taken not to confuse the two values: however, these subscripts will be adhered to as they appear in much of the impedance work). $\omega = 2\pi$ times the frequency (f) in Hz.

If $R\omega C < 1$ and $R_p < R_s$ which was always observed in the experimental situation, then eq. 42) and 43) can be approximated by

$$R = R_s + R_p \quad \text{or} \quad R_s = R - R_p \qquad 44)$$

$$C_s = C - 1/\omega^2 R^2 C_p \qquad 45)$$

Finally, the interelectrode capacitance, C_x, was subtracted from C_s as the two were assumed to lie in parallel.

The impedance, Z, of a system can be expressed by

$$Z = (R + jX) \qquad 46)$$

where R is the resistance and X the reactance. The reactance of a capacitor is $-1/\omega C$ so that the admittance, Y, (=1/Z) can be written as,

$$Y = (G + j\omega C) \qquad 47)$$

Thus, to obtain the impedance values of the muscle, the measured values of C_s and G_s were converted to R and -X values by the relations,

$$R = \frac{G}{G^2+(\omega C)^2} \quad ; \quad -X = \frac{\omega C}{G^2+(\omega C)^2} \qquad 48)$$

These values could then be expressed in the form of an R versus -X plot which gives a locus for every separate time constant. The results were then manipulated to fit the most suitable network model that describes the behaviour of the system as will be shown in the results chapter.

Intracellular Stimulation

Two independant microelectrodes were used, one to inject current into the cell and the other to record the electrotonic potential at various interelectrode distances. The current electrode was filled with 2M potassium citrate and the amount of current passed was controlled by a suitable guard resistor of 2 kMΩ-550 MΩ.

For reasons discussed in the results chapter, the angle which the two microelectrodes made with the vertical was zero degrees. It was found easier if one microelectrode penetrated a cell first and was left for a few seconds to stabilize itself. The second microelectrode was then advanced and a penetration attempted. This usually dislodged the first microelectrode but the number of penetrations achieved in this way was greater than if both microelectrodes were simultaneously advanced.

The criteria for successful penetrations had to be more rigorous than for extracellular stimulation. On recording a resting potential of 75 mV or more from both microelectrodes the system was left for at least 15 seconds so that both recorded resting potentials were stable. If action potentials could be recorded through both

microelectrodes with extracellular stimulation then - if the latter procedure did not dislodge the microelectrodes - readings were taken by passing 200 msec square pulses down the potassium citrate microelectrode. After taking measurements of the electrotonic interaction, if any, the distance between the two microelectrode tips was measured as shown by figure 6.

The measurable parameters were the angles the microelectrodes made with the horizontal (θ' and θ''), the two distances x' and x" - which could be read from the micromanipulator calibrators - and the surface distance, y, between the two microelectrodes. θ' and θ'' were estimated by measuring the geometric relations the micromanipulator microelectrode holders made with the horizontal. The difficulty with measuring x' and x" was knowing when the microelectrodes were at the surface of the trabecula. This was estimated by noting the calibration reading with the microelectrode intracellular and then withdrawing it completely from the trabecula. The microelectrode was then slowly advanced towards the trabecula until small voltage deflexions were seen. This was taken to mean that the microelectrode was at the surface of the trabecula. The distance, y, was measured under 50-fold magnification, using a calibrated eyepiece graticule. The estimated error in measurement of x and y was about 5μ in each case.

Figure 6 The geometrical relationships used to find the distance between the two microelectrode tips. The microelectrodes are represented by the lines x' and x'' so that the interelectrode distance is AB. The horizontal line, y, is the surface of the trabecula. Measurment of x', x'', y, θ' and θ'' are as described in the text.

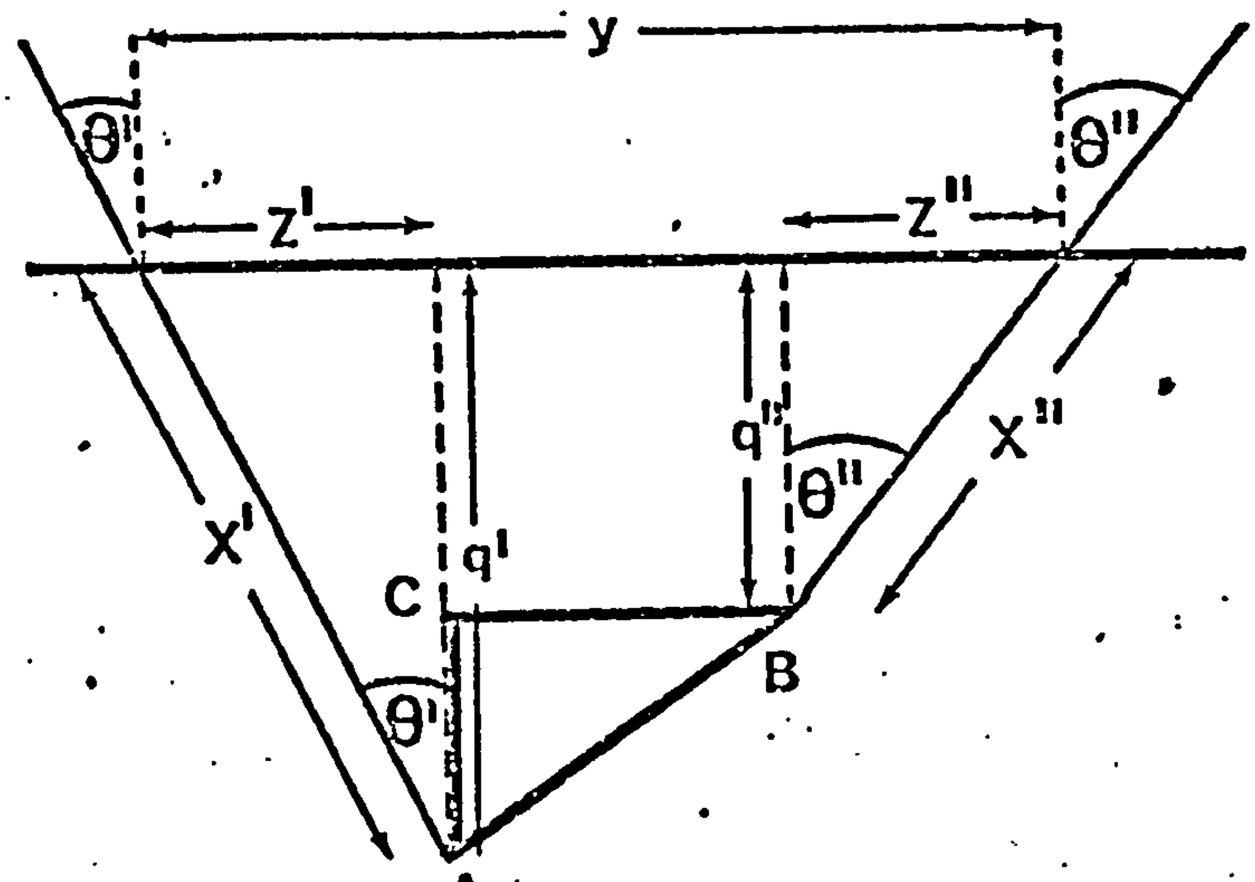

$$AB = \sqrt{BC^2 + AC^2}$$

$$\sin\theta' = z'/x' \qquad z' = \sin\theta'.x' \qquad BC = y - (z' + z'')$$

$$\sin\theta'' = z''/x'' \qquad z'' = \sin\theta''.x''$$

$$\cos\theta' = q'/x' \qquad q' = \cos\theta'.x' \qquad AC = q' - q''$$

$$\cos\theta'' = q''/x'' \qquad q'' = \cos\theta''.x''$$

$$\therefore AB = \left[(y - [\sin\theta'.x' + \sin\theta''.x'']\right)^2 + [\cos\theta'.x' - \cos\theta''.x'']^2\Big]^{1/2}$$

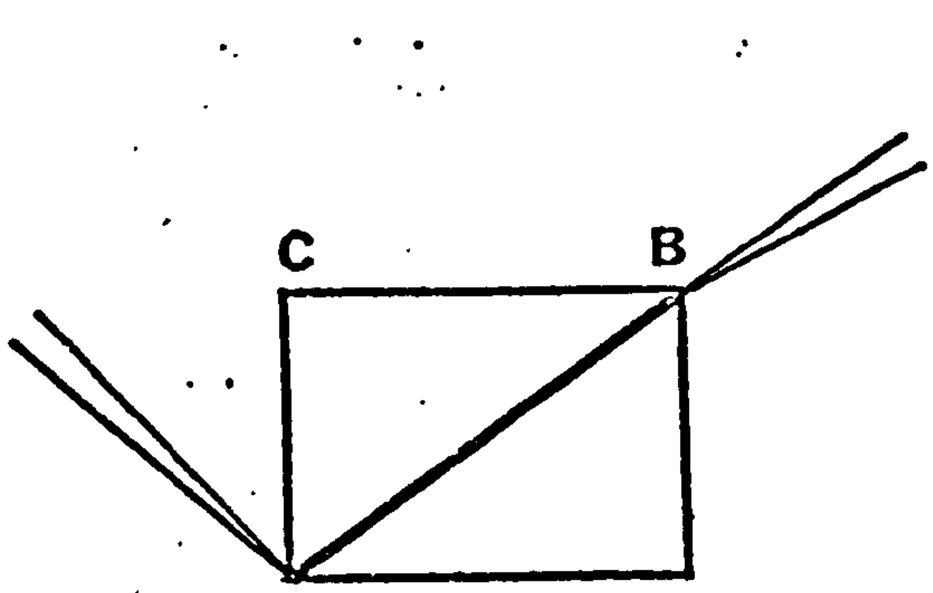

2-Dimensional case

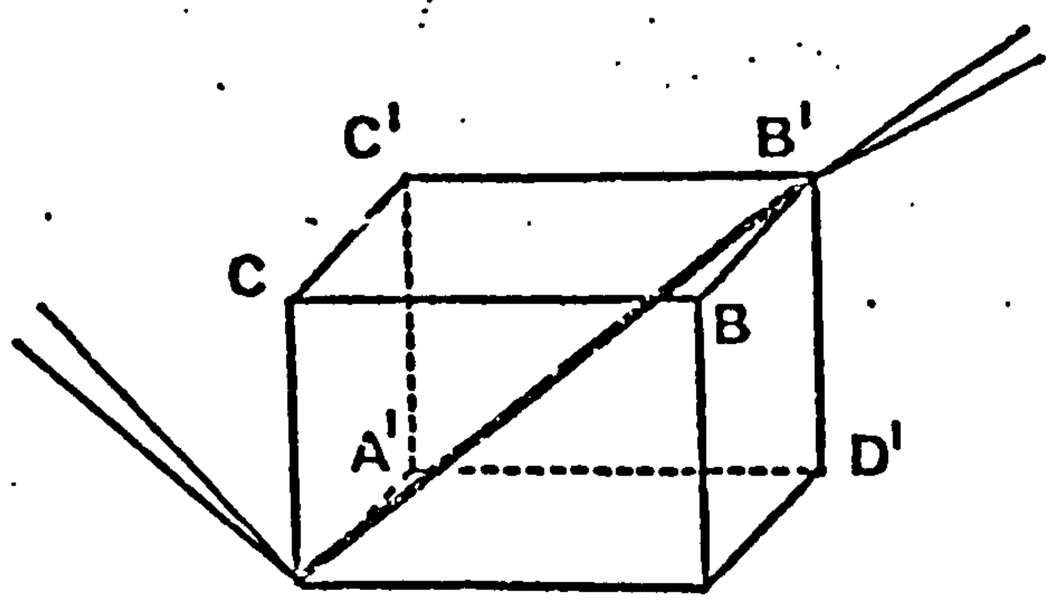

3-Dimensional case

$$\therefore AB' = (AA'^2 + AD^2 + AC^2)^{1/2}$$

$$\text{or,} \quad AB' = (AA'^2 + AB^2)^{1/2}$$

RESULTS

Measurement of the Cytoplasmic Resistivity, R_c

3 M, 1 M and 0.3 M KCl-filled microelectrodes were tried in these experiments. The microelectrodes filled with the lower electrolyte concentrations - i.e. 0.3 M and 1 M KCl-filled - had the advantage that they had a larger resistance and showed greater resistance changes when the external resistivity was changed. This reduced the contribution of the input resistance with the intracellularly determined value of R_{EL}. However, due to the arrangement of measuring R_{EL} - i.e. with R_{EL} in parallel with a 20 MΩ resistor - changes in R_{EL} were more difficult to measure with these electrodes. The 0.3 M KCl-filled microelectrodes also proved to be unreliable in having variable resistances throughout the course of an experiment so their use was abandoned.

Figure 7 shows examples of calibration curves of the three types of microelectrodes tested. As can be seen, a non-linear relationship exists between R_{EL} and the resistivity of the calibrating solution (R_{ext}). However, if R_{EL} is plotted against the logarithm of R_{ext} an approximately straight-line relationship is seen. Figure 8 shows a plot of R_{EL} versus R_{ext}, the latter on a logarithmic scale. With some microelectrodes the latter type of plot was slightly curvilinear, R_{EL} decreasing more than would be expected at higher concentrations of calibrating solutions.

For a successful experiment several criteria had to be fulfilled, which is best seen with reference to table 3. Firstly, it was necessary that R_{EL} measured in the Ringer surrounding the trabecula was the same before and after penetration of the cells. Any decrease

Figure 7 Calibration curves of microelectrodes used for the determination of the cytoplasmic resistivity. The microelectrodes were placed in solutions of differing resistivity (R_{ext}) and the microelectrode resistance (R_{EL}) measured as described in the methods section.

The three panels show examples of calibration curves from the three microelectrode types tested, filled with 3M, 1M and 0.3M KCl.

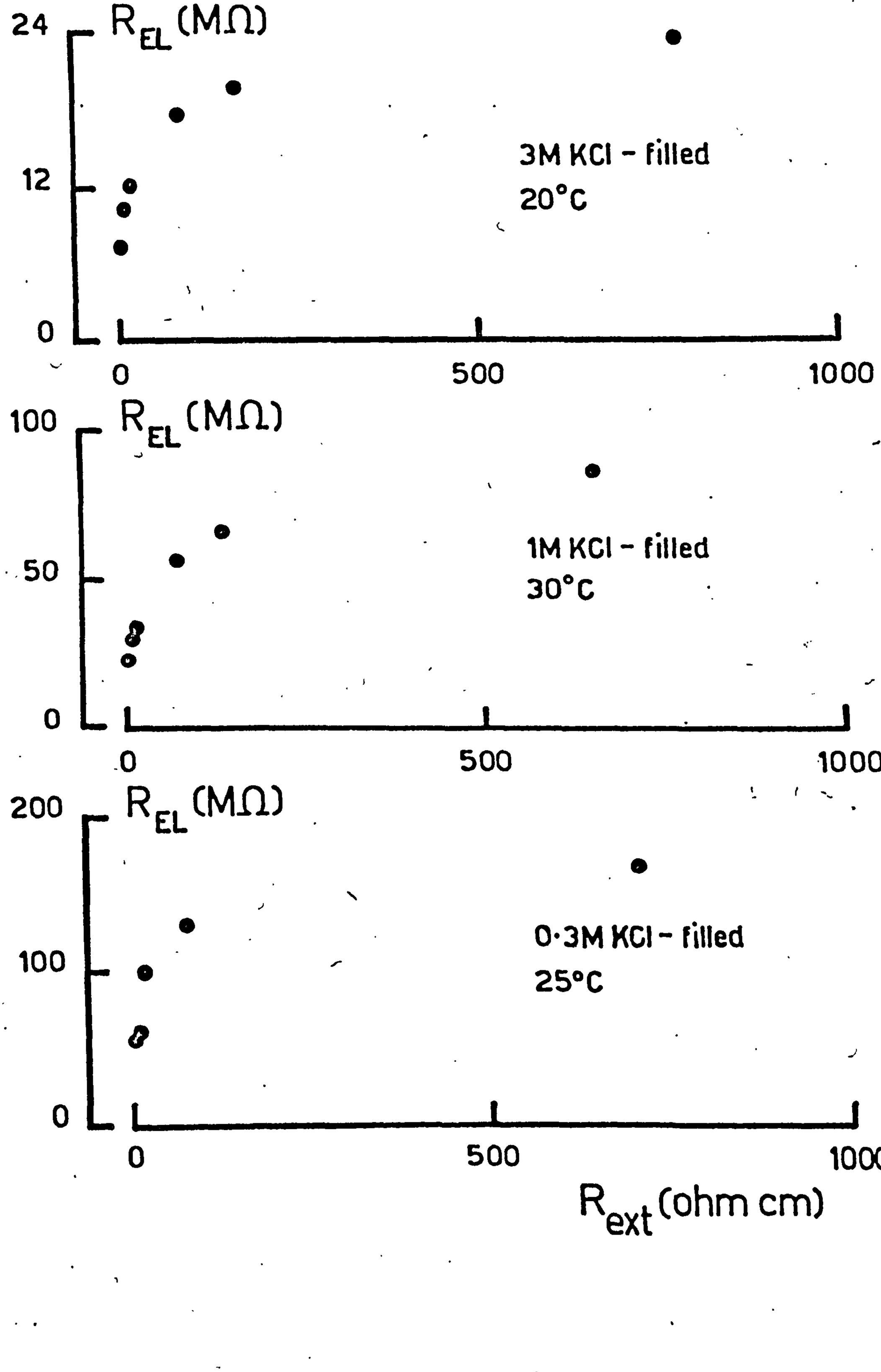
24
R_{EL} (MΩ)
12
0
0
500
1000
3M KCl - filled
20°C
100
R_{EL} (MΩ)
50
0
0
500
1000
1M KCl - filled
30°C
200
R_{EL} (MΩ)
100
0
0
500
1000
0·3M KCl - filled
25°C
R_{ext} (ohm cm)

Figure 8 A semilogarithmic plot of the microelectrode calibration curves used for the determination of the cytoplasmic resistivity. The microelectrode resistance (R_{EL}) is plotted against the resistivity of the bathing solution (R_{ext}), the latter on a logarithmic (to the base 10) scale. The data from the same three microelectrodes as shown in figure 7 is used.

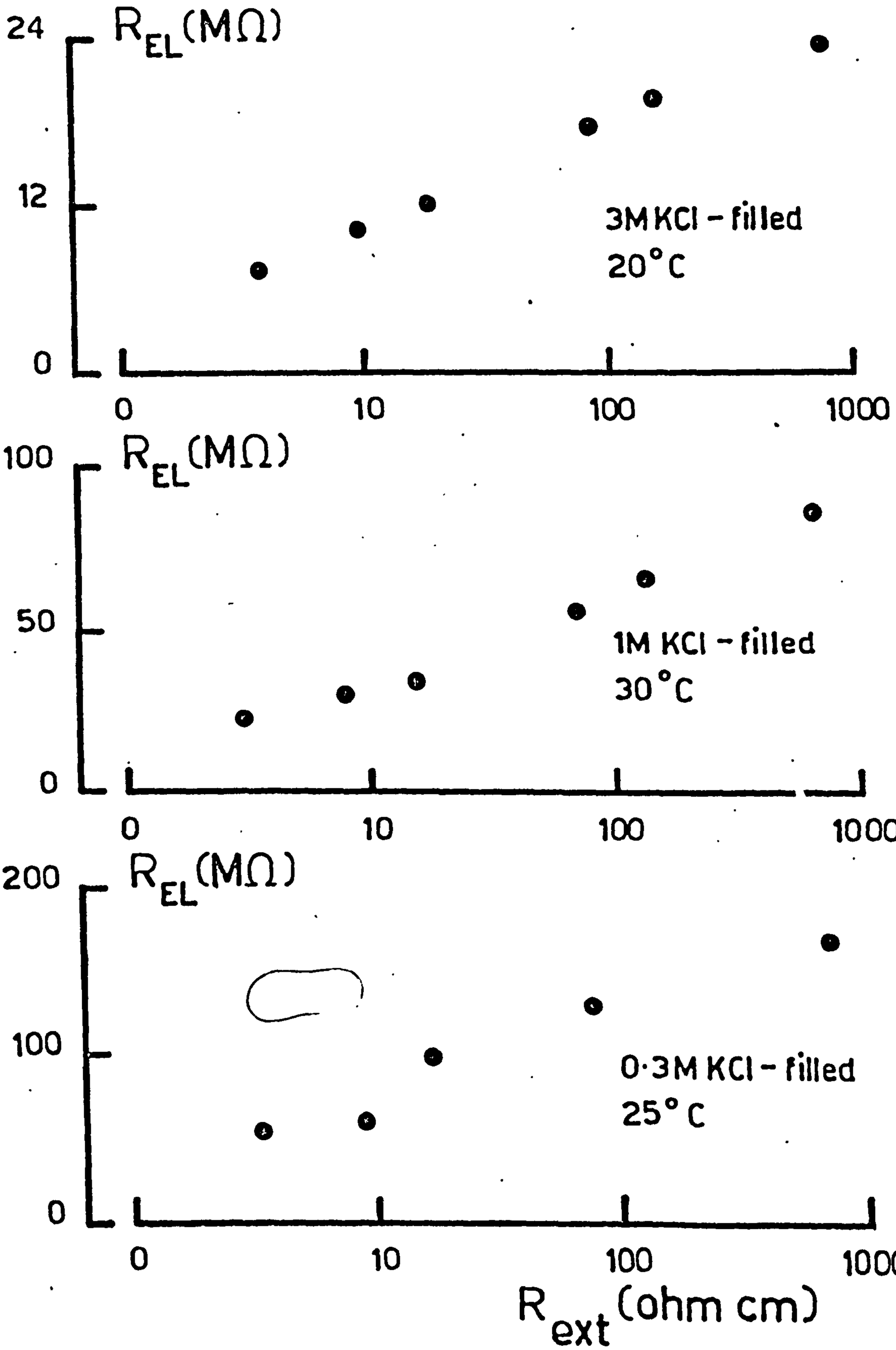
24
$R_{EL}(M\Omega)$
12
0
3M KCl – filled
20°C
0
10
100
1000
100
$R_{EL}(M\Omega)$
50
0
1M KCl – filled
30°C
0
10
100
1000
200
$R_{EL}(M\Omega)$
100
0
0·3M KCl – filled
25°C
0
10
100
1000
R_{ext} (ohm cm)

Table 3 Experimental Procedure for the Measurement of the Cytoplasmic Resistivity

Microelectrode position	R_{EL} (MΩ)	R_{inp} (MΩ)	R_{EL} (MΩ)(cor.)*	R_c (ohm cm)	R_{KCl} (ohm cm)
Ringer surrounding trabecula	10.9				
Intracellular	13.2	0.3	12.9	220	
	13.2	0.3	12.9	220	
	12.6	0.3	12.3	170	
	13.2	0.3	12.9	220	
	13.7	0.3	13.4	280	
Ringer surrounding trabecula	10.9				
Ringer	10.9				
10 mM KCl	15.8				782
50 mM KCl	14.2				116
100 mM KCl	11.2				86
500 mM KCl	7.3				18.7
1 M KCl	6.0				9.6
3 M KCl	4.6				3.7
Ringer	10.9				

* R_{EL} (cor.) = $R_{EL} - R_{inp}$

Electrode 38: 3 M KCl-filled microelectrode. Accuracy of R_{EL} determination to ± 0.2 MΩ.
Temperature 20°C.

Cytoplasmic Resistivity: 222 ± 39 ohm cm.

Table 4 Anomalous values of R_{EL} obtained during the determination of the Cytoplasmic Resistivity

Part 1 Electrode 41		Part 2 Electrode 26		Part 3 Electrode 20	
Microelectrode position	R_{EL} (MΩ)	Microelectrode position	R_{EL} (MΩ)	Microelectrode position	R_{EL} (MΩ)
Ringer surrounding trabecula	14.5	Ringer surrounding trabecula	18.2	Ringer surrounding trabecula	18.8
Intracellular	20.0	Intracellular	23.9	Intracellular	21.7
	20.0		25.6		22.4
	19.3		27.3		22.4
	18.6		25.6		22.8
	19.3		26.0		23.1
	20.0		36.1		23.9
Ringer surrounding trabecula	18.0		37.2	Ringer surrounding trabecula	17.9
			39.3	Ringer	9.7
		Ringer surrounding trabecula	21.0	10 mM KCl	15.4
				50 mM KCl	10.4
				100 mM KCl	8.5
				500 mM KCl	5.1
				1 M KCl	4.1
				3 M KCl	2.6
				Ringer	9.7

would indicate some breakage of the microelectrode tip and any increase would indicate some blockage of the tip. With some microelectrodes the intracellularly determined value of R_{EL} showed a gradual increase throughout the course of an experiment and this also would indicate some blockage of the microelectrode tip, presumably by intracellular components. Parts 1 and 2 of table 4 show two microelectrodes where such a tip blockage was indicated. In the first part the intracellular values of R_{EL} show no significant trend. Microelectrodes giving such results could not be used to determine the cytoplasmic resistivity.

After such extracellular and intracellular measurements a calibration curve was constructed by placing the microelectrode in a small volume - 10 ml - of KCl standard solutions and measuring R_{EL}. Before and after such a run R_{EL} was measured in a similar volume of Ringer. If these values - termed 'Ringer' in the microelectrode position column of tables 3 and 4 - were the same as the value obtained in the Ringer bathing the trabecula - termed 'Ringer surrounding trabecula' in tables 3 and 4 - the calibration curve was used. In a number of cases the value of R_{EL} as measured in a beaker of Ringer was less than the value measured in the extracellular medium. Such results were obtained in early experiments when a large volume of Ringer and calibrating solutions - about 50 ml - was used to construct the calibration curve. Subsequent calibrations were carried out in 10 ml of the solution, about the same volume as the dish in which the trabecula was fixed. The explanation for this phenomenon is not clear, but an example is shown in column 3 of table 4.

Table 5 Results for the determination of the Cytoplasmic Resistivity, R_c

Electrode no.	R_c (ohm cm)	Temperature (°C)	Electrode type
16	311 ± 71 (4)	30	1M KCl-filled
19	245 ± 117 (8)	30	1M KCl-filled
22	277 ± 54 (5)	30	1M KCl-filled
25	328 ± 90 (11)	30	1M KCl-filled
Mean	290 ± 37		
29	307 ± 80 (13)	16.5	1M KCl-filled
30	249 ± 134 (8)	16.5	1M KCl-filled
31	482 ± 67 (5)	16.5	1M KCl-filled
Mean	346 ± 121		
35	126 ± 28 (11)	25	3M KCl-filled
36	260 ± 63 (10)	25	3M KCl-filled
47	230 ± 42 (2)	25	3M KCl-filled
63	319 ± 105 (15)	25	3M KCl-filled
64	318 ± 38 (13)	25	3M KCl-filled
65	262 ± 58 (11)	25	3M KCl-filled
Mean	253 ± 71		
32	183 ± 35 (5)	20	3M KCl-filled
33	427 ± 0 (5)	20	3M KCl-filled
38	222 ± 39 (5)	20	3M KCl-filled
39	196 ± 29 (11)	20	3M KCl-filled
40	395 ± 93 (8)	20	3M KCl-filled
43	268 ± 56 (12)	20	3M KCl-filled
44	235 ± 98 (8)	20	3M KCl-filled
Mean	275 ± 97		
Mean of all results		282 ± 84	(23°C)
Mean of 1M KCl-filled electrodes		324 ± 80	(24°C)
Mean of 3M KCl-filled electrodes		265 ± 84	(22°C)
Mean of all results corrected to 16.5°C		346 ± 103	

The numbers in parenthesis refer to the number of penetrations made by that particular microelectrode. The results in the R_c column are thus the mean (± S.D.) R_c values calculated from the individual R_{EL} measurements.

It was also noted that the microelectrodes did not show any cation specificity - i.e. R_{EL} was the same in KCl and NaCl solutions of similar resistivity. This was not important for the determination of the cytoplasmic resistivity because KCl solutions were used to construct the calibration curves and K^+ ions are the predominant intracellular cation. Such specificity could be noted by comparing the R_{EL} values of Ringer and 100 mM KCl. Because the resistivities of 100 mM KCl and 117 mM NaCl (essentially Ringer) are similar any difference in the R_{EL} values would indicate some specificity.

The input resistance value used in these experiments was calculated from data using two microelectrodes less than 10 μ apart, one for passing current and the other for measuring the resulting change in membrane potential - see the section on intracellular stimulation for further analysis of these results. From the slope of the current-voltage relationship the input resistance was calculated. Figure 9 shows examples of two such determinations - in one both depolarizing and hyperpolarizing currents were passed whilst in the other only depolarizing currents were used. No rectification was apparent although in one of the curves (R_{inp} = 295 kΩ) higher currents elicited an action potential. From a total of 8 determinations a value of 320 kΩ (± 120 kΩ, S.D.) was obtained.

It was not possible to use the value of R_{inp} calculated from the cable equation

$$R_{inp} = (r_m \cdot r_i)^{1/2} \qquad 49)$$

because, as shown by George (1961), for a syncitial arrangement of cells - as can be assumed for frog ventricular myocardium - R_{inp} is

Figure 9 Two examples of the input resistance, R_{inp}, as measured by two intracellular microelectrodes, one for passing current, I ($\times 10^{-9}$ amp), and the other for measuring the resulting change in membrane potential, ΔV_m (mV). The two microelectrodes were less than 10μ apart as estimated by the protocol of figure 6, in the methods section.

In one experiment both hyperpolarizing and depolarizing currents were passed (filled circles) whilst in the other experiment only depolarizing currents were passed (filled squares).

Experiments were performed at 25°C and in 0.1 mM Ca^{2+} Ringer.

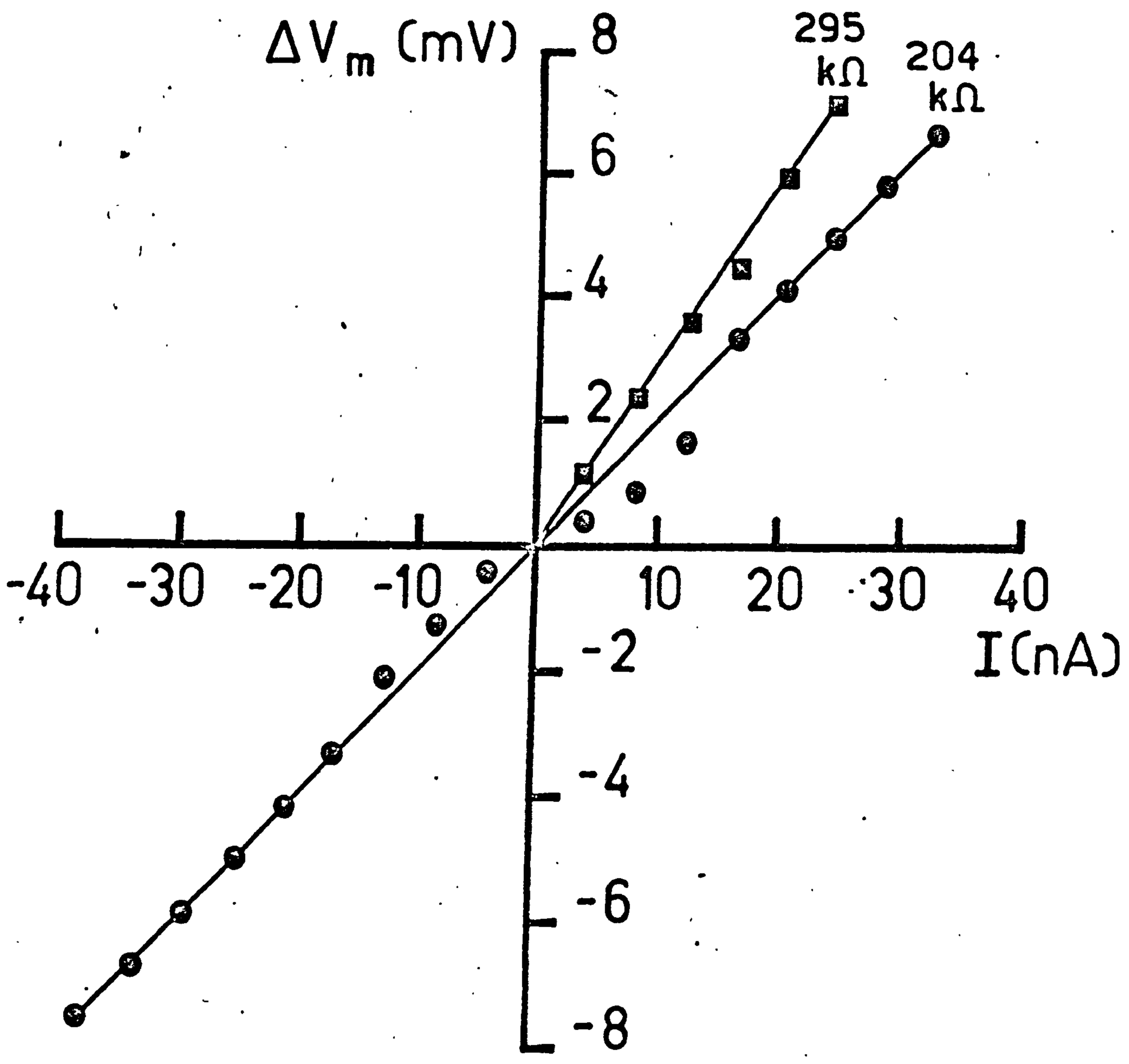
ΔVm (mV)
8
6
4
2
-2
-4
-6
-8
-40
-30
-20
-10
10
20
30
40
I(nA)
295
kΩ
204
kΩ

not proportional to $r_m^{0.5}$, but more nearly to $r_m^{0.25}$. This is seen to be evident in this tissue with the results presented in the intracellular stimulation section.

From such considerations the cytoplasmic resistivity was calculated for each microelectrode's data and the total results are seen in table 5. The results have been divided into sections depending on the type of microelectrode used - i.e. 1 M or 3 M KCl-filled - and the temperature of the determination.

Due to the large standard deviations in the mean results of each section there is no significant difference (at the $p = 0.05$ level) between them so that all of the data have been lumped together, giving a figure of $282 \pm 84\ \Omega$cm, at 23°C. To calculate the value at 16.5°C a Q_{10} value of 1.37, given by Hodgkin and Nakajima (1972) for the sarcoplasmic conductivity of skeletal muscle, was used, giving a value of $346 \pm 103\ \Omega$cm.

The Resistance to the Longitudinal Flow of Current, R_f

Figure 10 shows a typical set of intracellularly and extracellularly recorded action potentials from a tetrodotoxin-treated strip of ventricular myocardium, used for measuring the ratio of the intracellular to extracellular resistance.

One half of the preparation was perfused with tetrodotoxin (TTX)-containing Ringer for 15 minutes before recording was attempted. This was the time needed to inactivate a separate strip perfused wholly in TTX-Ringer as noted by the shortening of the action potential height and duration, similar to that observed by Hagiwara and Nakajima (1966).

Figure 10 An intracellularly and extracellularly recorded action potential used for the measurement of the resistance to the longitudinal flow of current. The numbers over each record refer to the two microelectrodes, via which the differential recording was made. Experiment performed at 20°C in 0·1 mM Ca^{2+} Ringer.

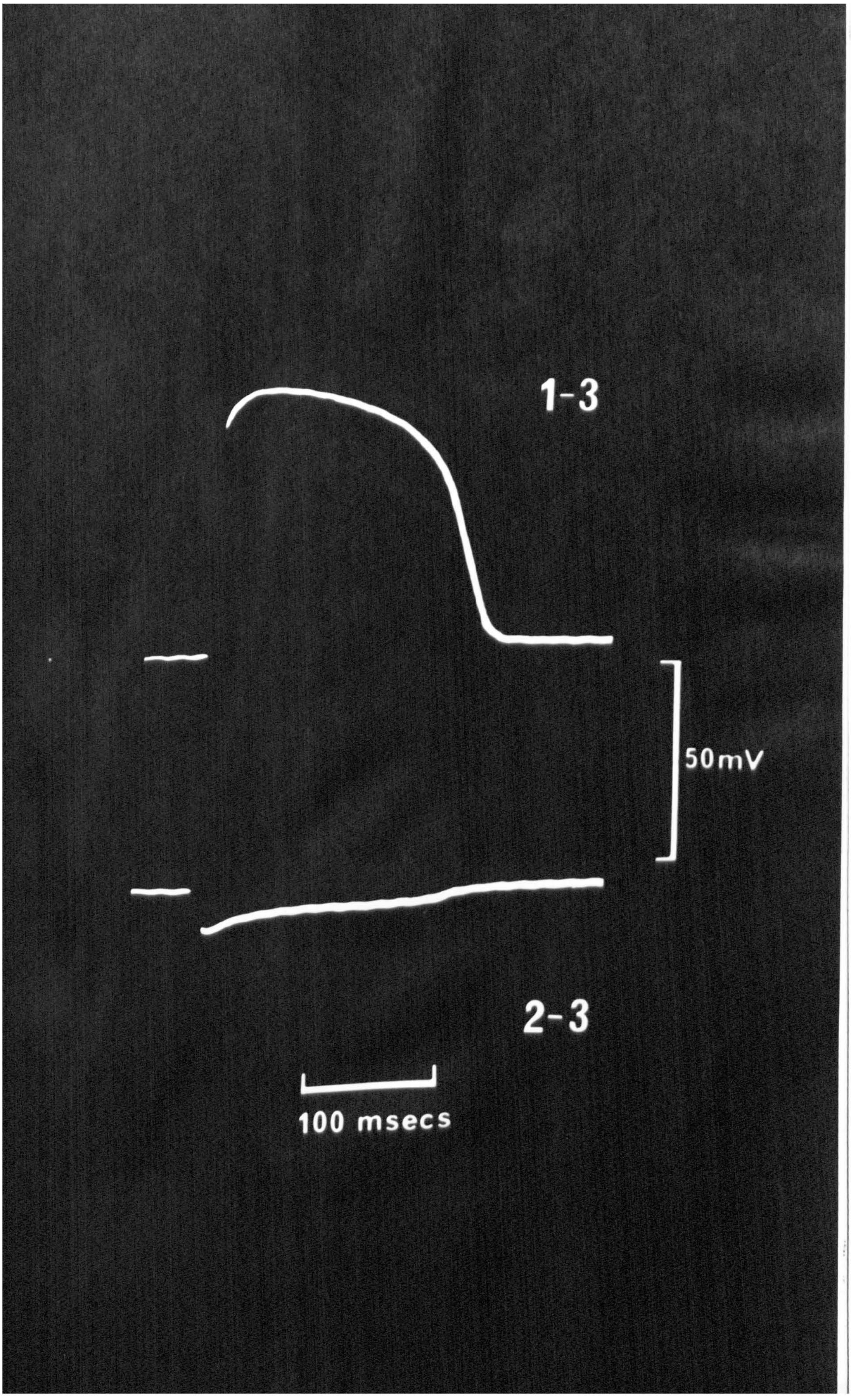
1-3
50mV
2-3
100 msecs

On several occasions a diphasic artifact was seen in the extracellular recording, as seen in figure 11. This was most likely due to propagation of the action potential into the TTX-treated part, so that the diphasic hump was due to the arrival of the action potential at the end of the strip. However, in this situation, the action potential would be expected to propagate quite slowly so that the initial high potential peak would be essentially unaffected by such an invasion. Thus, in these situations, the initial peak was taken as the extracellular action potential height.

From nine experiments a figure for the ratio of 6.70 (S.E. 1.09) was obtained, see table 6 for details.

To obtain the specific resistance it is necessary to know the relative cross-sectional areas occupied by each resistive component. A figure of 25% was used for the extracellular space of frog ventricular strips. This was calculated on the basis of data given by Niedergerke (1963) based on the inulin space and an assumed density of 1.05 for ventricular tissue.

However, in this experimental situation, there was a layer of Ringer of significant thickness surrounding the trabecula, which would contribute to the total extracellular pathway. This layer was measured with a binocular microscope under 50-fold magnification and, in general, was of the order of 100 μ - complete details are given in table 6. This method of measurement was convenient as the Ringer-paraffin oil interface could be observed easily due to their different refractive indices. This layer increased the extracellular space to about 44%, on average, of the total cross-sectional

Figure 11 An example of a diphasic hump in the extracellularly recorded action potential - bottom recording - due to the slow propagation of the action potential in the TTX treated portion of the strip. The horizontal line in each record refers to the zero potential level. Experiment performed at 20°C in 0·1 mM Ca^{2+} Ringer.

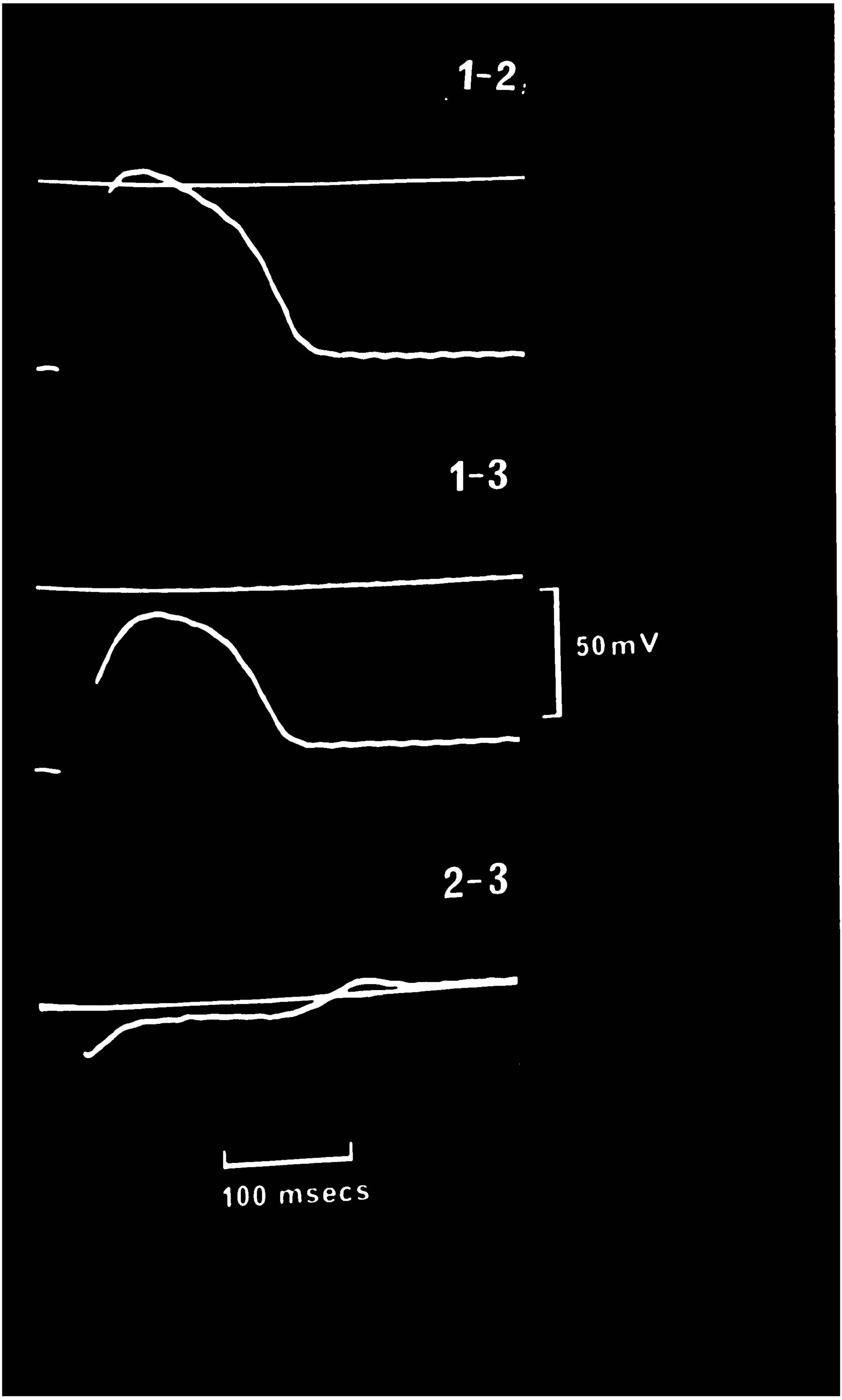
1-2
1-3
50 mV
2-3
100 msecs

Figure 11 An example of a diphasic hump in the extracellularly recorded action potential - bottom recording - due to the slow propagation of the action potential in the TTX treated portion of the strip. The horizontal line in each record refers to the zero potential level. Experiment performed at 20°C in 0·1 mM Ca^{2+} Ringer.

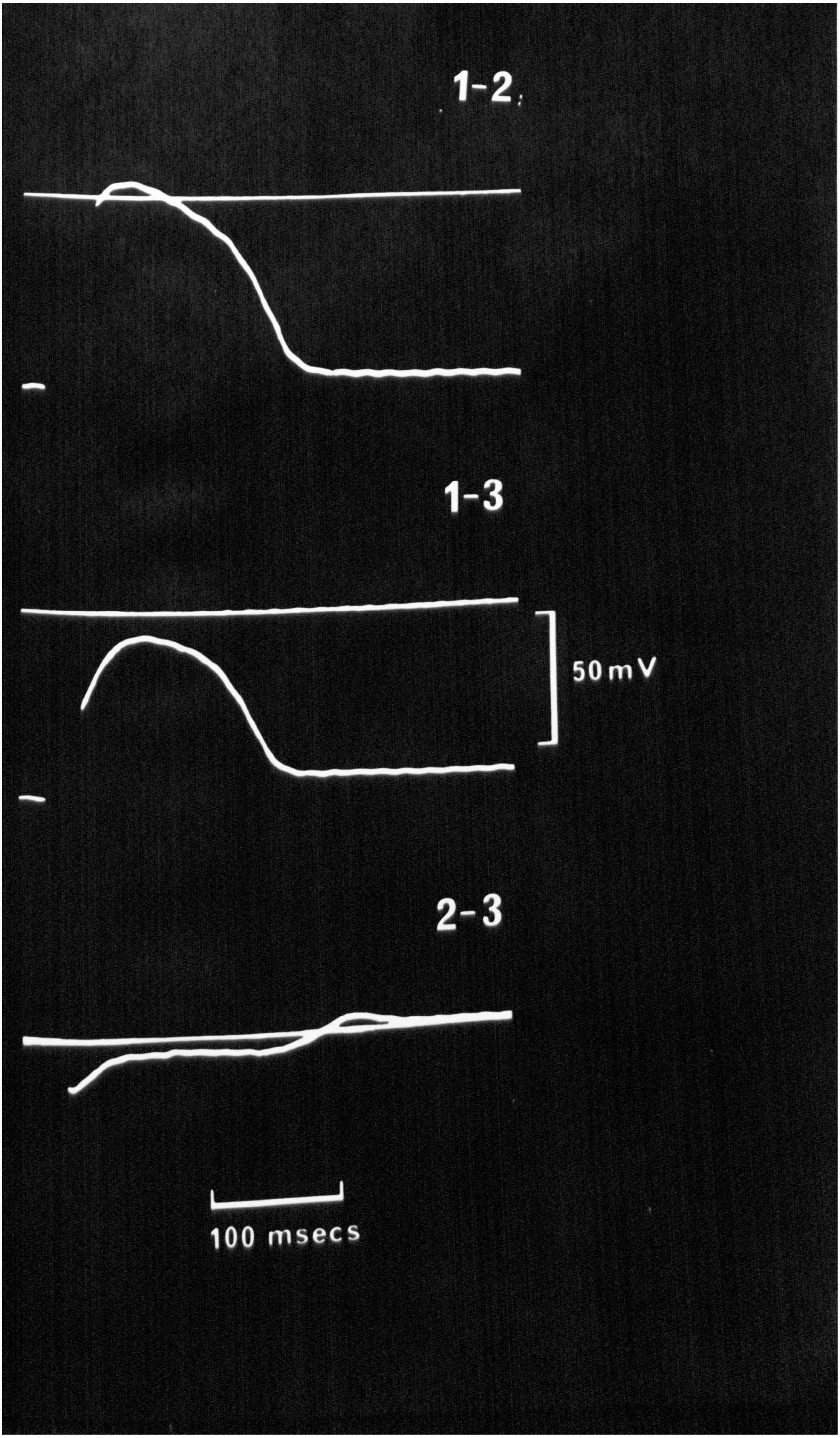
1-2
1-3
50 mV
2-3
100 msecs

Table 6 Experimental Data for the Determination of R_f

Experiment no.	$(A.p.)_i/(A.p.)_o$ *	Strip diameter (mm)	Fluid layer thickness (mm)	%age extracellular§ space
1	6.71 ± 0.10 (4)	1.82	0.13	42
2	6.20 ± 0.00 (3)	1.70	0.10	39
3	4.69 ± 0.44 (4)	1.50	0.11	42
4	6.55 ± 1.23 (9)	1.12	0.09	44
5	8.60 (1)	1.00	0.09	45
6	7.31 ± 0.30 (9)	1.00	0.10	44
7	6.55 ± 0.21 (2)	1.04	0.09	45
8	7.59 ± 0.46 (14)	0.90	0.09	47
9	6.12 ± 0.43 (9)	0.94	0.10	48
Mean ± S.E.	6.70 ± 1.09			44 ± 3

*R_f can be calculated from the ratio $(A.p.)_i/(A.p.)_o$ and the intracellular/extracellular space ratio, as described by equation 50) in the text.

§The extracellular space comprises the extracellular space within the trabecula and the fluid layer surrounding the trabecula - see text for details.

The numbers in parenthesis are the number of separate determinations in each experiment.

area, giving a ratio of intracellular to extracellular cross-sectional areas of 1.27 : 1 (56% : 44%).

From measurements with a conductivity bridge (M.E.L. type E7566/3) frog Ringer had a specific resistivity, R_o, of 69 Ω cm at 16.5°C. The bridge was calibrated with NaCl and KCl solutions of known resistivity and had a cell constant of 1.489 cm^{-1}.

Thus, from a knowledge of the specific resistivity of Ringer, the ratio of the intracellular and extracellular action potential heights and the relative cross-sectional areas of these spaces the specific longitudinal resistance was calculated as:

$$\frac{(A.p.)_i}{(A.p.)_o} = \frac{r_i}{r_o} = \frac{R_f \cdot a_o}{R_o \cdot a_i} \qquad 50)$$

where $(A.p.)_{i,o}$ are the intracellular and extracellular action potential heights and $a_{i,o}$ the cross-sectional areas of the spaces.

Thus, R_f was calculated to have a value of 588 Ω cm (± 95 Ω cm, S.E. 9 experiments).

The Specific Intercalated Disk Resistance, R_d

Interest in the resistance between cells stems mainly from the question as to whether the transmission of an impulse between contiguous cells is by an electrical process or by chemical means (i.e. a transmitter substance). The latter would be expected to show itself by a high resistance between adjacent cells, the former by a low resistance.

If the intracellular resistive pathway is considered to consist of the resistance of the cytoplasm in series with the junctional resistance between cells, the latter can be calculated from the preceding data. That is, subtraction of the cytoplasmic resistance

from the total intracellular resistance should give information about the junctional resistance. The term intercalated disk resistance is for convenience only and complies with the precedence set down by previous authors (Weidmann, 1966; Woodbury and Crill, 1970).

Calculation of the specific resistance of the junctional membrane requires a knowledge of the area occupied by such junctions. Three problems present themselves in the evaluation of such an area. Firstly, the intercalated disk cannot be presumed to be a flat structure lying perpendicular to the longitudinal axis of the cell. Many electron-microscopic studies with mammalian and amphibian intercalated disks (e.g. Sjöstrand, Andersson-Cedegren and Dewey, 1958) have shown that it has a highly convoluted structure. Secondly, not all of the intercalated disk may have a low electrical resistance and thirdly other regions apart from the intercalated disk may form low resistance pathways between cells - i.e. the desmosomes in amphibian ventricular myocardium (Grimley and Edwards, 1960). However, it will prove useful to calculate the intercalated disk resistance firstly by merely considering it as a uniform flat disk, lying perpendicular to the cell axis, to compare the result with values obtained from other studies using a similar criterion (Weidmann, 1966; Woodbury and Crill, 1970).

It is also essential to know the length of individual cardiac cells before any calculation concerning the specific disk properties can be made. Fabiato and Fabiato (1972) quote a figure of 15μ for the length of individual frog ventricular cells, separated by collagenase treatment. Similar collagenase treatment of rat heart was carried out in the present study with a view to finding a

unicellular cardiac preparation for voltage-clamping with two micro-electrodes. However, the cells were very difficult to impale and it seemed that they were in a slight state of contracture, which would underestimate the cell length. At the other extreme Barr, Dewey and Berger (1965) describe frog atrial cells as 175-200μ in length.

For seven species of mammal Marceau (1904) quotes a length/diameter ratio of about 8 and for two species of bird a value of 12.5. If a ratio of 10 is assumed for frog ventricular cells this gives a value of 50μ for the length of the cells. This value will thus be used in subsequent calculations of disk properties.

Thus, consider a centimetre cube of intracellular contents. The resistance between the two faces in the longitudinal axis will be 588Ω. A similar cube of cytoplasm will have a value of 346Ω. The remaining 242Ω will be due to intercalated disks. If there are 200 such disks per centimetre, 50μ apart, each disk will have a specific resistance of 1.2Ω cm^2.

A more reasonable procedure would be to calculate the relative surface area covered by desmosomes (assumed to be the low resistance junctions in the frog myocardium) - a measurement not yet achieved. Measurements of the desmosomal area in figures 2 and 4 of Staley and Benson (1968) and figure 1 of Sommer and Johnson (1969) which are (presumably random) longitudinal and transverse sections of ventricular trabeculae give a value of about 5% of the total cell membrane.

Thus, a 50μ long cylindrical cell, 2.5μ in radius, will contribute $242/(\pi a^2.200) = 6.2.10^6\Omega$ to the junctional resistance. If such a resistance is offered by 5% of the cell membrane area, the specific junctional resistance is calculated to be 2.4 Ωcm^2.

The Space Constant, λ

For measurement of the space constant, λ, hyperpolarizing pulses were passed down the trabecula, the size of the electrotonic potential decreasing with increasing distance from the partition. The decay of the steady-state amplitude along the trabecula is shown in figure 12A from which the space constant could be calculated as the distance along which the voltage drops to 1/e. This, of course, presumes that one-dimensional cable theory holds under these experimental conditions, which seems to be true because when the steady-state potential (on a logarithmic scale) is plotted against the distance from the stimulating partition the experimental points approximately fall on a straight line.

This series of experiments was performed over a period of two months on winter-conditioned frogs and it was noted that there was a drop in the average value of the space constant later in the series. The mean results ($\pm$ the standard error) obtained from frogs used on 11 separate days are shown in figure 13A. Day zero is the time when the series of experiments was begun, the frogs having been in captivity previous to this for several months, living at 4°C in a starved condition.

Statistically, the drop in the value of the space constant is not significant. Figure 13B shows the individual determinations from which figure 13A was constructed. The straight line is a least-squares best-fit line through the data points. The slope of the line is negative, with a drop of 2.6μ per day in the value of the space constant but the correlation coefficient has a value of only 0.39. However, it was found that on even later days it was necessary to add glucose to the Ringer to elicit normal electrical activity,

which is indicative of some deterioration in the state of the trabeculae - results obtained from such trabeculae were not used and the series of experiments terminated. In addition, if the fall in the value of the space constant was real this would be masked to some extent in that the frogs might be expected to begin their deterioration at different times, so that even to attempt to fit a straight line to the results would not be justifiable.

From the results shown in figure 13 the space constant was calculated to have a value of 328μ ($\pm$ 22μ , S.E. 11 experiments).

The Membrane Time Constant, τ_m

The transiently rising and falling tails of the electrotonic pulses, due to the discharging and charging of the membrane capacity, will have a time course dependant on the membrane resistance and capacitance. If the myocardium behaves as a one-dimensional cable then the measurement of the membrane time constant from these tails should be possible. Hodgkin and Rushton (1946) listed seven ways of measuring the membrane time constant. The two ways used in these experiments were to measure the half-value potential propagation, at a speed of $2\lambda/\tau_m$, and to fit the cable equation to the experimentally derived curves. The 'on' tails - i.e. the falling tail of the hyperpolarizing pulses - were used in both methods, although there is no reason in theory why the 'off' tails should have a different time course.

Figure 12B shows an example of the time taken for a pulse to reach 50% of the steady-state potential (V_{max}) plotted against the distance from the stimulating partition, giving a straight-line plot. Theory predicts that the slope of such a line has a value of $\tau_m/2\lambda$.

Figure 12 Experiment for the determination of the space constant, λ, and the membrane time constant, τ_m. Part A shows the decay of the steady-state electrotonic potential (mV) with increasing distance from the stimulating partition (note the logarithmic scale of the ordinate) for determination of λ. Part B shows the linear relationship between the time for the electrotonic pulse to reach $V_{max}/2$ and the distance from the stimulating partition. The slope of the line has a value of $\tau_m/2\lambda$. Part C shows tracings of the electrotonic pulses used to construct the curves of parts A and B. The points are obtained from equation 19 by inserting λ and τ_m as obtained above, at various distances, x, from the stimulating partition. The distances are expressed in terms of the dimensionless variable X (= x/λ).

Experiment was performed at 25°C and in 1 mM Ca^{2+} Ringer.

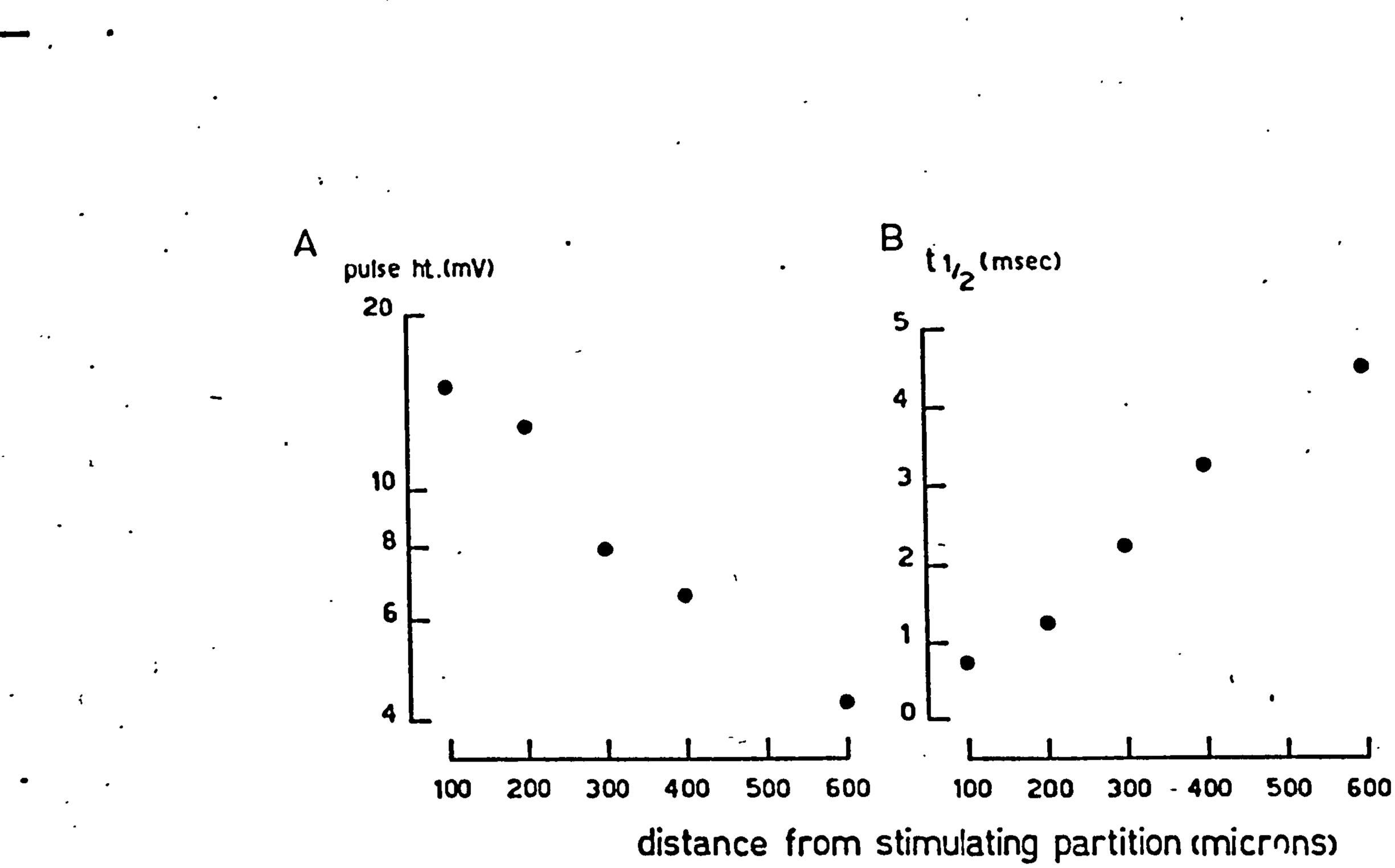
A
pulse ht.(mV)
20
10
8
6
4
B
t 1/2 (msec)
5
4
3
2
1
0
100 200 300 400 500 600
100 200 300 400 500 600
distance from stimulating partition (microns)
C
X = 0.27
X = 0.55
X = 0.80
X = 1.10
X = 1.60
5 mV
20 msec

Figure 13 Part A shows the mean value (± S.E.) of the space constant as the experimental series progressed. The figure above each mean value is the number of determinations made on that day. Part B shows the individual determinations of the space constant that have been used to construct part A. The straight line is a least-squares best-fit line through the points and has no special significance.

Experiments were performed at 20-25°C in 1 mM Ca^{2+} Ringer.

A

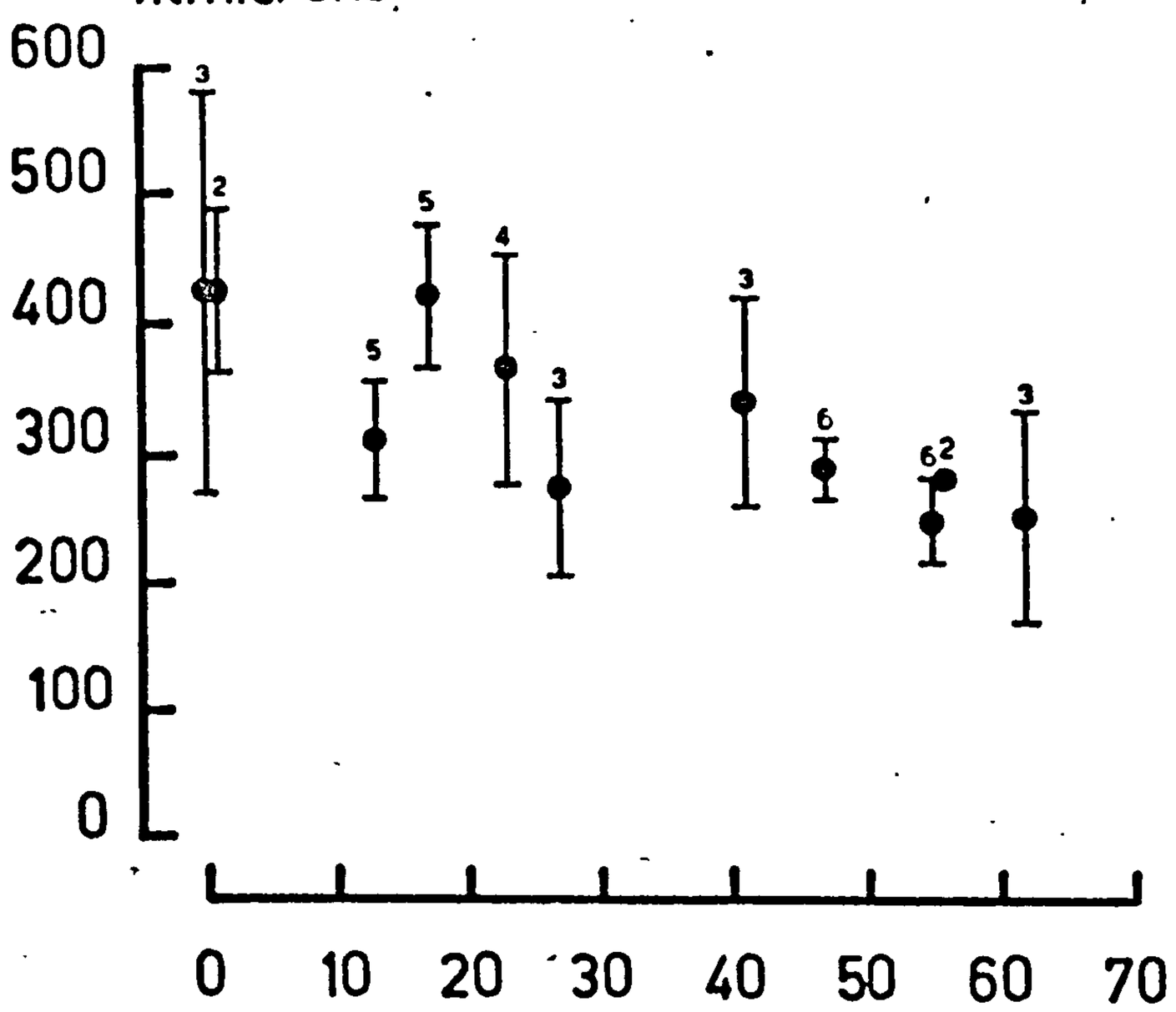
λ(microns)
600
500
400
300
200
100
0
3
2
5
5
4
3
3
6
6
2
3
0
10
20
30
40
50
60
70
days

B

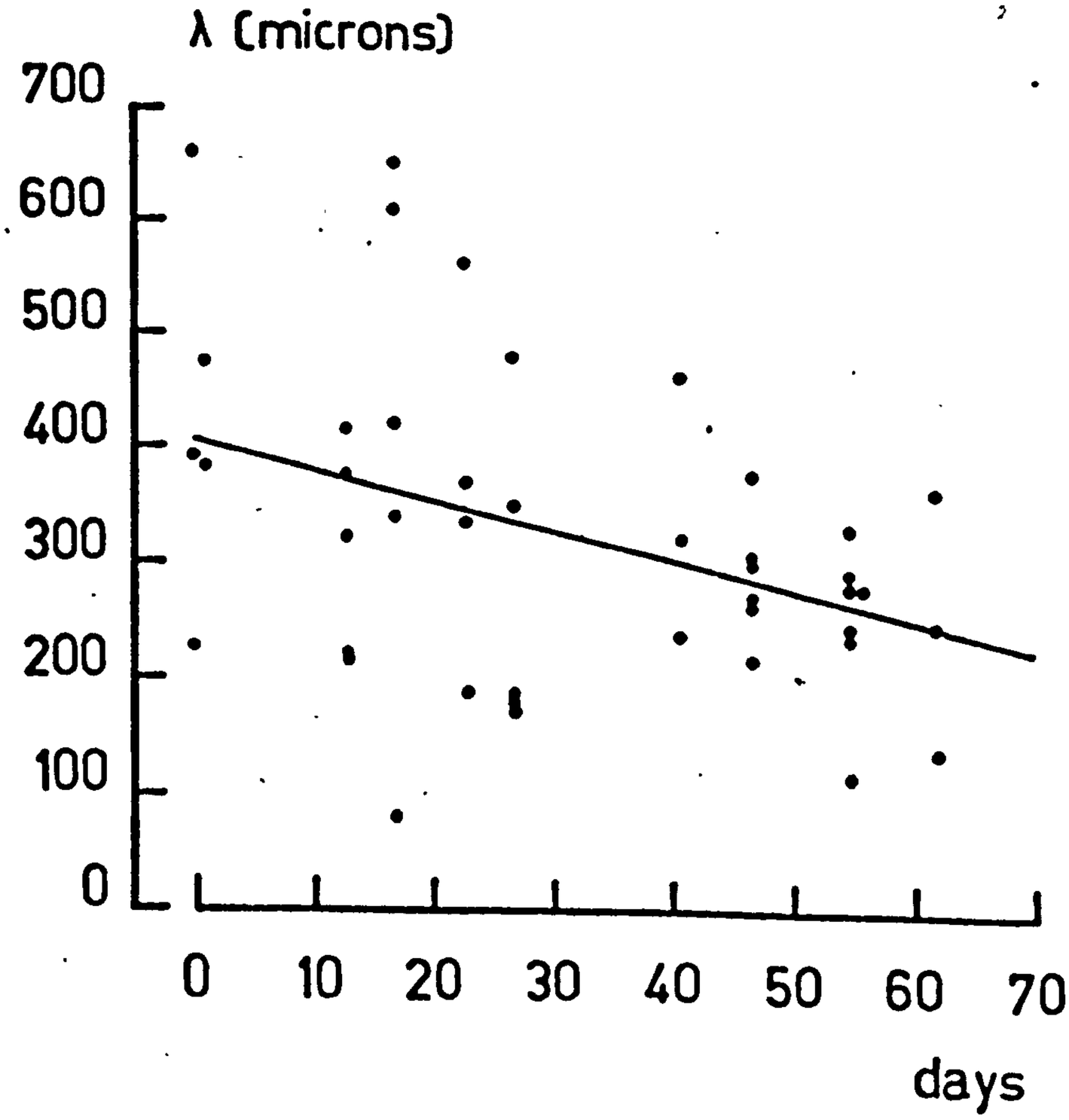
λ (microns)
700
600
500
400
300
200
100
0
0
10
20
30
40
50
60
70
days

These electrotonic potentials were always the same ones as used for the determination of the space constant, so insertion of that particular value of λ was used for each determination of τ_m. From a total of 7 different trabeculae a value of 4.15 msec (S.E. 0.55 msec) was obtained.

A final test was used for the applicability of one-dimensional cable theory in this preparation under this kind of stimulation, as shown in figure 12C. The curves are traces of the electrotonic pulses used for the determination of λ and τ_m in parts A and B, the values thus obtained were inserted into equation 19 and the points are the calculated voltages at various values of T ($= t/\tau_m$). There was some deviation during the initial part of the transients, which could have been due to some distortion produced by the intracellular capacity (see the longitudinal impedance section for discussion of this parameter), but this was not serious. Thus, with the assumption that one-dimensional cable theory can be applied to these transients, a curve-fitting procedure was applied which was achieved as follows. The distance ($X = x/\lambda$) from the stimulating partition was recorded for each transient. From theoretical plots of equation 19), for different values of X, the ratio of V/V_{max} at time T could be evaluated for each distance. The time to this amount of rise was taken as the time constant: e.g. for X = 1.0 at time T = 1.0 then $V = 0.635\ V_{max}$.

With the amount of photographic enlargement possible, this procedure was accurate to $\pm$ 0.5 msec. From random samples of 18 determinations of λ a value of 3.7 msec (S.E. 0.5 msec) was obtained for τ_m.

The Conduction Velocity, θ, and the Time Constant from the Foot of the Action Potential, $\tau_{a.p.}$

From measurements of the difference in delay of a propagated action potential, as recorded by two intracellular microelectrodes at a measured distance apart, the conduction velocity was calculated as 11.6 cm sec^{-1} (S.E. 1.1 cm sec^{-1}, 11 experiments) at 16.5°C.

Part 1 of the conduction velocity column of table 7 shows the mean results of the 11 experiments. The numbers in parenthesis are the number of determinations carried out in any individual experiment. In any single determination 5-10 records were taken and the mean value used. The stimulus pulse strength and duration were kept constant throughout the experiments. The interelectrode distance was never less than 500 μ and usually about 1 mm, because at smaller distances the variation in measurements was usually much greater. This was probably due to the fact that the actual geometrical position of the microelectrode within the trabecula became significant at small interelectrode distances - a factor which would not be of such great consequence at an interelectrode distance of 1 mm.

Care was taken to maintain a constant amount of stretch on the muscle preparation throughout the experiment at just over the resting length. Martin (1954) found that in frog sartorius muscle there was no variation in conduction velocity with a 30% change in the resting length - a phenomenon which was explained by the muscle fibre having a folded structure. A single experiment with a ventricular trabecula also indicated that this was true in this tissue, but the 10% variation recorded at each stretch level could have masked any effect.

Table 7 The Propagated Response Parameters, The Conduction Velocity and The Time Constant from the Foot of the Action Potential

Experiment no.	Temperature (°C)	Conduction Velocity (cm sec^{-1})			Time Constant from the foot of the action potential (msec)
		1	2	3	
7	16.5	10.8 ± 2.4 (2)			1.55 ± 0.00 (2)
8	16.5	9.5 ± 3.8 (2)			
9	16.5	15.0 ± 10.9 (2)			
10	16.5	15.2 ± 5.2 (5)			1.64 ± 0.11 (7)
12	16.5	17.6 ± 3.4 (4)			1.38 ± 0.46 (7)
13	16.5				1.59 ± 0.61 (3)
15	15.5	5.9 ± 0.1 (2)	11.7 ± 7.4 (2)	4.9 ± 1.1 (2)	1.49 ± 0.07 (7)
16	16.5	8.6 ± 3.5 (4)	6.3 ± 1.4 (2)	5.0 ± 0.6 (4)	1.73 ± 0.07 (3)
17	16.5	13.1 ± 6.7 (5)	11.7 ± 2.3 (2)	14.7 ± 1.2 (4)	2.07 ± 0.76 (3)
18	16.5	11.9 ± 5.6 (6)		14.1 ± 3.3 (2)	1.05 ± 0.26 (14)
19	16.5				1.63 ± 0.28 (4)
20	16.5	9.1 ± 4.5 (4)		10.2 ± 4.8 (6)	2.25 ± 0.26 (8)
21	16.5	11.1 ± 3.0 (5)	8.9 ± 1.0 (3)	16.4 ± 5.2 (4)	2.22 ± 0.14 (4)
Mean ± S.E.		11.6 ± 1.1 (11)			1.69 ± 0.11 (11)
Means of expts. 15-18,20,21		10.0 ± 1.2 (6)	9.7 ± 1.2 (4)	10.9 ± 2.3 (6)	

In the conduction velocity columns, column 1 is the conduction velocity measured in Ringer, column 2 that measured in hypertonic Ringer (containing 400 mM glycerol) and column 3 that measured on return to Ringer. The numbers in parenthesis are the number of determinations in each experiment.

The time constant from the foot of the action potential, $\tau_{a.p.}$, as defined by equation 31, was measured by plotting the logarithm of the voltage at the base of the action potential against time. A straight-line relationship was seen before the threshold for regenerative action was reached. Action potentials were randomly selected from those used to calculate the conduction velocity. Table 7 shows the values obtained from 11 experiments, the numbers in parenthesis are the number of action potentials selected for measurement in each experiment.

The time constant, as measured by the time taken for the voltage to reach a level V from V/e, was thus calculated to have a value of 1.69 msec (S.E. 0.11 msec, 11 experiments) at 16.5°C. An example of one such determination is seen in figure 14.

The Effect of Glycerol on the Conduction Velocity

It has been shown by Hodgkin (1954) that the conduction velocity of an impulse in a continuous fibre is given by the equation

$$\theta = \left(\frac{\zeta P}{R_i A} \right)^{\frac{1}{2}} \qquad 51)$$

where A is the fibre surface area, P is the fibre volume, R_i the internal resistivity and ζ is a constant. Thus, any change in the conduction velocity should reflect any changes in other parameters. It was of interest to study the conduction velocity during and after glycerol treatment as Strosberg, Katzung and Lee (1972) have observed structural changes in guinea-pig cardiac muscle during and just after such treatment. It would thus have been useful to see if electrophysiological changes occured during this treatment also.

Figure 14 A semilogarithmic plot of the foot of the action potential. The line is a regression line through the experimental points. Experiment performed at 16·5°C in 0·1 mM Ca^{2+} Ringer.

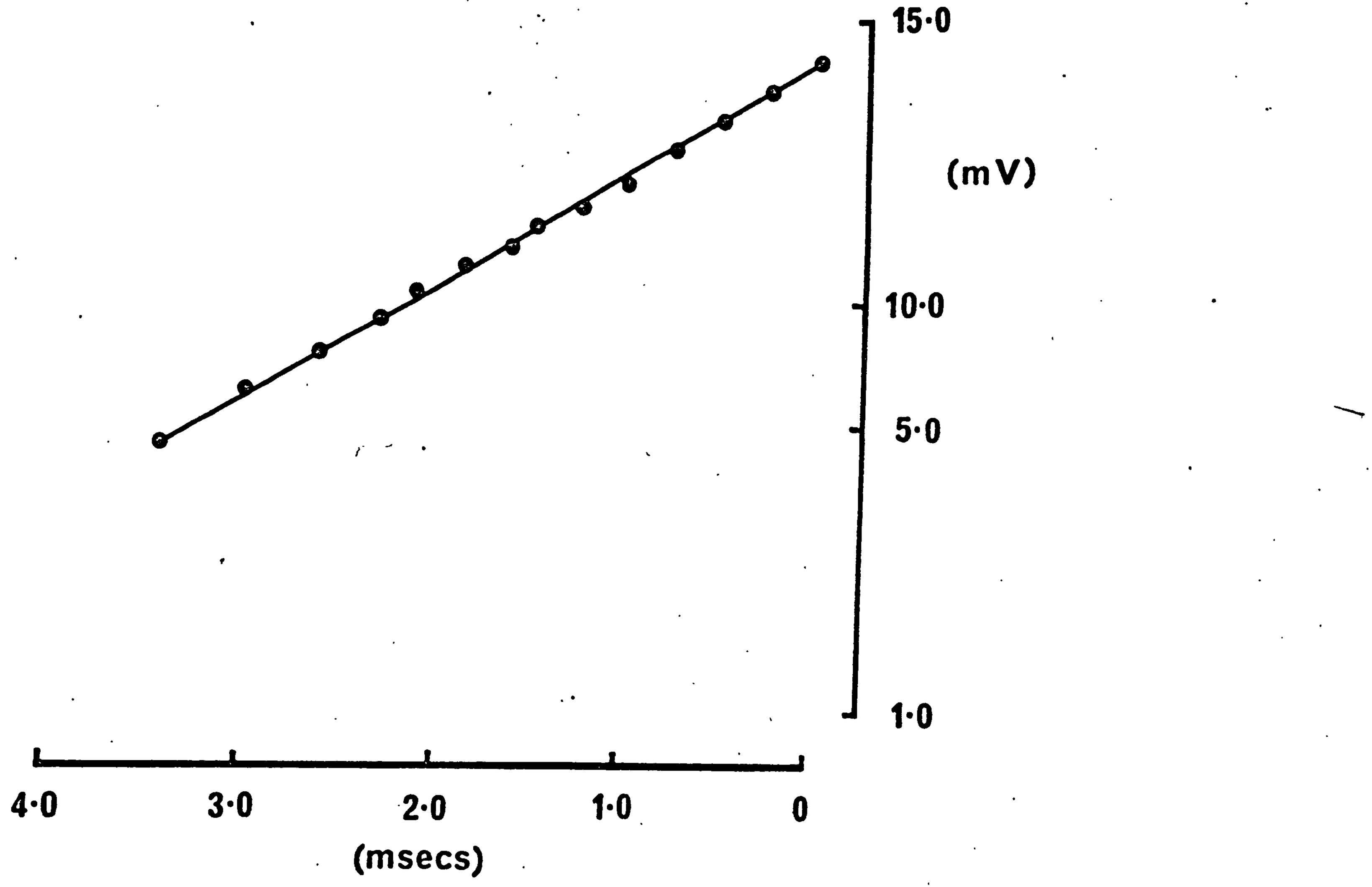
15·0
(mV)
10·0
5·0
1·0
4·0
3·0
2·0
1·0
0
(msecs)

Results of six experiments measuring the conduction velocity before, during and after glycerol treatment - i.e. perfusion by hypertonic Ringer, containing 400 mM glycerol - gave the following respective results: 10.0 $\pm$ 1.2 cm sec^{-1}; 9.7 $\pm$ 1.2 cm sec^{-1}; 10.9 $\pm$ 2.3 cm sec^{-1}. These results are shown as experiments 15-18, 20 and 21 in parts 1, 2 and 3 respectively of the conduction velocity column of table 7.. The results of measurements taken during and after glycerol treatment have been lumped together as no significant trends were found during these periods. Thus, it can be concluded that either no changes in fibre area, volume or internal resistivity occured, or that changes in one were balanced by changes in other parameters.

It should be noted that the absence of any change in the conduction velocity is not, in itself, any proof for the absence of a T-tubular system. (Electron-microscopic studies of frog ventricle, Staley and Benson, 1968, and electrophysiological studies in frog auricle, Chapman, 1971, however indicate that the T-tubular system is absent in frog cardiac muscle.) Glycerol treatment of skeletal muscle has been shown to cause a lesion of the T-tubular system with the surface membrane - i.e. upon return to normal Ringer from the glycerol-containing solution - thus greatly reducing the membrane area (Howell and Jenden, 1967; Howell, 1969). However, similar treatment of cardiac muscle preparations with a T-tubular system does not produce such lesions (Niemeyer and Forssman, 1971; Strosberg, Katzung and Lee, 1972), presumably due to the fact that the T-tubules in cardiac muscle

are shorter and wider and so more resistant to osmotic stress. Thus, no change in membrane area would occur so producing, per se, no change in the conduction velocity.

Calculation of the Membrane Resistance, R_m, and Capacitance, C_m

The estimation of the membrane parameters relies on calculations using the experimentally derived parameters. By use of equation 26) and 33) to 35) estimates can be made. Consideration of equation 26), which requires a frequency analysis of the membrane impedance, will be left until later.

An estimate of the membrane resistance can be made from the d.c. space constant. Using the relationships of equation 33), the specific membrane resistance is given as:

$$R_m = \frac{2R_i \lambda^2}{a} \qquad 52)$$

Using the experimentally derived values of $R_i = 588\,\Omega$cm and $\lambda = 328\,\mu$ a figure of 5.06 k $\Omega\,cm^2$ is obtained for R_m. R_f is the most appropriate value to use for R_i. As the space constant is greater than one cell length we will be considering the lumped intracellular resistance provided by R_f (e.g. Abe and Tomita, 1968).

Again from equation 33) the membrane capacity can be calculated from

$$\tau_m = C_m R_m$$

in which τ_m was calculated from the same transients as for the calculation of the space constant, and hence R_m. Thus using values of τ_m = 3.7 msec and R_m = 5.06 kΩ cm^2, the specific membrane capacitance has a value of 0.73 μF cm^2.

Equations 34) and 35) are designed for measurement of the membrane capacity from the foot of the action potential, although it must be remembered that the additional information of τ_m is needed for equation 35). With equation 34) inserting a value of 588 Ωcm for R_i (again R_f is the most appropriate parameter to use as we are considering propagated responses) and values of 11.6 cm sec^{-1} for θ, 1.69 msec for $\tau_{a.p.}$ and $2.5.10^{-4}$cm (2.5 μ) for the fibre radius, a, a figure of 0.94 $\mu F\ cm^{-2}$ (range 0.63 to 1.46 $\mu F\ cm^{-2}$) is obtained for the specific membrane capacity. However, as previously explained, the approximation used in the determination of equation 34) is not valid for frog ventricular myocardium, so that the more complete equation 35) must be used. By inserting the additional value of 3.7 msec for τ_m a value for C_m of 0.64 $\mu F\ cm^{-2}$ (range 0.40 to 1.06 $\mu F\ cm^{-2}$) can be calculated.

The two estimates of C_m are not independent as both require a knowledge of τ_m, but they do act as a test of self-consistency in the determination of the parameters required for the calculation of the specific membrane capacity.

Longitudinal Impedance Measurements: Theory

Measurements of the longitudinal impedance were primarily made in order to ascertain whether the intracellular pathway is purely resistive or whether there is a reactance in the system which would manifest itself by a frequency-dependant behaviour.

With this experimental situation, account must be taken of membrane properties manifesting themselves in the results. Current will have to cross the surface membrane of the cells to reach the intracellular pathway and not via the cut ends of the preparation, the latter being expected to heal over in the external calcium concentration of 1 mM. Thus, current will cross the membrane at a distance of up to about one space constant in the oil gap (c.f. Cole and Hodgkin, 1939), so that the longitudinal pathway will not be the exact length of the trabecula in the oil gap. An estimate can be made of this error, in that if the external resistance, r_o, is made equal to the internal resistance, r_i, (both per unit length) the space constant will have a value of 232 μ (obtained from $\lambda = 328\,\mu$, when r_o is zero). This phenomenon will occur at both ends of the oil gap making a distance of about 460 μ not included in the intracellular pathway - i.e. 9% if the total oil gap length is 5 mm. If r_o is greater the error will decrease as λ is reduced.

The single time constant model

With the experimental situation used, impedance measurements will be of the type recorded by Cole and Baker (1941) on the squid giant axon. If the internal pathway is purely resistive and the only impedance element that the current encounters is the surface

membrane capacitance then a single time constant model can be constructed. The longitudinal impedance of such a membrane model will be given by (Falk and Fatt, 1964):

$$Z = R + jX = \frac{(r_i r_m)^{\frac{1}{2}}}{2\left[(r_m \omega c_m)^2 + 1\right]^{\frac{1}{2}}} \cdot m - jn \qquad 53)$$

where $$m = \frac{1}{2}\left\{\left[(r_m \omega c_m)^2 + 1\right]^{\frac{1}{2}} + 1\right\}^{\frac{1}{2}}$$

and $$n = \frac{1}{2}\left\{\left[(r_m \omega c_m)^2 + 1\right]^{\frac{1}{2}} - 1\right\}^{\frac{1}{2}}$$

r_m, c_m are the membrane resistance and capacitance respectively and r_i is the internal resistance.

The absolute value of the membrane impedance, z_m, has been shown by Cole and Baker (1941) to be proportional to the square of the absolute value of Z, so that:

$$z_m = r_m + jx_m \qquad Z^2 = R^2 - X^2 + j2RX \qquad 54)$$

Figure 15A,B shows a Z^2 and Z plot for a simple one time constant model of a parallel resistance and capacitance. Thus, a plot of Z^2 can be used for determination of the circuit parameters that give the observed complex-plane plots.

The two time constant model

If a membrane impedance does exist somewhere else than at the surface membrane this will introduce a further time constant into the model. If the two time constants are different this will show itself as two dispersions in the complex-plane plot.

There are four possible four-element equivalent circuits having two time constants, as shown in figure 16A-D. The intracellular pathway will also be assumed to have a resistor, r_c, in series with any impedance element, corresponding to the resistance

Figure 15 Part A is a complex-plane plot of the impedance, Z^2, of a single time constant system, consisting of a parallel resistance and capacitance. The example shown is that calculated for the surface membrane of the frog ventricular myocardium using the experimentally determined values of R_m and C_m. The example has a time constant of 3.52 msec, so that the characteristic frequency (where -X is a maximum) has a value of 45.2 Hz - see equation 55). Part B is a plot of the longitudinal impedance, Z, of the above system. The plot was drawn by inserting the experimentally obtained values of r_i, r_m, and c_m into equation 53). The characteristic frequency is shown.

A

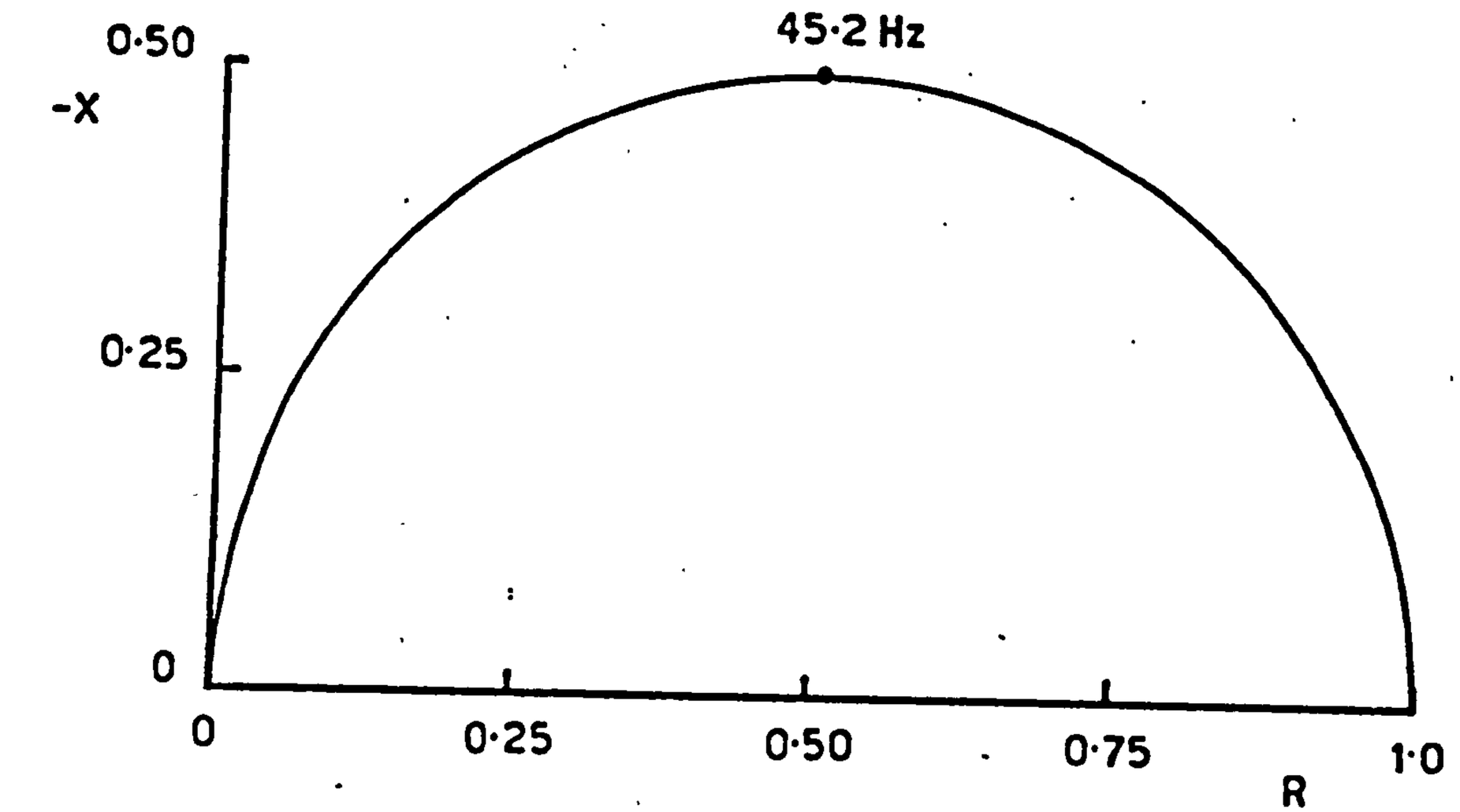
0·50
-X
0·25
0
45·2 Hz
0
0·25
0·50
0·75
1·0
R

B

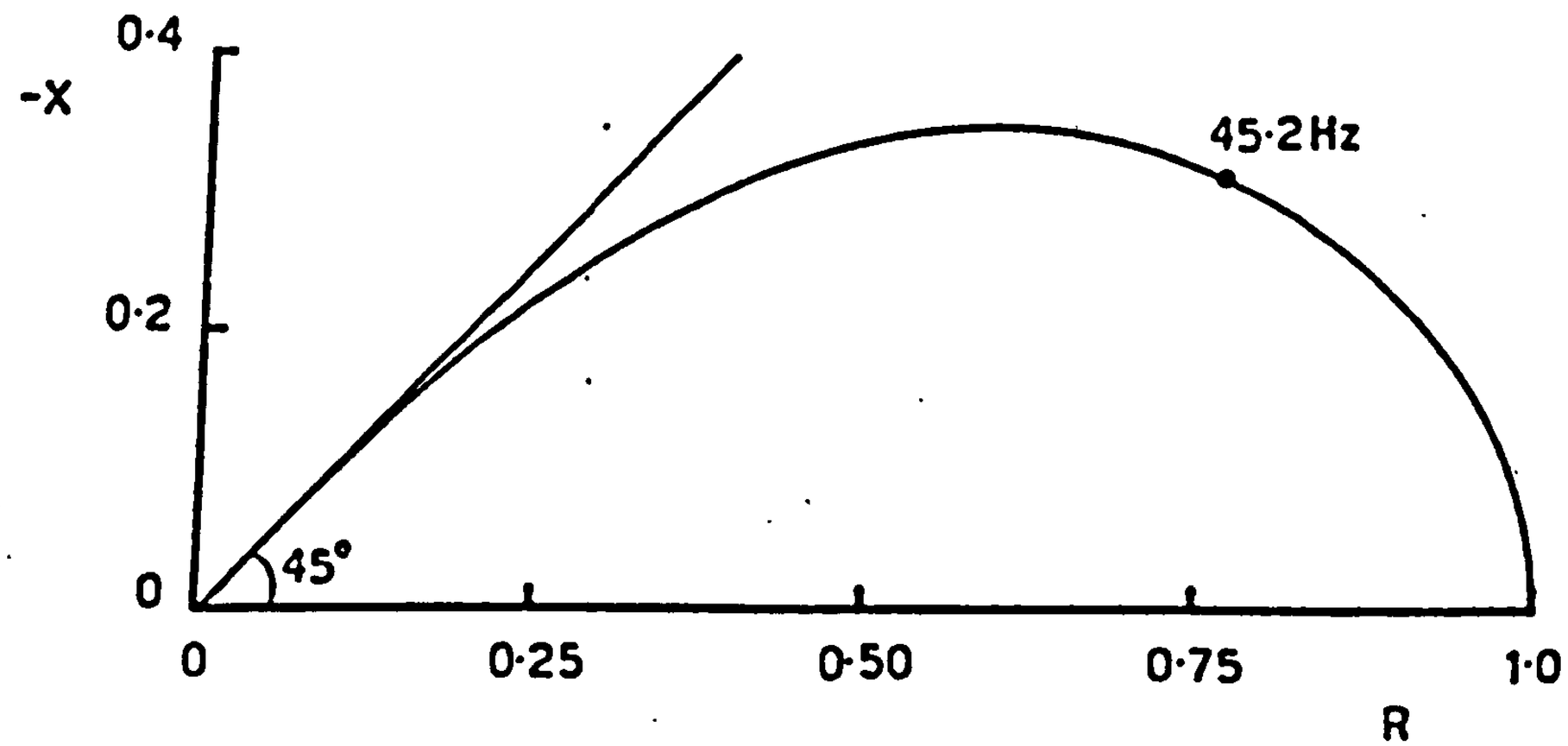
0·4
-X
0·2
0
45°
45·2Hz
0
0·25
0·50
0·75
1·0
R

Figure 16 Parts A-D show the four possible four-element, two time constant equivalent circuits, consisting of resistors and capacitors only. Part E is a complex-plane plot of a two time constant network - in the example the two time constants differ by a factor of ten. The dotted line shows the complex-plane plot of one of the time constants in the model.

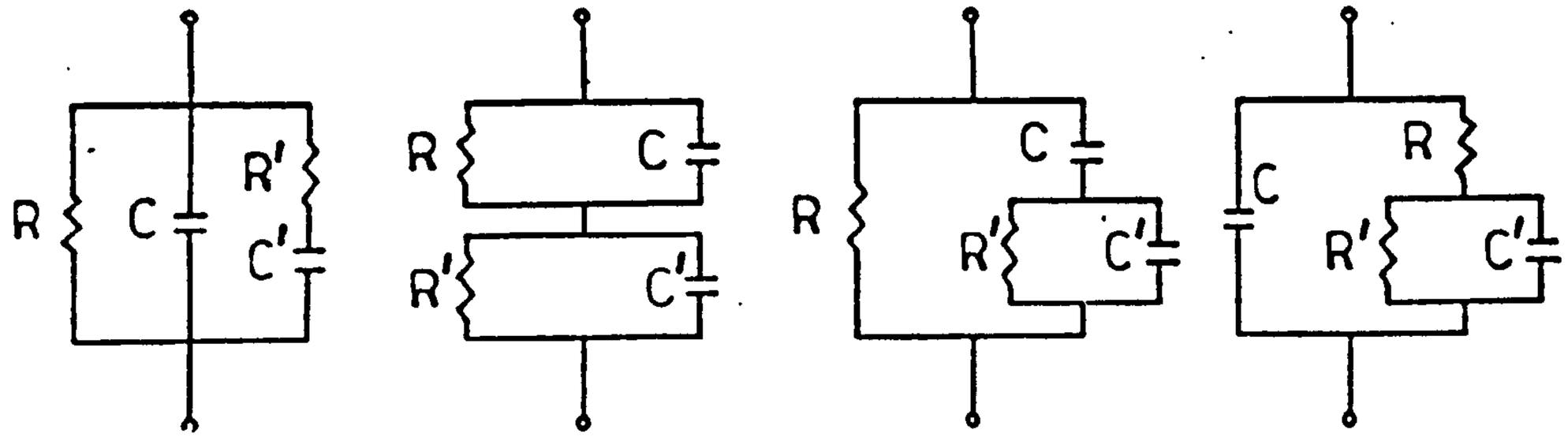

A

B

C

D

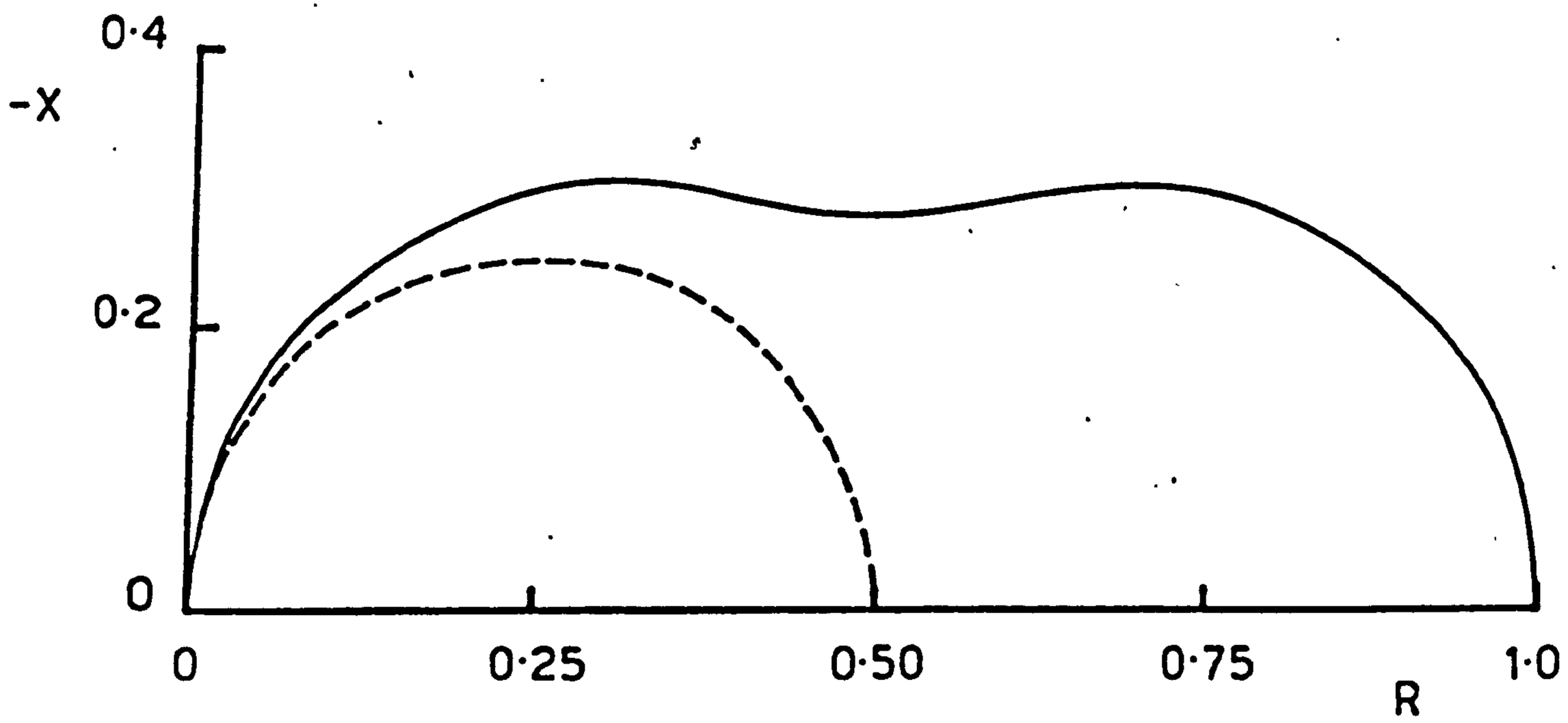

E

of the cytoplasm. There will also be an extracellular shunt, r_o, in parallel with the whole sample. For the purposes of this analysis, the resistance at which the high-frequency limb of the complex-plane plot cuts the resistance axis will be the parallel combination of r_c and r_o.

Figure 16E shows a plot of a two time constant impedance locus based on the circuit of figure 16B. The two time constants were chosen to differ by a factor of ten but even so the two dispersions are incompletely separated. The dotted-line semicircular locus within the main plot is that of each individual parallel resistance and capacitance.

Thus, the purpose of the experiments was to see whether a one or two time constant system could be explained by the results and what physical features could explain the observed locus.

Longitudinal Impedance Measurements: Results

Figure 17 shows an example of the platinum blacked electrodes' resistance and capacitance values before and after plating. The constant residual resistance seen after plating can be presumed to be that of the Ringer solution between the two electrodes, so that the electrodes themselves had virtually no resistance. The reactance also was very much reduced, as is seen by the large increase in series capacitance. In this condition the blacked electrodes offered little impedance (about 0.1%) to the total circuit. Changing the interelectrode distance altered the values of both the measured resistance and capacitance so a constant interelectrode distance of 0.6 cm was maintained throughout the experiments.

Figure 17 The two parts of the figure show the platinum electrodes' electrical characteristics before and after coating with platinum black. The upper part shows the capacity before - filled triangles - and after - filled squares - plating, as measured at various measuring frequencies. Note the change in ordinate from μF to mF. The lower part shows the resistance before and after plating, the same symbols are used.

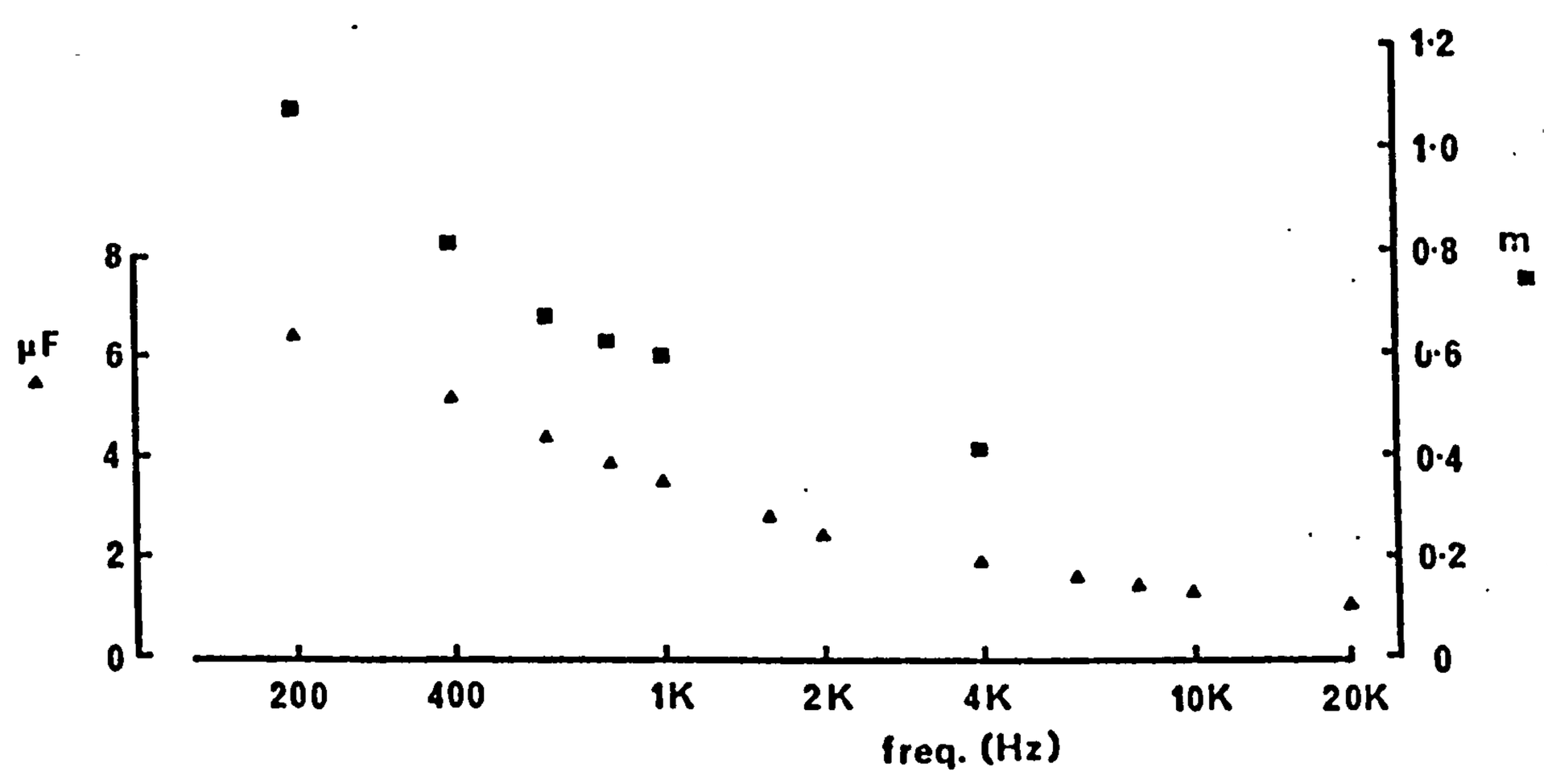
μF
8
6
4
2
0
1·2
1·0
0·8
0·6
0·4
0·2
0
m
200
400
1K
2K
4K
10K
20K
freq. (Hz)

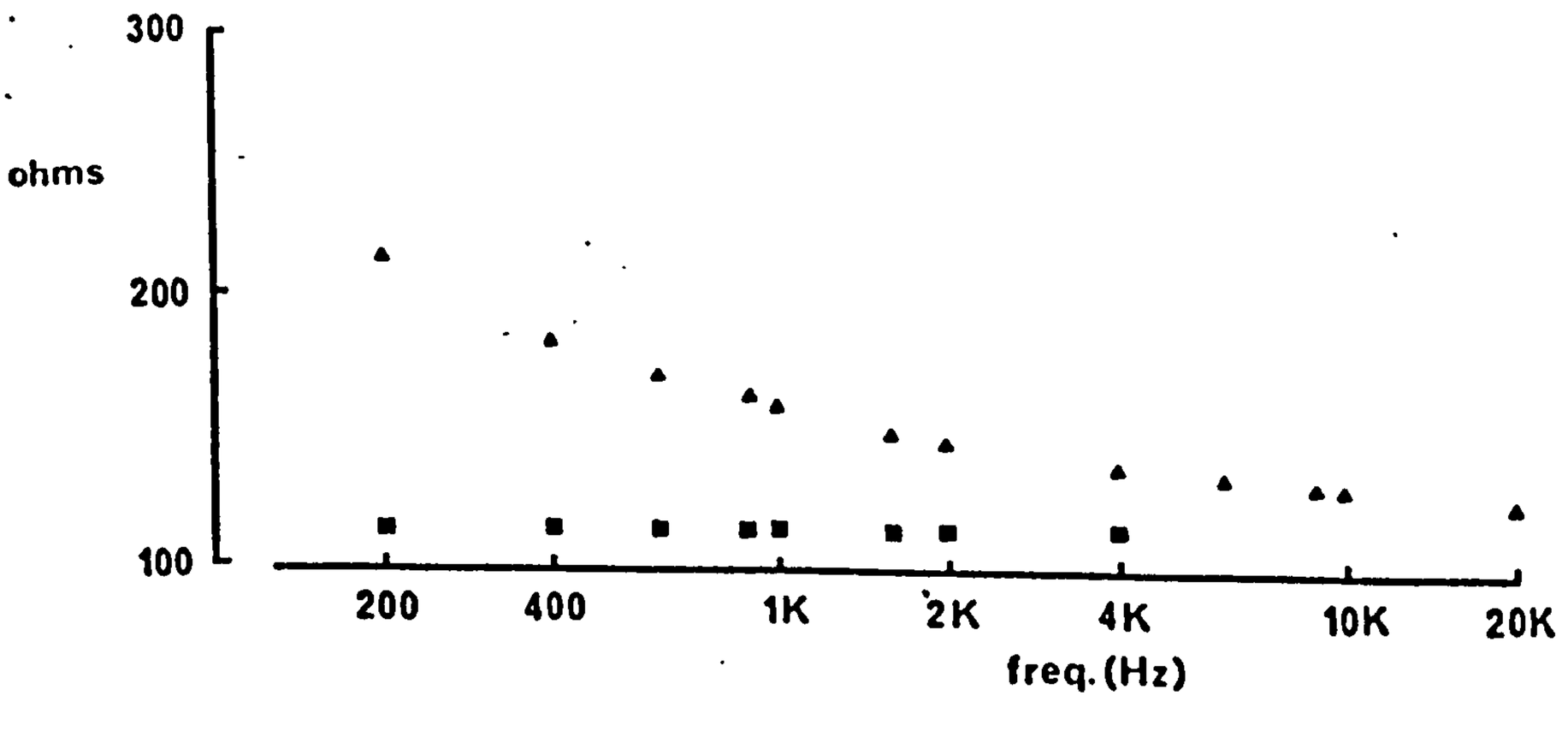
ohms
300
200
100
200
400
1K
2K
4K
10K
20K
freq. (Hz)

Figure 18A shows a typical longitudinal impedance complex-plane locus for a ventricular strip measured over a range of frequencies from 80 Hz to 40 kHz. Over such a frequency range one major dispersion is evident, although at lower frequencies a further dispersion seems to be present. The lower frequency dispersion could be due to the surface membrane as it would be manifest over such a frequency range - see figure 15.

To study the high-frequency dispersion any effect of the membrane properties had to be discounted. It was assumed that the high-frequency region of the plot was free of any membrane effect - i.e. at frequencies of 6 kHz or greater - and the high frequency dispersion was calculated around these points. With a pure capacity, at high frequencies R and -X will diminish together and so the plot will approach the R axis at a 45° angle, and at low frequencies will approach the R axis at a 90° angle. If the capacity has a certain amount of dielectric loss so that the phase angle is less than 90°, i.e. ϕ°, (a model assumed by Cole and Baker (1941) to account for their high-frequency data) then the high-frequency region of the locus will approach the R axis at $\phi/2^{\circ}$ and the low-frequency will approach at ϕ°. Thus, the phase angle, ϕ°, could be determined from the high-frequency data and the locus was obtained by comparison with theoretical longitudinal impedance loci for ϕ° according to the recommendations of Falk and Fatt (1964). Figure 18B shows the data above duly corrected.

Figure 18 Longitudinal impedance of a frog ventricular trabecula, expressed as a complex-plane plot. Part A shows the -X and R values obtained from the experimentally derived values of the conductance and capacitance - see methods section for details - taken over a frequency range of 80 Hz to 40 kHz. Part B is the longitudinal impedance locus after correcting for the contribution due to the surface membrane - see text for details. Part C is the impedance locus obtained from part B, calculated from equation 54).

Experiment performed at 20°C with 1 mM Ca^{2+} Ringer bathing the preparation in the two outer chambers.

A

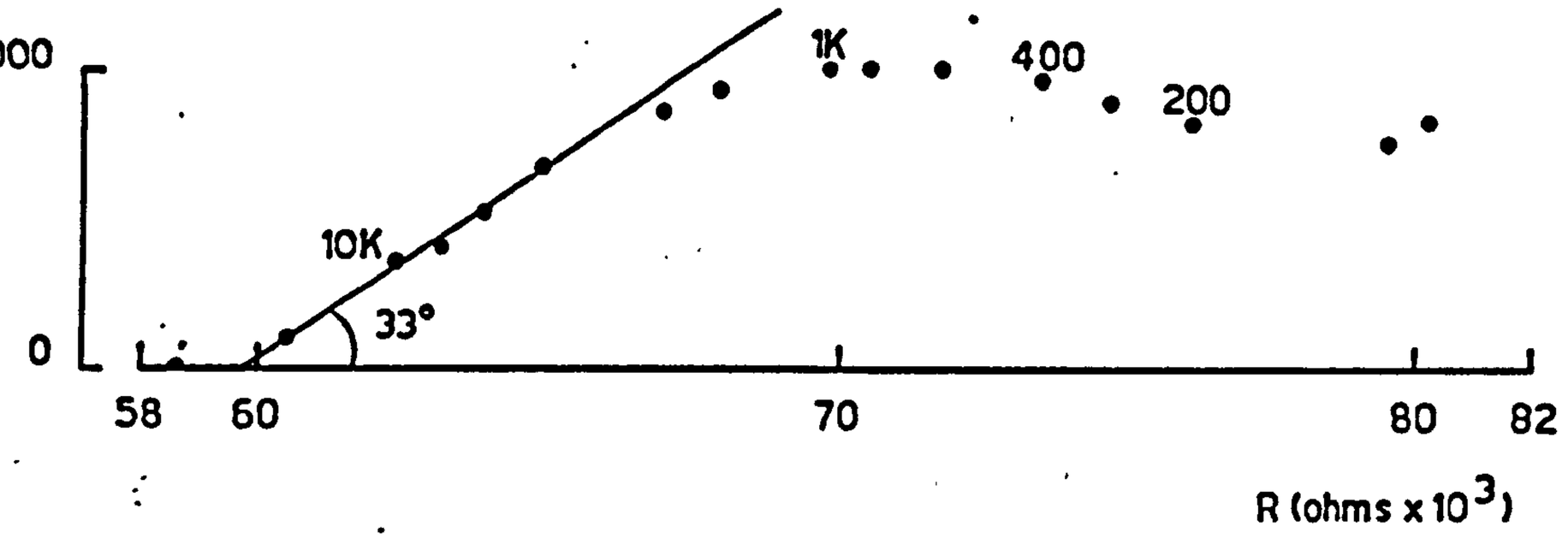
5000
-X (ohms)
0
1K
400
200
10K
33°
58
60
70
80
82
R (ohms x 10^3)

B

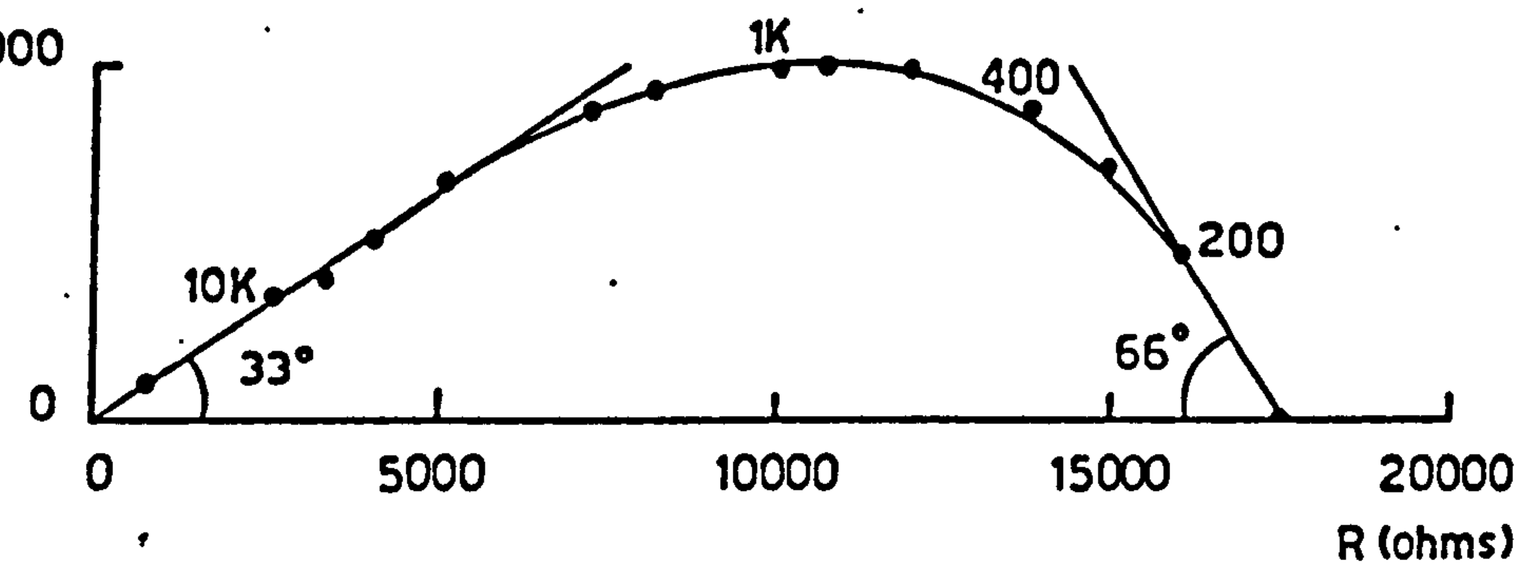
5000
-X (ohms)
0
1K
400
200
10K
33°
66°
0
5000
10000
15000
20000
R (ohms)

C

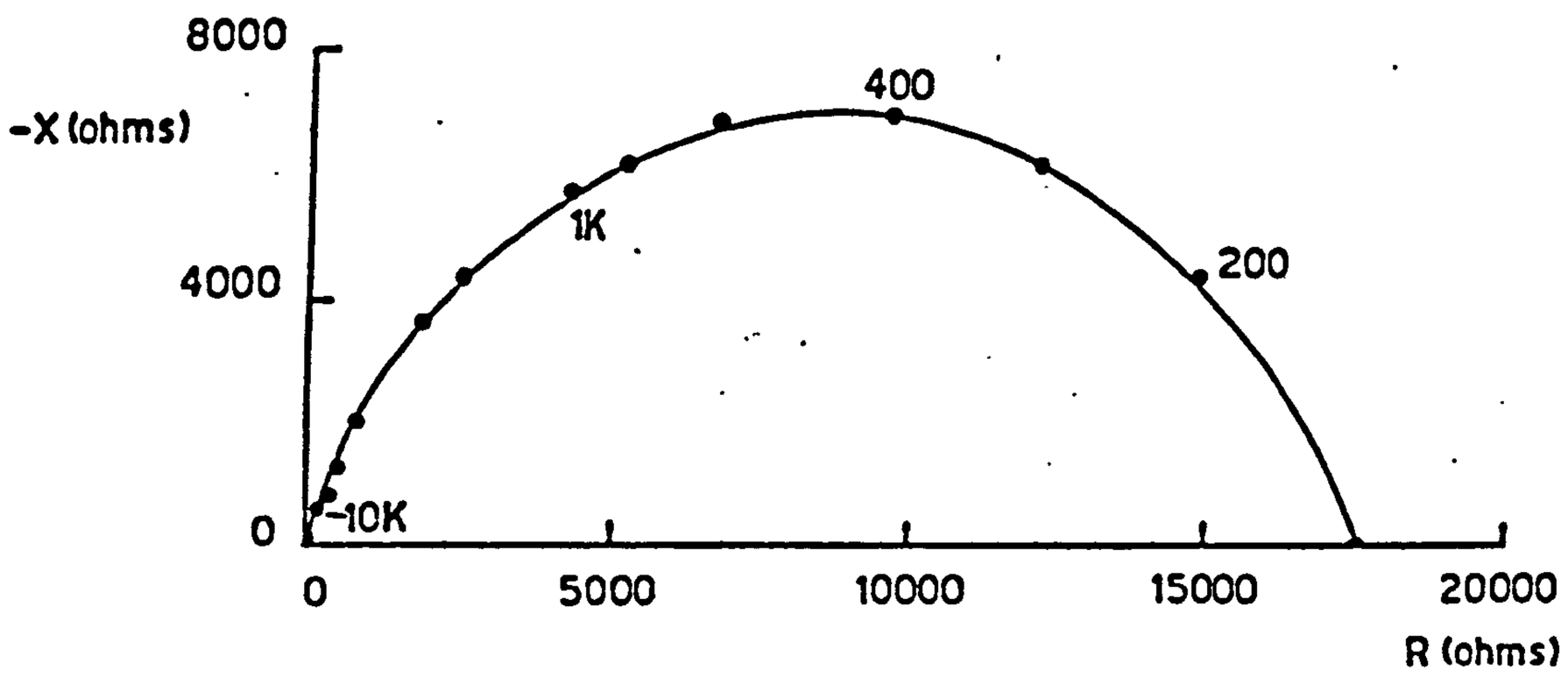
8000
-X (ohms)
4000
0
400
1K
200
10K
0
5000
10000
15000
20000
R (ohms)

Table 8 Longitudinal Impedance Measurements

Experiment no.	ϕ °	freq*	area ($\times 10^{-3}$ cm^2)	R_d (ohm cm)	C_d (mF cm^{-2})	τ_d (msec)
1	66°	450	2.12	0.96	0.28	0.27
2	53°	500	0.94	1.05	0.30	0.32
3	50°	500	2.49	1.42	0.22	0.31
4	56°	600	5.89	1.23	0.32	0.39
5	48°	450	0.94	1.04	0.34	0.35
Mean				1.14	0.29	0.33
± S.D.				0.19	0.05	0.04
6	72°	1600	5.89	0.29	0.28	0.08
7	42°		0.94			

freq* is the characteristic frequency of the locus, from which can be calculated ω^* of equation 55)

R_d and C_d are the specific resistance and capacitance, respectively, of the membrane causing the observed dispersion and are equivalent to R and C of the general equation 55)

the cross-sectional area of the trabecula is given in column 4.

To obtain information about the parameters of the dispersion the longitudinal impedance data was converted to an impedance locus by the relationship previously described, i.e. equation 54)

$$z_m = r_m + jx_m \qquad Z^2 = R^2 - X^2 + j2RX$$

Figure 18C shows the above data corrected to an impedance locus. Such a locus can be produced by a parallel resistance and capacitance, as seen in figure 15A. The capacitance of such a circuit is given by the equation:

$$R\omega^* C = 1 \qquad 55)$$

where R is the resistance of the circuit and is given by the resistance between the high and low frequency transects of the locus with the R axis and ω^* is the characteristic frequency, at which -X is a maximum, occuring at a resistance of R/2. It will be noted that the two arms of the locus approach the R axis at a tangent of ϕ° - i.e. 66° in the above example. Data from a total of five experiments is given in table 8, experiments 1-5.

It is now necessary to place a physical interpretation upon such a dispersion. Cable analysis of skeletal muscle (Falk and Fatt, 1964) and Purkinje fibres (Fozzard, 1966) has suggested that part of the surface membrane lies in series with a resistance and that such membrane may lie in the tubular system or the narrow clefts between cells, respectively. The electrical separation of the surface membrane of the above tissues had been indicated previously when low frequency measurements of the capacity gave high values (Fatt and Katz, 1951; Weidmann, 1952). Thus, Falk and Fatt (1964) and Fozzard (1966) used the circuit of figure 16A to describe the

surface membrane more completely. However with the frog ventricular preparations it has been found that the low frequency measurements of the membrane capacity gave much lower values, of about 1 $\mu F\ cm^{-2}$ - values similar to those obtained with giant axons (Hodgkin and Rushton, 1946) where the membrane geometry is much better defined. Thus, it seems reasonable that such a separation of the frog ventricular myocardial membrane does not occur, at least to the same extent as in Purkinje or skeletal muscle fibres. Indeed Beeler and Reuter (1970a) found that in a single sucrose-gap voltage-clamp system contamination by sucrose of the muscle in the test region produced a resistance in series with all of the membrane, in mammalian ventricular preparations.

A model electrically equivalent to that of figure 16A is that of figure 16B. This model has been used by Freygang and Trautwein (1970) and is similar to one used by Stibitz and McCann (1974), suggesting that the second parallel resistance and capacitance lies in the internal pathway - e.g. the desmosomes. The data in table 8 has been calculated on the basis of such a model.

To calculate specific values it was necessary to measure the length of the preparation in the oil gap and the cross-sectional area of the trabecula. It was again assumed that 25% of the total cross-sectional area was extracellular space, the length of the individual cells was 50 μ and 5% of the surface membrane was desmosomal area.

One other possible explanation of the high-frequency dispersion is to treat the individual cardiac cells as short cables so that the current could be pictured as threading in and out of the cells. Such a behaviour has been proposed by Falk and Fatt (1973) to account for current flow through rod suspensions. The characteristic frequency of such a dispersion is given by:

$$f = \frac{2.48.a}{R_c C_m l^2} \qquad 56)$$

where R_c is the resistivity of the intracellular contents, C_m the specific membrane capacity, l the length of the cell, a the fibre radius and f is the characteristic frequency. Using the previously determined values of $R_c = 346\ \Omega$ cm and $C_m = 0.69\ \mu F\ cm^{-2}$ and values for $a = 2.5\ \mu$ and $l = 50\ \mu$, the characteristic frequency has a value of 33 kHz. It must be stressed however that the value is highly dependant on the length of the individual cells, so that if $l = 100\ \mu$ the characteristic frequency will have a value of 8 kHz. However, this is still about an order of magnitude higher than the observed values of the characteristic frequency.

Moreover, it is questionable whether it is entirely justifiable to treat individual cells singly, i.e. as stacks of short cables. The previous d.c. analysis has indicated that the junctional area between cells does not form a significant barrier to current flow so that, per se, these regions will not force current over the surface membrane to produce the threading pathway of current.

To account for so large a capacitance as 290 $\mu F\ cm^{-2}$ requires that there be a space where ions can be accumulated or depleted. Such a mechanism was proposed by Fatt (1964) to account for a capacity of about 50,000 $\mu F\ cm^{-2}$ found in transverse impedance measurements of skeletal muscle, and was placed at the mouths of the T-tubular system. The capacity per unit area of such a system was given by Fatt as:

$$C = \frac{F^2\ s\ c}{2\ R\ T} \qquad 57)$$

where F is the Faraday constant, R the gas constant, c the concentration of external ions and s the space width in which the ions could be accumulated or depleted. Using a value of 0.12 M for c, a value of 116 Å for the space width can be calculated. Sjöstrand, Andersson-Cedegren and Dewey (1958) quote a value of 120 Å for the space between adjacent membranes at the intercalated disk of frog ventricular myocardial cells and Fawcett and Selby (1958) give a value of 150-200 Å for the membrane separation at desmosomes in the turtle atrium - a tissue anatomically very similar to frog ventricular myocardium. Thus, it does not seem unreasonable to suppose that the capacitance lies at this structure.

It is a consequence of equation 57) that changing the external concentration of ions should change the capacity - providing the intermembranous space stays constant. Two experiments were performed, one in which the Ringer was made twice tonic by doubling the concentration of all ions in the Ringer and in the other all but 10% of the external sodium ions were replaced by sucrose.

Figure 19 Impedance loci of trabeculae bathed in hypertonic and hypoösmotic Ringer - parts A and B respectively. The loci were obtained as described in figure 18 and the text.

Experiments performed at 20°C with 1 mM Ca^{2+} in the modified Ringers.

A

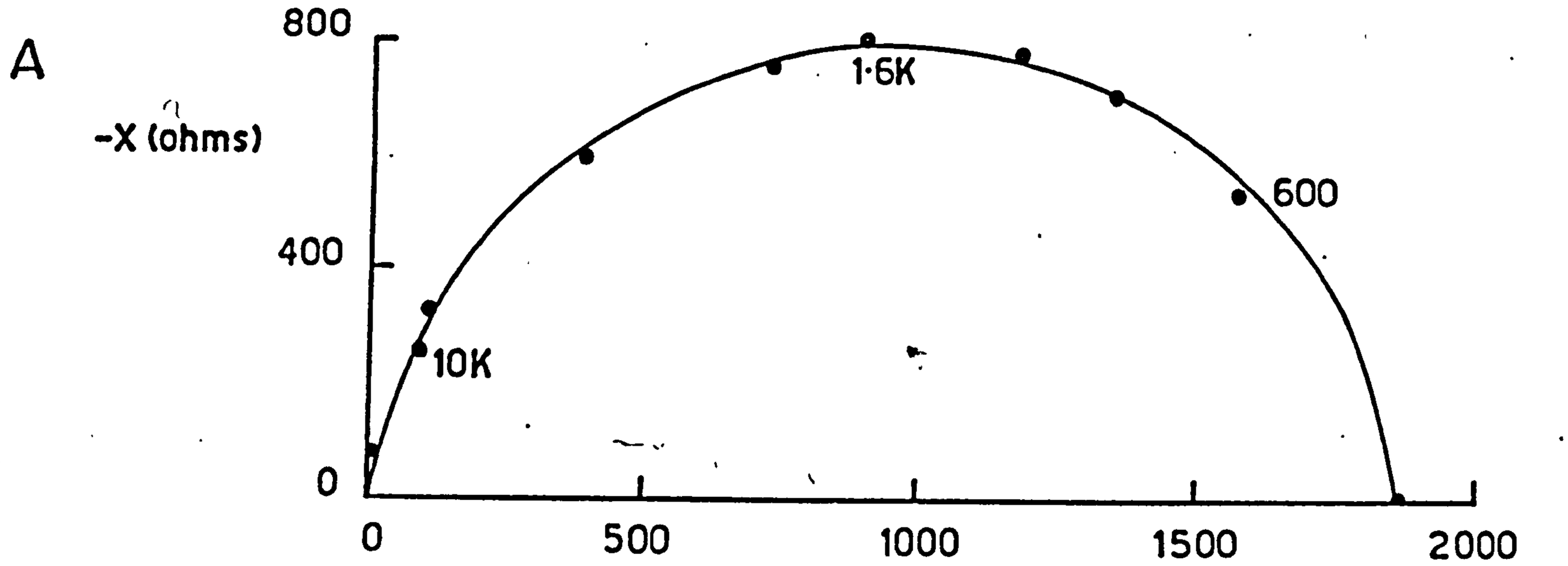
800
400
0
-X (ohms)
1·6K
600
10K
0
500
1000
1500
2000
R(ohms)

B

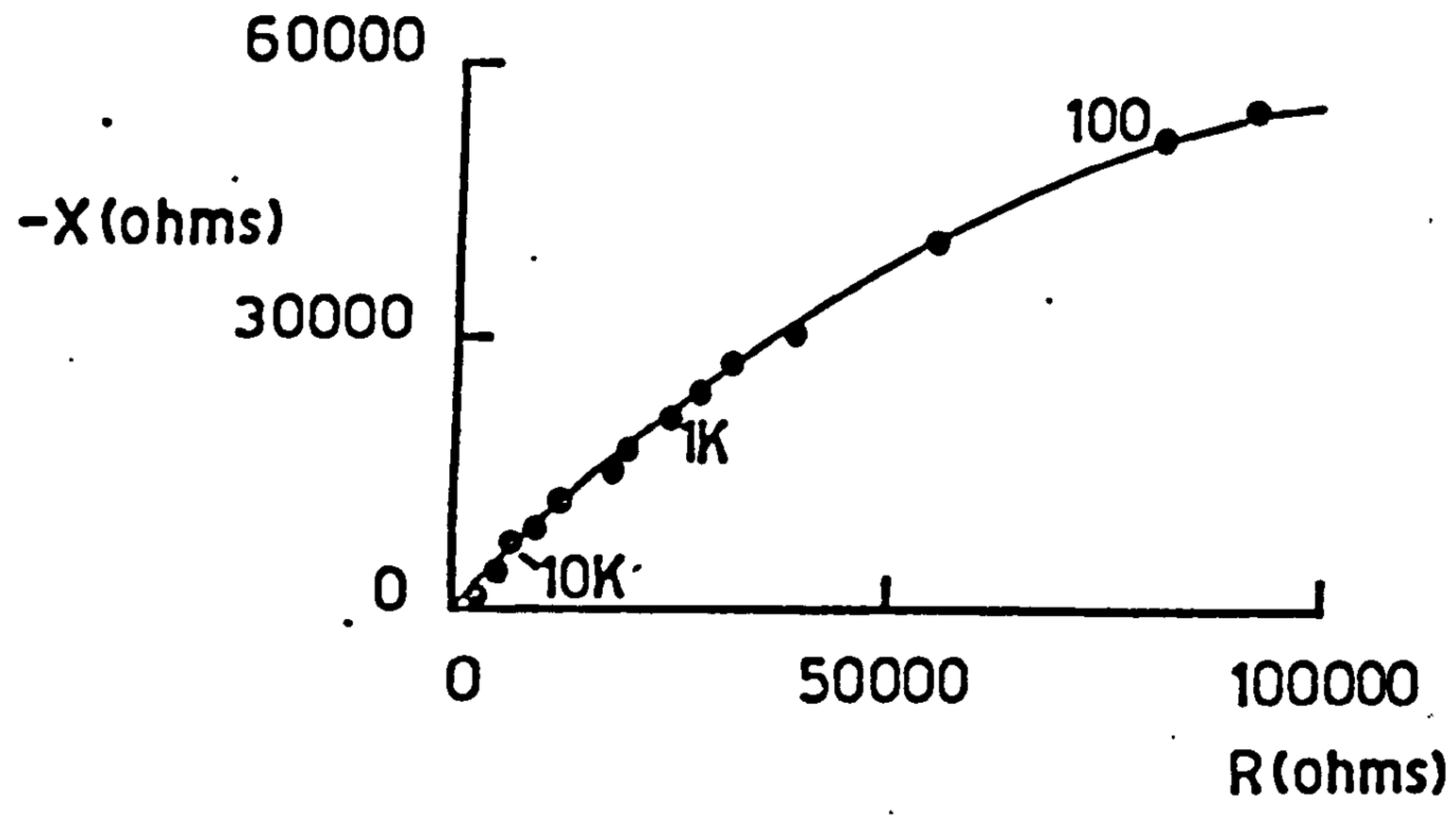
60000
30000
0
-X(ohms)
100
1K
10K
0
50000
100000
R(ohms)

These are quoted as experiments 6 and 7 in table 8. The procedure was to remove all the oil from the central chamber after an initial frequency run in normal Ringer, and leave the trabecula for about 30 minutes in the modified Ringer. The central compartment was then drained of Ringer and replaced by oil so that a new frequency run could be made.

Figure 19 shows the impedance loci for the trabeculae in the modified Ringer solutions after subtraction of the surface membrane contribution and conversion to an impedance locus. The characteristic frequency is changed in each Ringer solution, it being raised in the hypertonic Ringer and lowered in the hypoösmotic Ringer, although in the latter case the exact value of the characteristic frequency could not be determined. The result of experiment 6 shows that the disk capacity, C_d, has a value of 0.28 mF cm^{-2} as compared to a value of 0.29 mF cm^{-2} in normal Ringer. Fatt (1964) also noted a lack of change in a similar capacity following similar manoeuvres. The only explanation is that, assuming the intermembranous space is constant, the space is not easily accessible to the extracellular space under these conditions.

Passage of Alternating Current along the Trabecula

With direct current pulses, the space constant is a measure of the ratio of the square roots of the membrane and intracellular resistances. In terms of alternating current theory the same analysis can be applied. Thus, for an ordinary four-terminal network the ratio of input to output voltages is:

$$\frac{V_1}{V_2} = \frac{I_1}{I_2} = e^{\gamma} \qquad 58)$$

In this situation, γ - the propagation constant - is a complex function

$$\gamma = \alpha + j\beta \qquad 59)$$

where α - the real part of the equation - is the attenuation function and can be analogized to the direct current space constant. In the imaginary part of the equation, ($j\beta$), β is the phase function and is a measure of the phase difference between the two ends of the network, whilst j is the complex operator $\sqrt{-1}$.

For this purpose, the core-conductor model can be considered as a set of lumped impedances.

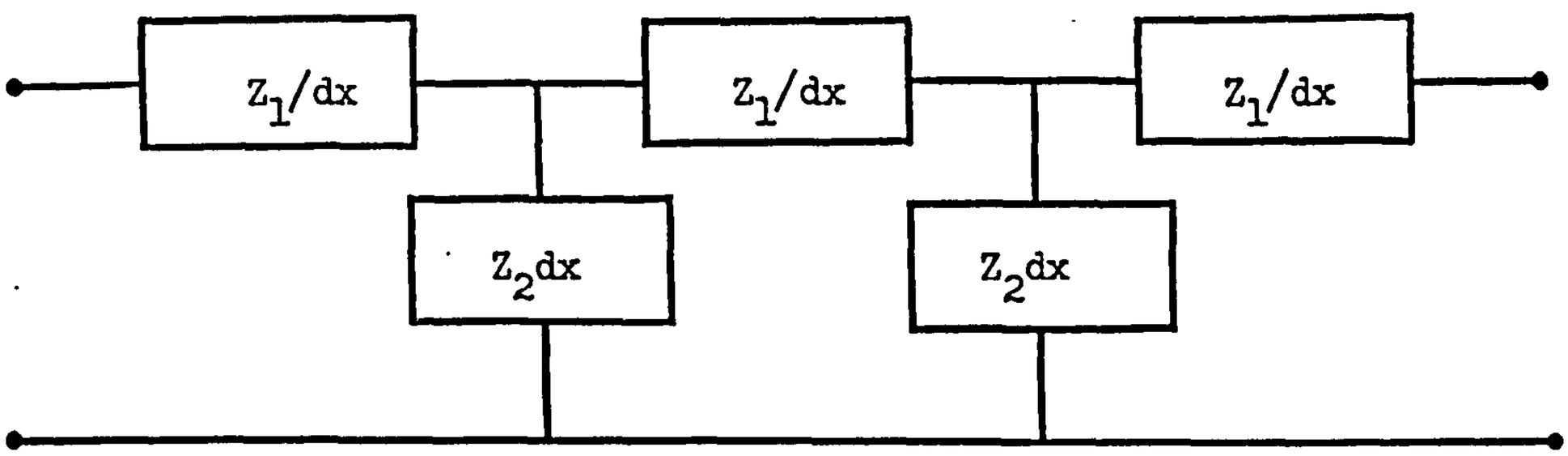

where Z_1/dx represents the intracellular impedance per unit length and Z_2 dx the membrane impedance for unit length. Again the extracellular impedance has been assumed to be negligible, as for the case of a trabecula immersed in a large volume of fluid. It will also be assumed initially that the intracellular pathway can be reduced to a resistance only - i.e. there is no reactive behaviour - as in equation 24. As has been seen, however, this simplification is not wholly justifiable and will be considered in the analysis.

Analysis of the network can be simplified by considering the system as a series of symmetrical T-sections in series so that it will behave as a filter. If the membrane impedance is represented as a capacitor with a parallel resistor then the system will be a low-pass filter.

Thus, if a measure of the impedance can be taken at a number of frequencies it will enable a network to be constructed which fits

such a behaviour. Measurements of this type have been attempted by Tasaki and Hagiwara (1957) and Falk and Fatt (1964) with skeletal muscle fibres. In the two sets of work current was passed down one microelectrode and recorded via another so that all the current was injected into the fibre. In addition Falk and Fatt (1964) largely carried out their measurements at very small interelectrode distances so that no factors due to the loss of current were involved. With the frog ventricle, however, the use of such a technique was not practical. A microelectrode used as a source of current will not provide a one-dimensional flow of current as is demanded of the technique so that a stimulating partition was used. The disadvantage of such a method is to determine what proportion of current passes down the trabecula. However, it was observed that the stimulating electrodes passed the same current at all frequences tested. Also in the work of Falk and Fatt an interelectrode distance of 30 μ was considered to be equivalent to a zero distance due to the relatively larger space constant. With frog ventricle, however, even a distance of 30 μ will produce a sizeable decay of current so that the effect of interelectrode distance must always be taken into account.

Figure 20 shows a plot of the recorded voltage - i.e. the peak-to-peak value of the sinusoid - V, versus frequency at two recording distances from the stimulating partition. The line passing through each of the experimental plots is that calculated from equation 25 using the experimentally determined values of $\lambda = 328\,\mu$ and $\tau_m = 3.7$ msec. r_i was calculated from the specific total resistance to the flow of current, R_f, using a value for the fibre radius of $2.5\,\mu$, as before. The theoretical curve was then normalised around the experimental value at 1 Hz.

Figure 20 The frequency response of the fibre membrane as measured at two different distances from the stimulating plane. The filled squares are the data for a recording distance of 100μ from the plane, whilst the filled triangles are the data for a distance of 260μ. The lines are theoretical plots of eq. 25) using values of R_i: 588 Ω cms, λ = 328μ and τ_m = 3·7 msecs and normalised around the experimental value obtained at 1 Hz (see text for details). Experiment performed at 20°C in 0·1 mM Ca^{2+} Ringer.

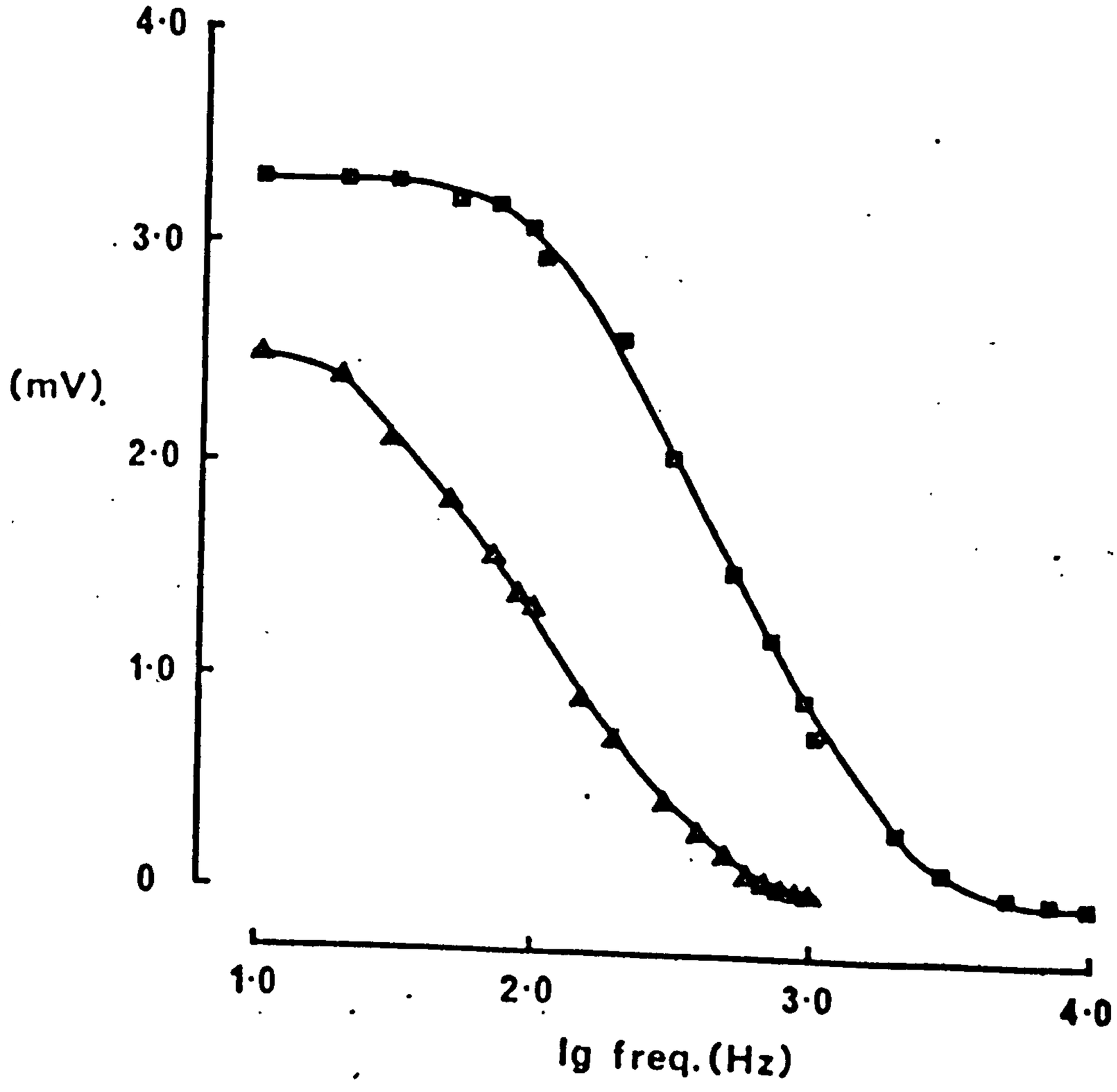
4·0
3·0
(mV)
2·0
1·0
0
1·0
2·0
3·0
4·0
lg freq.(Hz)

The plot shows that a one time constant model is adequate to describe the results. We must now consider why such a model will fit the results when two time constants have been indicated in the previous section on longitudinal impedance. Results similar to those above were obtained by Tasaki and Hagiwara (1957) with skeletal muscle fibres. However, Falk and Fatt (1964) on repeating the experiments obtained results consistent with a two time constant model and explained the previous results in the authors' failing to account for stray capacitative artifacts. Falk and Fatt pointed out that the variation of |Z| (equivalent to the recorded peak-to-peak sinusoidal voltage, assuming a constant current) with frequency was an insensitive test for the presence of one or more time constants and as long as the system contained only resistances and capacitances it was bound to decay monotonically with frequency.

Evaluation of the present data according to the one-dimensional cable theory of equation 25 presumes a constant value for the internal resistance. However, in the previous section it has been suggested that a further time constant exists in the intracellular pathway, so the question is what effect this would be expected to have on the measurement of |Z| over the frequency range used.

The intracellular pathway can be considered to consist of the cytoplasm resistance, r_c, in series with a parallel combination of the disk resistance, r_d, and capacitance, c_d. Using the previously obtained values of 350 Ω cm for the specific cytoplasmic resistivity and 1.14 Ω cm^2 and 0.29 mF cm^{-2} for the specific resistance and capacitance of the disc membrane (from the longitudinal impedance measurements), at an infinite measuring frequency the intracellular impedance will be 61 % of the d.c. impedance. At frequencies of 100 Hz and 1 kHz the intra-

cellular impedance will be 93% and 73% respectively. Thus, if the data is to be evaluated in terms of one-dimensional cable theory, then emphasis should be placed on data obtained at lower frequencies. Thus, the second reactive component, which would be expected to become manifest at its characteristic frequency of about 500 Hz, would be important in the upper extreme of the frequency used at the usual recording distance of 200-300 μ from the stimulating partition. It is doubtful whether such a two time constant model could be resolved considering the errors in recording the sinusoid at the higher frequencies.

Over much of the useful recording range - upward of 40 Hz, where $2\pi f\tau_m > 1$ - the internal resistance can be considered constant within a margin of 10-15%.

Taking into consideration the above limitation, to obtain more information about the individual circuit parameters producing such a response, the analysis was continued according to equations 26) and 27), assuming a single inside-outside admittance, as just discussed...

At $x = 0$, it is a consequence of equation 26) that the recorded voltage will be directly proportional to $f^{-\frac{1}{2}}$, giving a straight-line plot passing through the origin. At finite distances, however, this will not be true due to the exponential term which will produce an attenuation of the recorded voltage, increasing with distance. Thus, with increasing distances from the stimulating partition there will be an increase in the sigmoidal nature of the curve as it approaches the origin. Figure 21 shows such a plot of recorded voltage (again as the peak-to-peak value of the sinusoid) versus $f^{-\frac{1}{2}}$. Even at a recording distance of 100 μ from the stimulating partition the curve does not approach the origin by a straight line, so that no estimate of the membrane parameters

Figure 21 A plot of the intracellularly recorded peak-to-peak potential of the stimulating sine wave against the reciprocal of the square root of the frequency. The same data as in figure 20 are used. The lines are plots of equation 26) with the same parameter values as used in figure 20.

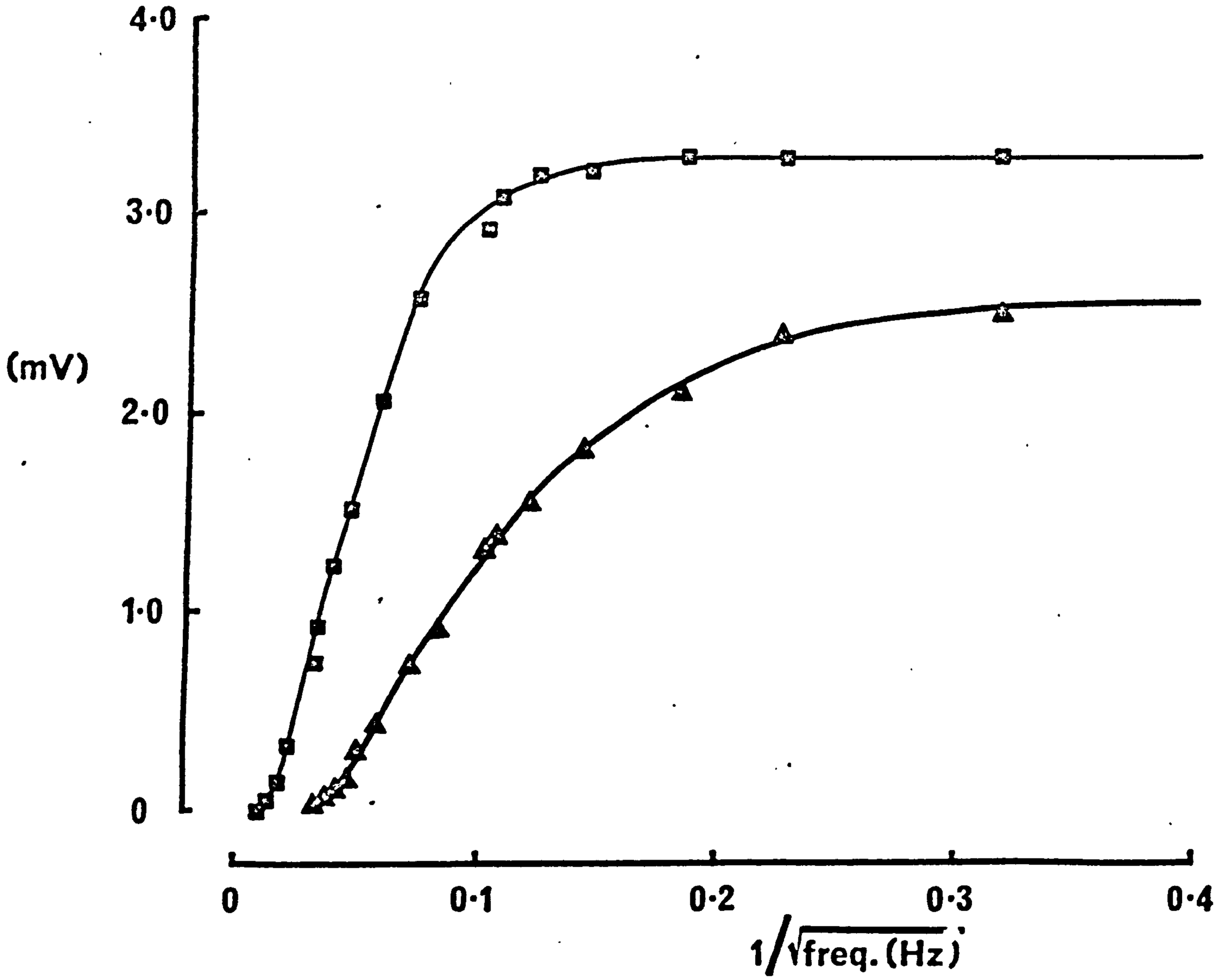
4·0
3·0
(mV)
2·0
1·0
0
0
0·1
0·2
0·3
0·4
1/√freq. (Hz)

can be made from the slope. It will also be noticed that the curve deviates from a straight line at $f^{-1/2} > 0.1$. This represents the invalidity of the approximation that $2\pi f \tau_m > 1$ that has been assumed in the calculation of equation 26 from equation 25.

Equation 26 can be rearranged, however, to give a straight-line plot as in equation 27, regardless of the recording distance, x, from the stimulating partition. In this case log $V.f^{1/2}$ is a linear function of $f^{1/2}$. Figure 22 shows such a plot with a straight-line relationship observed at frequencies greater than 150 Hz with the line through the points calculated from equation 25. Equation 25 was used as it predicted the voltage below the frequencies when $2\pi f \tau_m$ was not greater than unity. Thus, due to the logarithmic nature of the $V.f^{1/2}$ axis, such a quantity should decay exponentially with the square root of the frequency so that the frequency range where has fallen to 1/e (37 %) corresponds to $1/(x^2 r_i c_m)$ or $a/2x^2 R_i C_m$ from equation 27 on the condition that R_i and C_m are independent of the measuring frequency. Again, x is the distance from the stimulating partition and a is the fibre radius. The slope of the line is thus essentially a measure of the product $R_i C_m$ so that providing one is known the other can be calculated.

Thus, an estimate can be made of the membrane capacity by inserting the appropriate value of R_i. As has been suggested previously the value for the total resistance to current flow, R_f, seems the most suitable as this resistance takes into account the resistance of the cytoplasm and any intercellular junctions. The value of the bulk cytoplasmic resistivity would not account for the latter. Thus, if R_i has a value of 588 Ωcm, a value for the membrane capacity of 0.70 $\mu F\ cm^2$ (S.E. 0.29 $\mu F\ cm^{-2}$, 16 experiments) is obtained.

When f = 0 in equation 25, the equation reduces to the familiar form for direct current spread. Thus, it is evident that the quantity m in the exponential term of equation 25 will be a measure of the shortening

Figure 22 A plot of the logarithm of the product of the recorded potential and the square root of the frequency against the square root of the frequency. The same data are used as in the construction of figure 12. The lines are theoretical plots of a rearrangement of eq. 25). Equation 27) did not represent the observed results below 200 Hz as $2\pi f \tau_m \not> 1$. The slope of the straight line region above 200 Hz was used for a determination of the specific membrane capacitance.

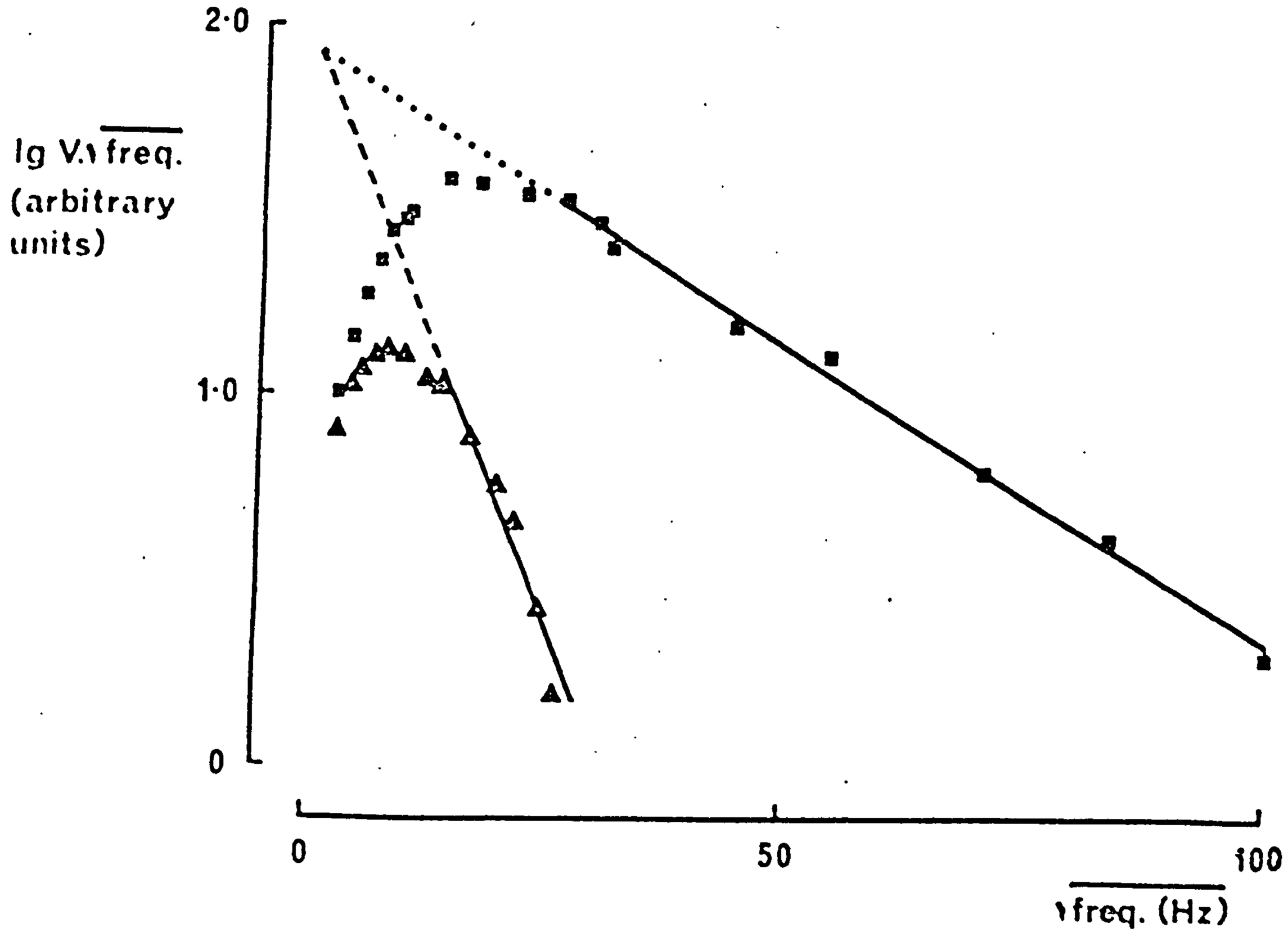
2·0
1·0
0
lg V freq.
(arbitrary
units)
0
50
100
√freq. (Hz)

of the space constant with increasing frequency. The quantity 1/m can now be defined as the attenuation function of equation 59). The concept can be understood more easily if one considers it merely as a gradual reduction in the membrane impedance due to the membrane capacity offering increasingly less impedance with higher frequencies, so that more current will leak through the membrane. The alternating space constant, $\lambda_{a.c.}$, will be related to the direct current space constant, $\lambda_{d.c.}$, as

$$\lambda_{a.c.} = \lambda_{d.c.}/m = (z_m/r_i)^2 \qquad 60)$$

The membrane resistance, r_m, has been replaced by the membrane impedance, z_m, so that the shortening of the space constant with frequency will be a measure of the membrane impedance with frequency. Again the assumption is made that r_i remains constant over the frequency range under test.

Figure 23 shows the results of one such experiment, in which the space constant was measured at different frequencies in a single trabecula. The line passing through the experimental points is that of 1/m - calculated on the basis of a single time constant model with a time constant of 3.7 msec and normalized around the value of the attenuation function at a frequency of 600 Hz. The close fit between experiment and theory indicates the adequacy of a single time constant model as a representation of the trabecula under these experimental conditions.

Intracellular Stimulation

Theory: A point source of current in a three-dimensional syncitium cannot be expected to have a simple distribution; two factors will contribute to the deviation from an exponential decay, the first of which is the radial currents within the cell and the second of which is the flow of currents through side

Figure 23 Decrease in the value of the attenuation function - or a.c. space constant - with increasing measuring frequency. The line is a theoretical plot of 1/m with a value for τ_m of 3·7 msecs and normalised around the space constant value obtained at 600 Hz. Experiment performed at 20°C in 0·1 mM Ca^{2+} Ringer.

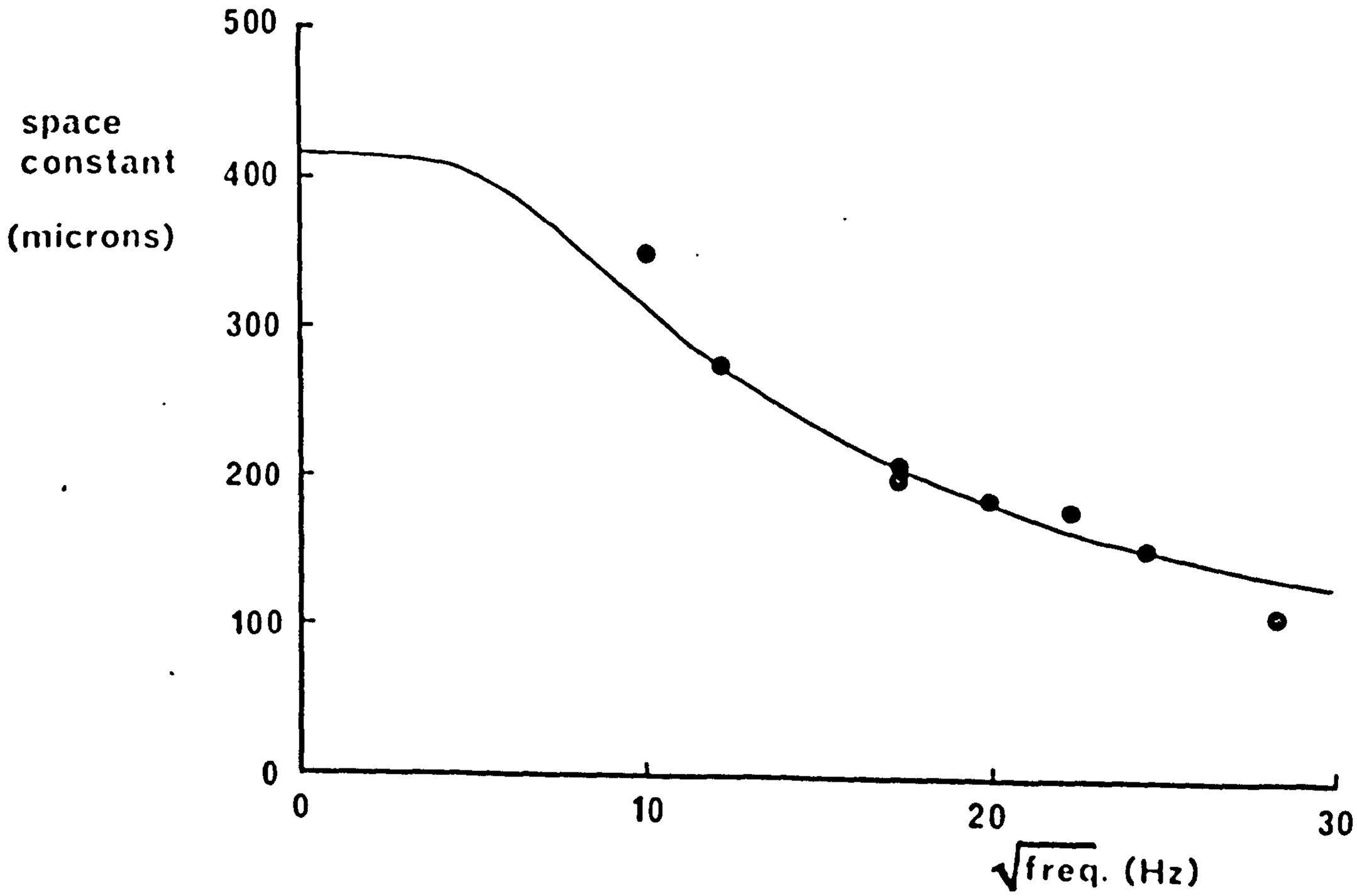
space
constant
(microns)
500
400
300
200
100
0
0
10
20
30
√freq. (Hz)

connexions to other cells. The first problem has been dealt with by Eisenberg and Johnson (1970), who produced a solution to the potential distribution problem in terms of a one-dimensional decay multiplied by some correction factor. This correction factor was a function of the interelectrode distance and the angle subtended between the two microelectrodes. It was for this reason that the two microelectrodes penetrated the trabecula vertically, so as to remove one variable quantity. However, for the case when the space constant is very much greater than the fibre radius, the correction factor quickly approaches unity, i.e. at a five micron interelectrode distance, the factor has a value of 1·01, so that this factor would in most cases be negligible.

The flow of current through side branches will produce a more serious deviation from unidimensional flow as it occurs at all points within the syncitium. A two-dimensional solution to the problem has been considered by George (1961) and Tanaka and Sasaki (1966), who proposed that the potential distribution was described by a Bessel function. The three-dimensional situation would be expected to produce an even steeper distribution of potential with distance.

A simplified approach to the problem has been made. There are two extremes for a syncitial system. Either the side connexions are so far apart that only flow along the axis is important (the solution of which is in Eisenberg and Johnson, 1970) or they are so close together that there is an equal probability that current will flow in any direction (neglecting for the moment any resistive barrier due to intercellular connexions). The latter case will thus be expected

to produce a series of spherical isopotentials radiating from the source of current.

Consider, in the first instance, a sphere of purely resistive conducting fluid of conductivity σ, which is homogeneous and isotropic throughout. Thus, Laplace's equations (eqs 12)) will hold.

In Cartesian coordinates, Laplace's equation is:

$$\nabla^2 V = \frac{\partial^2 V}{\partial x^2} + \frac{\partial^2 V}{\partial y^2} + \frac{\partial^2 V}{\partial z^2} \qquad 62)$$

making the transformations of x, y, z into spherical coordinates

$$x = r \sin\theta \cos\phi \qquad 63)$$

$$y = r \sin\theta \sin\phi \qquad 64)$$

$$z = r \cos\theta \qquad 65)$$

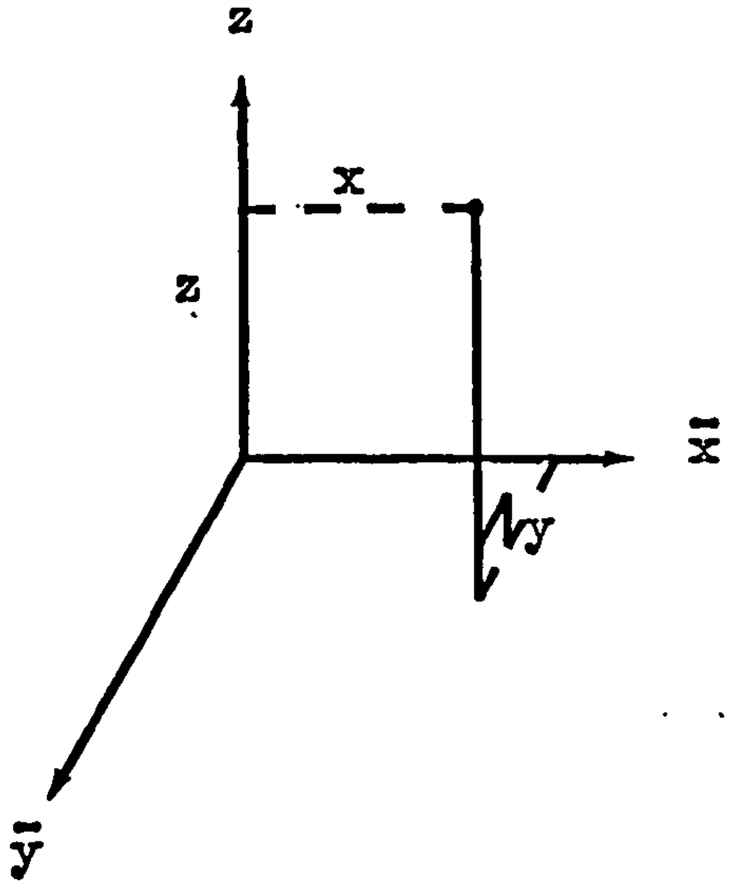

Cartesian coordinates

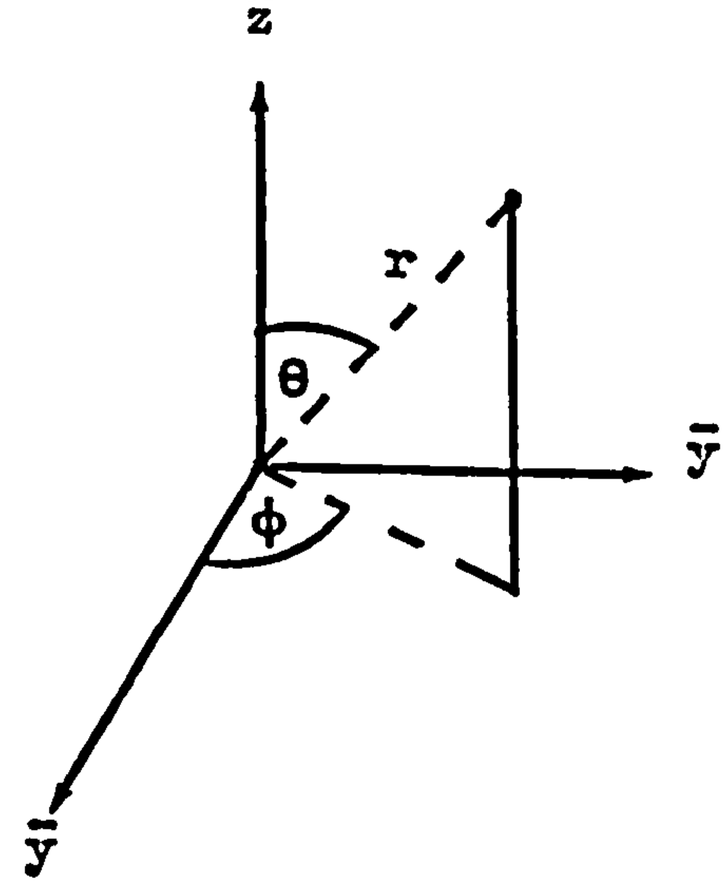

Spherical coordinates

Thus, Laplace's equation becomes:

$$\nabla^2 V = \left[\frac{1}{r^2}\frac{\partial}{\partial r}\left(r^2 \frac{\partial V}{\partial r}\right) + \frac{1}{\sin\theta}\frac{\partial}{\partial\theta}\left(\sin\theta \frac{\partial V}{\partial\theta}\right) + \frac{1}{\sin^2\theta}\frac{\partial^2 V}{\partial\phi^2}\right] \qquad 66)$$

When $\nabla^2 V = 0$, as previously discussed, there will be no current loss from the system and Laplace's equation can be solved accordingly. However, we must consider the situation when there is a current loss from the system, to a zero potential infinite in extent, which is proportional to the voltage and area. Thus, at every isopotential, current loss will be proportional to its area and the voltage at that region, if we assume it has an infinitesimally small thickness.

Thus, $\nabla \cdot \underline{j} = -k'V$ 67)

with $\underline{j} = \sigma \underline{E}$ 68)

and $\underline{E} = \text{grad } V = -\partial V / \partial r \ (\nabla V)$ 69)

where ∇ is the divergence (div) of the current vector flowing through a medium of conductivity, σ, and k' is a measure of the current loss which we will define later. From the relation

$$\text{div grad } V = \nabla \cdot \nabla V = \nabla^2 V \qquad 70)$$

the Laplace equation becomes

$$\nabla^2 V = (k'/\sigma)V = k'V. \qquad 71)$$

If we make the further assumption that V is a function of r (the distance from the point of stimulation), only so that there is no angular dependence, then

$$\frac{1}{r^2} \frac{d}{dr}\left(r^2 \frac{dV}{dr} \right) = k'V \qquad 72)$$

or

$$\frac{d^2V}{dr^2} + \frac{2}{r}\frac{dV}{dr} - k'V = 0 \qquad 73)$$

for $r \neq 0$.

If we make the substitution $u = rV$, then:

$$\frac{du}{dr} = V + r\frac{dV}{dr}\,;\ \frac{d^2u}{dr^2} = 2\frac{dV}{dr} + r\frac{d^2V}{dr^2}\,. \qquad 74)$$

Thus eq. 73) becomes

$$\frac{d^2u}{dr^2} - k'u = 0 \qquad 75)$$

which has a solution

$$u = A \exp (k')^{\frac{1}{2}}r + B \exp - (k')^{\frac{1}{2}}r. \qquad 76)$$

If we set the boundary condition that as $r \longrightarrow \infty$, $V \longrightarrow 0$, then $A = 0$, so that substituting for V

$$V(r) = \frac{B}{r} \exp - (k')^{\frac{1}{2}}r \qquad 77)$$

B can be evaluated by setting the potential V_R at some small distance R, so that

$$V(r) = \frac{V_R R}{r} \exp - (k')^{\frac{1}{2}}r. \qquad 78)$$

It is interesting to note that if there is no current loss - i.e. $k' = 0$ - then the solution reduces to

$$V(r) = \frac{V_R R}{r} \qquad 79)$$

which is that obtained by solution of Laplace's equation $\nabla^2 V = 0$.

To find a physical representation for k', let us consider Laplace's equation with a similar loss of current, in one dimension

$$\frac{d^2V}{dx^2} - k''V = 0. \qquad 80)$$

This has a solution in V of the form

$$V = a \exp (k'')^{-\frac{1}{2}}x + b \exp - (k'')^{-\frac{1}{2}}x \qquad 81)$$

with the same boundary conditions as before,

$$V(x) = V_o \exp - (k'')^{-\frac{1}{2}}x. \qquad 82)$$

Thus, $(k'')^{-\frac{1}{2}} \equiv$ the space constant, λ .

Thus, $(k')^{-\frac{1}{2}}$ will be equivalent to the three-dimensional space constant. The actual meaning of the space constant is not exactly equivalent to the experimental parameter due to the fact that the membrane area at any distance $[(r + \delta x) - r]$ from the stimulation point will not equal the surface area of that sphere; however, the voltage distribution will still be proportional to $1/r.\exp^{-r}$.

Finally, let us picture the situation when current flows preferentially along the longitudinal axis of the trabecula and, to a smaller extent, in the direction perpendicular to the axis - as indicated by Woodbury and Crill (1961). Thus, the isopotentials look like a series of prolate spheroids. This anisotropy can be defined by the conductivity tensor

$$\sigma_{i,j} = \begin{bmatrix} \Sigma & 0 & 0 \\ 0 & \sigma & 0 \\ 0 & 0 & \sigma \end{bmatrix} \quad \text{mhos cm}^{-1} \qquad 83)$$

so that if we consider the system in Cartesian coordinates, as we do not want angularly dependant solutions,

$$\Sigma \frac{\delta^2 V}{\delta x^2} + \sigma \frac{\delta^2 V}{\delta y^2} + \sigma \frac{\delta^2 V}{\delta z^2} = k'V \qquad 84)$$

For ellipsoidal surfaces of equipotential, the transformations are made that:

$$x = x' \; ; \quad y = y' \frac{\sigma}{\Sigma} \; ; \quad z = z' \frac{\sigma}{\Sigma} \qquad 85)$$

thus

$$\frac{\delta^2 V}{\delta x'^2} + \frac{\delta^2 V}{\delta y'^2} + \frac{\delta^2 V}{\delta z'^2} = \frac{k'}{\Sigma} V \qquad 86)$$

The form of the solution will thus be the same as equation 84) except that the loss factor, k', will depend on whether the potential is measured on the axis or perpendicular to it. Thus, if $\Sigma > \sigma$, a potential measured on the axis will be Σ/σ times greater than the potential measured at an equidistant point perpendicular to the axis, so that a 'cone' of results can be expected, the width of which will depend on the Σ/σ ratio.

A plot of the recorded potential versus the interelectrode distance is shown in figure 24 as a semi-logarithmic plot, for all the results obtained. The results for each 10μ group of interelectrode distances have been collected together (i.e. 10-19μ, 20-29μ interelectrode distances) and the mean interelectrode distance for each group plotted with the standard deviation.

Superimposed upon the experimental results are plots of three possible types of voltage distribution. Curve 1 is a plot of equation 78) using a value of 328μ for $(k')^{-\frac{1}{2}}$. It represents a three-dimensional flow of current in the continuum model just described. Curve 2 is for a modified Bessel function of the second kind of order zero (K_o),

Figure 24 The electrotonic spread of potential for a point source of current. The data for each decade of interelectrode distances were collected. The horizontal bars represent standard deviation of the interelectrode distances of each decade, whilst the vertical bars represent the standard deviation of the recorded potentials within the decade. The superimposed lines are theoretical plots of the potential distribution in different cable conditions. Line 1 is a plot of eq. 78) representing a three-dimensional spread of current. Line 2 is of the Bessel function $K_o(x/\lambda)$ and line 3 is of an exponential plot. In all cases, λ has a value of 328μ. Data are the accumulated results of all experiments performed. The experiments were performed at 20°C in 0·1 mM Ca^{2+} Ringer.

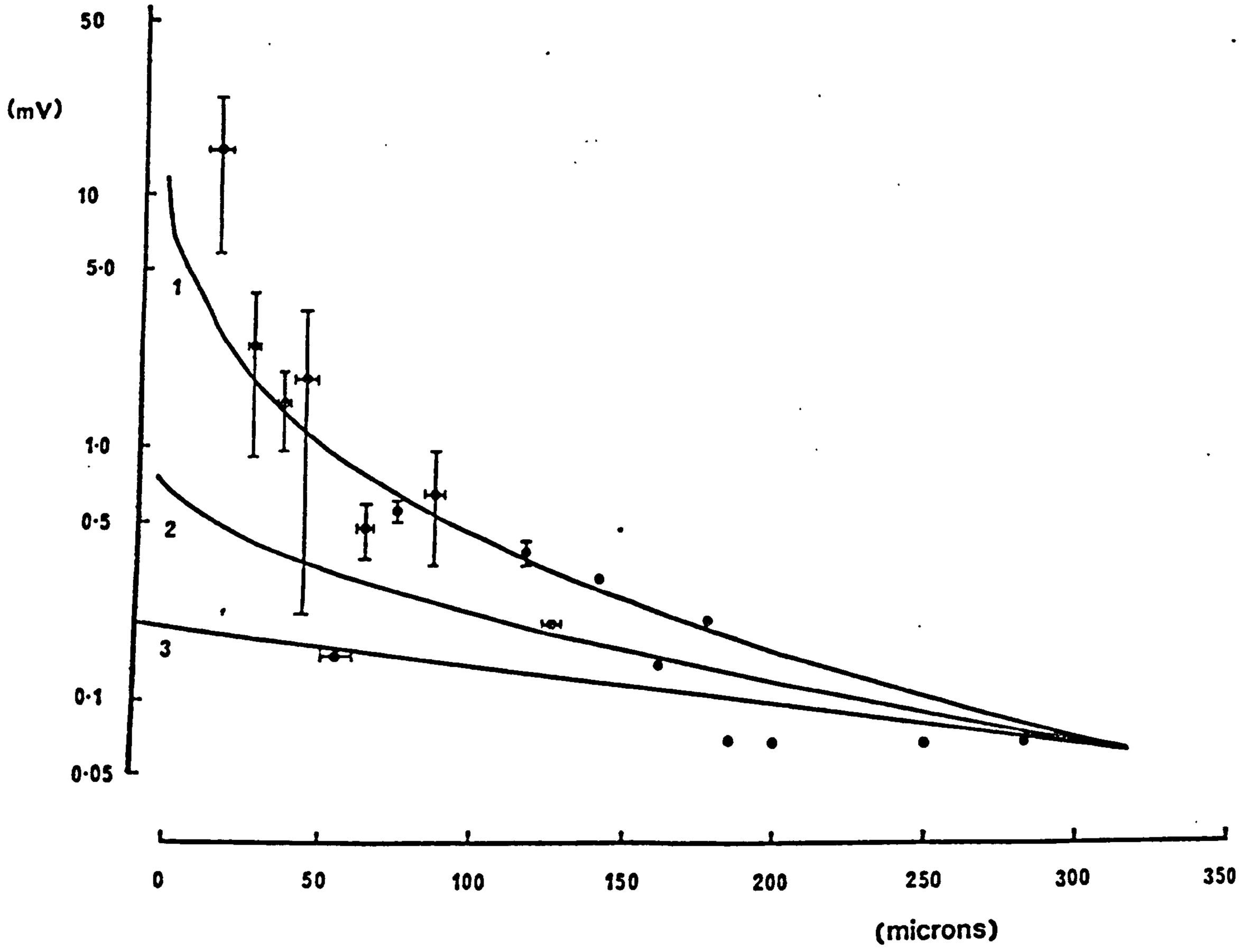
50
(mV)
10
5·0
1·0
0·5
0·1
0·05
1
2
3
0
50
100
150
200
250
300
350
(microns)

which should predict the voltage distribution of a two-dimensional network according to Tanaka and Sasaki (1966). Curve 3 is a simple exponential with a space constant of 328 μ.

As can be seen, one-dimensional cable analysis cannot be applied to this tissue with point stimulation, as is possible with Purkinje fibres (Weidmann, 1952). Thus, although it is not possible to determine precisely the degree of loss of current from the tissue or the Σ/σ ratio with any certainty, it seems that the distribution of potential follows that which would be expected from a freely-connecting three-dimensional syncitium of fibres. One important feature, thus, is that current is observed to spread from cell-to-cell without any large resistive barrier, which presumes that the inter-cellular connexions present little resistance to current flow. Thus, interaction was observed at interelectrode distances of up to 260 μ, which would include at least five intercellular barriers.

It must be admitted, however, that on many occasions - about 30% - no interaction was observed. These were usually at interelectrode distances of greater than 80 μ, although one case of non-interaction was observed at a 44 μ separation and another at 61 μ. However, these distances quoted are the minimum possible interelectrode distances - i.e. a straight line connecting the two microelectrode tips - and the actual current path may well have been more tortuous.

Table 9 Measured and Calculated Electrical Properties of Frog Ventricular Myocardium

Cytoplasmic resistivity, R_c, ohm cm	346 (±24, S.E. 20 experiments)
Resistance to the longitudinal flow of current, R_f, ohm cm	588 (±34, S.E. 9 experiments)
Intercalated disk resistance, R_{d_1}, ohm cm^2	1.2 (range 0.9 - 1.5)
R_{d_2}, ohm cm^2	2.4 (range 1.8 - 3.0)
R_{d_3}, ohm cm^2	1.14 (±0.19, S.D. 5 determinations)
Intercalated disk capacitance, C_d, mF cm^{-2}	0.29 (±0.05, S.D. 5 determinations)
Intercalated disk time constant, τ_d, msec	0.33 (±0.04, S.D. 5 determinations)
Space constant, λ, mm	0.328 (±0.022, S.E. 11 experiments)
Surface membrane time constant, τ_{m_1}, msec	4.15 (±0.55, S.E. 7 experiments)
τ_{m_2}, msec	3.7 (±2.0, S.D. 18 determinations)
Conduction velocity, θ, cm sec^{-1}	11.6 (±1.1, S.E. 11 experiments)
Time constant from the foot of the action potential, $\tau_{a.p.}$, msec	1.69 (±0.11, S.E. 11 experiments)
Membrane resistance, R_m, kohm cm^2	5.06 (range 4.22 - 6.00)
Membrane capacitance, C_{m_1}, μF cm^{-2}	0.73 (range 0.28 - 1.35)
C_{m_2}, μF cm^{-2}	0.64 (range 0.40 - 1.06)
C_{m_3}, μF cm^{-2}	0.70 (±0.29, S.E. 16 experiments)

Notes: S.D. values are given when only one experimental determination per trabecula (experiment) was obtained, i.e. in the longitudinal impedance measurements, and in the calculation of τ_{m_2} where random transients were chosen regardless of experiment.

. Parameter values calculated from measured values include a range of values which are calculated from the S.D. or S.E. limits of the measured parameter values.

R_{d_1} is the intercalated disk resistance calculated from the assumption that the disks are flat plates, 50 microns apart.

R_{d_2} is the intercalated disk resistance calculated from the desmosomal area.

R_{d_3} is the intercalated disk resistance calculated from measurements of the flow of alternating current along the trabecula.

τ_{m_1} is the membrane time constant calculated from propagation of the half value electrotonic potential.

τ_{m_2} is the membrane time constant calculated from curve-fitting the one-dimensional cable equations to the experimental records.

C_{m_1} is the membrane specific capacity calculated from the membrane time constant, τ_{m_2}.

C_{m_2} is the membrane specific capacity calculated from the foot of the action potential.

C_{m_3} is the membrane specific capacity calculated from measurements of the flow of alternating current along the trabecula.

DISCUSSION

The Intracellular Impedance

In the equations describing the core-conductor model, a single component, r_i, was designated to describe the interior of the model. This symbol gives no clue as to the precise electrical properties of the intracellular pathway and as has been shown, this component has reactive as well as resistive properties.

Knowledge of both the lumped component, r_i, and its subdivisions is important - the former for consideration of processes occurring over several cell lengths, i.e. propagated responses and electrotonic spread of current, the latter for characterization of the discrete units that comprise the cardiac syncitium.

In those tissues that can be treated as a one-dimensional cable with a point source of current, e.g. skeletal muscle fibres and Purkinje fibres, r_i can be calculated from the input impedance, using a microelectrode as a point source of current, with the equation:

$$R_{inp} = \left(\frac{V}{I}\right)_{x=0} = \tfrac{1}{2}\sqrt{r_m r_i} \qquad 87)$$

This has been attempted in Purkinje fibres by, among others, Weidmann (1952) and Fozzard (1966) and from the cross-sectional area of the fibres they could calculate the specific resistivity of the intracellular contents - see table 1. Such a procedure is not even theoretically possible in a syncitial structure such as the frog ventricular myocardium - even though it has been attempted by van der Kloot and Dane (1964) - because the use of a microelectrode as a current source does not produce a one-dimensional distribution. George (1961) has shown that in a closed syncitial

arrangement, in which fibres branch and re-join further along the network

$$R_{inp} \propto r_m^{\kappa} \qquad 88)$$

where κ varies between 0.5 and 0.25, the exact value depending on the frequency of branching and r_m.

The measurement of the resistance to flow of current is essentially a measure of r_i. It has been designated with the symbol R_f (the value can be directly calculated in specific values of ohm cm as the cross-sectional area of tissue is involved in the calculations) as it is primarily a practical concept, whilst r_i remains, in this tissue at least, a theoretical parameter.

The value of 588 Ωcm obtained for R_f of frog ventricle at 16.5°C is similar to the value of 470 Ωcm calculated by Weidmann (1970) at 37°C for mammalian ventricular trabeculae. However, it must be remembered that strips of frog ventricle were used for these experiments whilst trabeculae were used for the remainder of the d.c. cable analysis. Thus, although the fibres in the strip had the appearance of running in the same direction, the orientation of fibres along the longitudinal axis may not have been so good as within the trabeculae. This would show itself as a greater density of intracellular connexions per unit length, thus increasing the resistivity.

The specific resistivity of the cytoplasm has been measured by following changes in microelectrode resistance, R_{EL}, when a micro-electrode was transferred from outside to inside a myocardial cell.

Microelectrodes are unpredictable tools for measuring resistance changes, in that when they are intracellular various cytoplasmic and membranous components can be expected to attach themselves to the tip of the microelectrode which might cause changes in R_{EL}. However, the value of the method is that it provides information that is difficult to obtain by other means. Thus, the criteria for acceptance of data as listed in the results section were strictly adhered to. This is evinced in that only 27% of the microelectrodes fulfilled all the criteria.

It is necessary to know what volume of solution must surround the microelectrode tip for it to 'measure' its resistivity. The internal milieu of a cell consisting of a number of organelles, such as myofibrils, mitochondria, etc., will be composed of a number of high-resistance bodies in a more conductive enviroment. However, Schanne (1966) has estimated that if a microelectrode is surrounded by 3-5 microns of cytoplasm reliable measurements can be made. As this distance is close to the diameter of the cell it seems that the microelectrode will 'sense' the average impedance of the surrounding contents, so that provided the electrode is not close to the surface membrane its position should not seriously affect the measurements. Schanne (1966) quotes as a rule of thumb "that the cytoplasmic resistivity can be determined in a cell in which the membrane potential can be measured."

To compare the figure of 346 ohm cm obtained for frog ventricular myocardium at 16.5°C with estimated values from mammalian ventricle it will be best to calculate the value for frog ventricle at 37°C, at which temperature the mammalian experiments were mainly performed.

Assuming a Q_{10} of 1.37 (Hodgkin and Nakajima, 1972, for skeletal muscle), the value at 37°C is 182 ohm cm. Weidmann (1970) obtained a value of 470 ohm cm for R_f at 37°C in sheep and calf myocardium. If the intercalated disks are flat plates spaced at intervals of 125 microns (Marceau, 1904) with a specific resistance of 3 ohm cm^2 (Weidmann, 1966) the cytoplasmic resistivity has a value of 230 ohm cm. Using the same microelectrode method as described here however Schanne, Thomas and Ceretti (1966) found a value of 120 ohm cm for rat atrial cells.

The values for the total resistive pathway of Purkinje fibres are consistently lower however. Weidmann obtained figures of 105 ohm cm and 154 ohm cm at 37°C from input resistance measurements - Weidmann (1952) and Coraboeuf and Weidmann (1954), respectively - and a value of 181 ohm cm for R_f (Weidmann, 1970). Freygang and Trautwein (1970) obtained a figure of 110 ohm cm at 35-37°C from longitudinal impedance measurements. These values would not even account for the intercalated disk resistance if it is assumed that they have the same resistive properties as those in ventricular myocardium and are spaced at similar intervals (Freygang and Trautwein, 1970, assume a 100 micron spacing). However, it is of interest to note that the latter authors estimated that the disk specific resistance had a much lower value of 0.18 ohm cm^2. This would give values of 92-163 ohm cm for the cytoplasmic resistivity of Purkinje fibres at 35-37°C.

Similar values of 100-150 ohm cm at 35°C were estimated for the cytoplasmic resistivity of smooth muscle cells by Tomita (1966) and Abe and Tomita (1968), using impedance measurements.

Skeletal muscle fibres do not have the complications of intercellular junctions so that their values of r_i should be that of the cytoplasmic resistivity. Thus, values ranging between 159 ohm cm (Hartree and Hill, 1921) and 260 ohm cm (Katz, 1948) have been obtained at 20°C.

The general agreement between the figures for the three types of muscle suggests that they have a similar internal ionic enviroment, so that the data given by Conway (1957) concerning the internal milieu of skeletal fibres can be extended to cardiac and smooth muscle.

The electrical properties of the intercellular junctions are a more controversial subject. Work has been carried out in both amphibian and mammalian preparations and caution must be exercised in applying conclusions of one to the other. It was mentioned in the introduction that nexuses, present in the mammalian myocardium, are absent in the amphibian tissue and from the lack of any other structure it has been presumed that the desmosomes form the means whereby information is transferred from cell to cell.

Most of such studies have been carried out with mammalian tissues (cf. Woodbury and Crill, 1961; Tanaka and Sasaki, 1966; Weidmann, 1966) and the general body of opinion is that the individual cells are connected by low-resistance junctions - presumed to be the nexuses - so that the local circuits that precede an action potential can pass from cell to cell and transmission can proceed electrically. However, there is a view that the resistance between cells is high so that ephaptic electrical transmission or chemical processes would be needed

to mediate information transfer along the tissue. Most of the information leading to the latter conclusion emanates from the laboratory of Sperelakis and his co-workers (see Sperelakis, 1969, for references) and the location of acetylcholinesterase near the disks (Joo and Csilik, 1962) added support for their theory of chemical transmission. Plausible alternative explanations exist for most of their experiments with frog and mammalian tissues which do not necessitate the postulation of high resistance junctions. These have been amply summarized by Weidmann (1969), so that consideration here would be repetitious.

Measurement of the intercalated disk resistance has been undertaken by many authors who have found it to have a low value. An early demonstration of low-resistance pathways was with an elegant experiment of Barr, Dewey and Berger (1965). They showed that conduction, blocked in frog auricular trabeculae by placing the central portion in isotonic sucrose, could be recorded when a sufficiently low electrical shunt was placed across the sucrose-gap. This would have been possible only if both the extracellular and intracellular resistances were sufficiently low.

To calculate the specific electrical properties of the intercellular junctions it is, of course, necessary to have some knowledge of the geometry of the junction. The method that has been employed here is the least unsatisfactory procedure of measuring the relative desmosomal areas from electron micrographs. However, until the topological structure of the surface membrane is understood no figure can be attained with any certainty. An approach

to the problem has been made in mammalian preparations where it has been assumed that the low-resistance junctions lie within the intercalated disk. The mammalian intercalated disk is extensively folded and specialized into regions (Sjöstrand, Andersson-Cedegren and Dewey, 1958). Certain of these regions are believed to be the site of resistive coupling - i.e. the nexuses. In a study of rat ventricle Matter (1973) measured a disk surface to cellular cross-section ratio of 3.56, of which 7.5% of the disk surface was covered by nexuses. Thus, the nexal specific resistance would be much lower than the specific disk resistance based on the assumption of a functionally uniform intercalated disk. In their study of electrotonus in cultured heart cells, Jongsma and van Rijn (1972) took into account the ratio of nexal to total disk area and obtained a value of 0.25-1.25 ohm cm^2, depending on the degree of folding of the disk.

From consideration of the electrotonic spread of current, Woodbury and Crill (1961) obtained a value of 1.2 ohm cm^2 in rat atrial myocardium, making some assumptions about the disk geometry. An upper limit of 2 ohm cm^2 was obtained by Tanaka and Sasaki (1966) by similar experimental techniques. Impedance measurements, as described in the text, have given lower values for Purkinje fibre disk resistances of 0.18 ohm cm^2 (Freygang and Trautwein, 1970). Whether such a difference is significant or not is difficult to say, but there could be some advantage in Purkinje cells having a lower electrical contact resistance in view of their conducting rôle. It is of interest to note that Tomita (1966) - by similar impedance measurements on a smooth muscle preparation - gave a value of 1.8 ohm cm^2, similar to that of ventricular myocardium.

Another approach taken by Weidmann (1966) was to measure the resistance to the flow of radioactive potassium along a trabecula as compared to the resistance to its flow over the surface membrane. A figure of 3 ohm cm^2 was obtained for the specific intercalated disk resistance. This work has been extended by Imanaga (1974) and Weingart (1974), who have shown that, using the dye Procion Yellow and C^{14}-labelled TEA respectively, the disk is much more permeable than the cell membrane. The ratio of nexus to surface membrane permeability is 9,600 for K^+ (mol. wt 39), 21,000 for TEA (mol. wt 130) and 220 for Procion Yellow (mol. wt 700). From such considerations, Weingart estimated that the mammalian nexuses have pores of about 10 Å in diameter connecting one cell to another.

Theoretical calculations arrive at a similar conclusion. Heppner and Plonsey (1970) and Woodbury and Crill (1970) have considered a model of two inexcitable membranes separated by some small distance (80 Å), similar to that found at the desmosomes. From considerations of the potential field in the intergap region it was calculated that the maximum possible value for the junctional resistance was 4 ohm cm^2 if electrical transmission was to occur.

Further evidence that the cells are connected by low-resistance junctions has been given by the electrotonic spread of current. With a microelectrode as an intracellular source of current, membrane potential changes have been recorded as far as 280 microns distant. The voltage distribution follows fairly closely the simplified three-dimensional model that has been presented, which presumes a lumped intracellular conductivity comprised of the intracellular contents

and the junctional membranes. This is contrary to the experience of Tarr and Sperelakis (1964) who found a sharp discontinuity of current spread at distances greater than 60 microns. However Woodbury and Crill (1961) working with a pinned-out rat auricle, found that interaction was evident at 500 microns from the current electrode, so that current did flow from cell to cell. In rabbit myocardium Tille (1966) recorded interaction up to 800 microns from the stimulus point, but stressed that such pathways were relatively rare and suggested that the fibres might be arranged in small bundles with resistive connexions within each bundle but rarer between bundles. More extensive measurements made by Tanaka and Sasaki (1966) in mouse preparations showed that there was no great discontinuity in the potential distribution between 20 and 250 microns, and described the current as flowing in a two-dimensional syncitium.

In the results described here no attempt has been made to divide the records into those obtained on the axis or transverse to the fibre axis as was done by Woodbury and Crill and Tanaka and Sasaki. Even if the two microelectrodes were on the same axis the problem of side-to-side connexions would still arise if they were at different depths. As the accuracy of measurement of the microelectrode tip position was 5 microns (the same as the cell diameter) such a procedure was not justifiable. Rather, any difference in the transverse or longitudinal resistances would show itself in the Σ/σ ratio - the scatter of results at any one interelectrode distance.

An inherent error in such measurements was that the microelectrode distance was a straight line between the two microelectrode tips. The real pathway may however have been more tortuous, so that the quoted distances will always be minimum ones.

The explanation presented in the results section to account for the large capacity in the longitudinal pathway is that the region between the membranes of opposing cells at the desmosomes is one in which ions can be accumulated or depleted - similar to that suggested by Fatt (1964). How such a process can be acheived will have to await the finding of whether or not the membrane is excitable in this region. In much of the theoretical work it has been assumed to be inexcitable (e.g. Heppner and Plonsey, 1970).

One possible explanation is an extension of the studies of Woo and Wei (1973) with artificial membranes. They suggested that the capacity of such films could be represented by three capacities in series - the capacity of the hydrocarbon film flanked by two interface capacities, the latter due to the dipole layer at the membrane surface and the diffused double layer in the aqueous phase adjacent to the membrane. The former capacity was always predominant as it had a value some 50 to 100 times less than the latter. They calculated that at conditions approximating the extracellular or intracellular space in ionic strength and pH such interface capacities would have a value of about 0.1 mF cm^{-2}. If in a situation where the hydrocarbon capacity was short-circuited, as is possible at the intercalated disk, the interface capacity would become predominant. This presumes that this capacity should be dependent on the ionic strength, contrary to observation, and it can only be presumed that under the conditions used the desmosomal space was not affected by changes in the extracellular solution.

It is interesting to note that the maximum reactance offered in the longitudinal pathway - at about 700-800 Hz - corresponds fairly closely to the frequency of the rising phase of the action potential. Thus, the impedance offered at such frequencies will be most sensitive to any perturbations in the frequency. Whether this has any functional significance is not known but a similar correlation may exist with Purkinje fibres.

The Membrane Capacity and Resistance

The value of about 0.7 $\mu F\ cm^{-2}$ for the surface membrane capacity of frog ventricular muscle agrees well with estimations from mammalian ventricular muscle (Sakamoto, 1969; Sakamoto and Goto, 1970; Weidmann, 1970) and is in reasonable agreement with values from auricular preparations (e.g. Sakamoto and Goto, 1970; Bonke, 1973) - see table 1. It has been assumed in the calculation of these values that the fibres are cylinders with a circular cross-section. It has been shown that there is no T-tubular system in the frog ventricular myocardium which would serve to increase the surface area (e.g. Staley and Benson, 1968). However, Lorber and Bertaud (1971) have demonstrated the presence of micropinocytotic vesicles on the surface of frog atrial cells. Similar vesicles have been seen in ventricular cells also, which may increase the surface area by as much as 15%, although no rigorous study has been made of this point (P.-Y. Hatt, personal communication). Also an increase in the ellipticity of the cell will increase the surface-to-volume ratio. All of these factors will increase the

assumed surface area and so decrease the membrane capacity. A converse correction factor suggested by Weidmann (1970) is that fusion of the membranes of adjacent cells might reduce the membrane area - there is some evidence for such a situation in mammalian fibres (Sommer and Johnson, 1968) but less evidence in the frog myocardium. Thus, until the relative magnitude of these corrections can be estimated, a precise value of the membrane properties cannot be attained.

Weidmann (1952) and Fozzard (1966) applying a similar analysis to Purkinje fibres found that the calculated membrane capacity varied according to whether it was determined from the membrane time constant - using d.c. pulse analysis - or the time constant from the foot of the action potential; the former being about five times larger than the latter. They suggested that the membrane was electrically separated into two regions - one portion was the outer membrane of the bundle of Purkinje fibres and the other consisted of the membrane in the clefts that separate the individual cells in a Purkinje fibre bundle. Thus, the model consisted of part of the membrane being in series with a variable resistor - the series resistance - having an equivalent electrical circuit of figure 16A.

The only way to show that more than one capacitance is involved in the inside-to-outside admittance of a cell is to examine the passive electrical properties at different frequencies. This was the case in the above work with Purkinje fibres. However, in frog ventricular myocardium τ_m and $\tau_{a.p.}$ are so similar in value that they provide no information in themselves whether there is one or more time constants associated with the surface membrane. However the low value of the

membrane capacity indicated little electrical separation of the surface membrane so the second time constant, observed in the longitudinal impedance experiments, was placed at the desmosomes and not at the intrafibral clefts, i.e. at a position less accessible to the extracellular electrical continuum. Such a model places the desmosomal membrane in the intracellular pathway, although it may be morphologically continuous with the surface membrane.

The exact value of the membrane resistance is subject to the same uncertainties as is the capacity, due to an inadequate knowledge of the membrane topology, so that an underestimation of the membrane area will tend to underestimate the specific resistance. A value of 5.06 kohm cm^2 is obtained using a value of 588 ohm cm for R_i, which is in reasonable agreement with values from mammalian ventricular and auricular preparations (Sakamoto, 1969; Sakamoto and Goto, 1970; Weidmann, 1970; Bonke, 1973) - see table 1.

The studies carried out involving action potential measurements were performed with an external calcium concentration of 0.1 mM - including the intracellular stimulation studies - and the remainder were carried out in 1 mM calcium. It has been shown by Weidmann (1955) with Purkinje fibres and Haass (1975) with mammalian ventricular muscle that large changes in the external calcium concentration have little effect on the membrane resistance and a similar situation has been assumed in the frog ventricular myocardium. This finding is contrary to that found in skeletal muscle, however (Tamashige, 1951).

From studies of radioactive potassium flow, Weidmann (1966)

calculated that the K^+-resistance of the surface membrane of ventricular fibres was 13.8 kohm cm^2, as compared to the electrical resistance of 9.1 kohm cm^2. This presumes that there is some other ionic flux over the membrane. In frog ventricle however the flux studies of Lamb and McGuigan (1968) have estimated that the potassium conductance in a quiescent state is 200 μmho cm^{-2} which compares very favorably with the measured electrical resistance. In both cases however the major permeant ion is not chloride, unlike the position in skeletal muscle (see also Carmeliet, 1961).

Studies with Artificial Membranes

The concept of the cell membrane as we regard it today was laid down by the studies of Gorter and Grendel (1925) and Danielli and Davson (1935). Basically, the structure is a bimolecular sheet of lipid molecules arranged so that the hydrocarbon tails - consisting of long-chain fatty acids - lie in the centre of the membrane, whilst the polar groups face the outside. Covering the bilayer on both faces are attached protein molecules, which may penetrate the lipid region.

The arrangement and type of protein molecule confers the various properties on the particular cell membrane (see for example, Kavanau, 1965). The lipid portion on the other hand is believed to give the gross physical characteristics to the membrane.

Because the individual membrane components - especially the proteins - are so little understood, various studies have been directed towards the properties of artificial lipid membranes and membranes formed from extracts of various cellular and membranous material.

Stable lipid bilayers were first described by Müller, Rudin, Tien and Wescott (1962a,b). The appearance of these films was similar to the black soap films whose thickness was of the order of 100 Å, or less. Thus, the study of such films should give some information as to the characteristics of biological membranes, which have a similar thickness.

The capacity of such membranes is about 0.6 $\mu F\ cm^{-2}$ (Fettiplace, Andrews and Haydon, 1971). These authors found that the capacitance decreased if solvents of shorter chain length were used, finding a value of 0.4 $\mu F\ cm^{-2}$ using n-decane, rather than n-hexadecane. The latter figure was similar to results obtained by other authors (e.g. Hanai, Haydon and Taylor, 1965; White, 1970; White and Thompson, 1973) and was attributed to the presence of solvent remaining in the lipid film and so increasing its thickness.

The similarity of these results to that of the frog myocardial cell membrane indicates that the membrane capacity is primarily located in the hydrocarbon region of the cell membrane.

If the lipid bilayer membrane is treated as a parallel-plate condensor with a static impedance, C_a, then

$$C_a = \frac{\varepsilon_o \varepsilon_m A_m}{4\pi d_m} \qquad 89)$$

where $\varepsilon_o = 1.11.10^{-12}$ F cm^{-1} (the specific capacitance of free space), ε_m is the effective membrane dielectric coefficient and d_m and A_m are the membrane's thickness and area, respectively. Thus, a lecithin black film of 0.6 $\mu F\ cm^{-2}$ capacitance (Fettiplace, Andrews and Haydon, 1971) will have a thickness of 31 Å, assuming a dielectric coefficient of 2.1.

Some estimate of the properties of the hydrocarbon region of the plasma membrane can thus be made. The plasma membrane has been measured

as 60 Å thick in mammalian cardiac cells (James and Sherf, 1970) which includes the outer protein layers, whilst Casper (personal communication in Fettiplace et al.) has estimated from X-ray diffraction studies that the hydrocarbon region in nerve myelin has a thickness of 35 Å. If the latter figure is inserted into equation 89) then with a measured capacity of 0.7 $\mu F\ cm^{-2}$ a value of 2.77 is obtained for the dielectric coefficient of the hydrocarbon region. This is similar to the dielectric coefficient of many oils and unsaturated fatty acids (see table 9) indicating that the latter do occur in the plasma membrane. This value of the dielectric coefficient is smaller than the value of 6-10 assumed by Tasaki (1955) with nerve fibre measurements. However, this was used in conjunction with a value of 3-7 $\mu F\ cm^{-2}$ for the surface membrane capacity, higher than is usually accepted today.

The capacitance of the two membrane interfaces must therefore be very much greater than that of the hydrocarbon region, if it is presumed that all three capacities lie in series. Each interface capacity will be due to the dipole layer at the membrane surface and the diffuse double layer in the phase immediately adjacent to the membrane. The capacity arises due to the effect of the fixed negative charges on the membrane. The large electrical field due to the membrane will polarize and immobilize neighbouring water molecules, resulting in a decrease in the dielectric constant immediately around the ions compared to the value in the bulk solution or around single mobile ions (Stern, 1924). Such a dielectric decrease increases ion and dipole interactions so that the counter-ions nearest to the membrane are adsorbed to form the so-called Stern layer. The more distant counter-ions, which form the

Gouy-Chapman layer, are more mobile, but the membrane electric field still hinders their movement. Thus, changes in ionic strength would be expected to change the width of such layers, especially the latter, as even at low ionic strengths from 60 - 85% of the counter-ions are in the Stern region (e.g. Stigter and Mysels, 1955). Such an approach has been undertaken by Woo and Wei (1973), who found the interface capacity to fall in low ionic strength and low pH solutions, using black lipid membranes. However, such interface capacitances were always greater than 8 $\mu F\ cm^{-2}$ whilst the hydrocarbon capacity was about 0·45 $\mu F\ cm^{-2}$, so that the latter capacity was always predominant. They regarded such large capacities as ensuring the stability of the membrane against a variety of conditions.

The resistance of such lipid films does not give comparable values to biological membranes however. Thus, whilst the latter have values in the range of 10^3 - $10^4\ \Omega\ cm^2$, lipid films have values from 10^6 - $10^8\ \Omega\ cm^2$ (Henn and Thompson, 1969). However, a number of substances added to such films reduce the resistance to more biological values. Usually, they are macromolecular components such as those isolated from retina or white matter - which also induce a gating reaction to d.c. stimuli - or nonactin. However, Läuger et al. (1967) have observed that substituting iodide for chloride ions also greatly reduces the resistance. However, it can be reasoned that the permeability of the biological membrane to substances is largely dependant on the protein coat which imparts the particular specificity peculiar to one type of membrane. Ling (1973) has suggested that proteins on the cell surface, acting in concert with layers of polarised water deeper in the

membrane - possibly surrounding and constricting a pore diameter - could serve to make the membrane semipermeable: a process which would certainly allow diffusion through such a pore to occur (Patlak, 1973).

The Space Constant

The most important conclusion that can be drawn from the value of the space constant is that when a trabecula is reduced to a one-dimensional system, so that it is presumed that current does not flow between lateral connexions, electrotonic interaction can be observed in adjacent cells in the longitudinal axis - i.e. the space constant is greater than a single cell length.

The space constant in itself is merely a ratio of the square root of the membrane and internal resistance and as the internal resistance can vary depending in which direction within the trabecula it is estimated the coordinate system in which the space constant was measured should be specified. Thus, if the dimension along which current was passed was perpendicular to the average fibre direction, it would be expected that the space constant would be smaller. This would be due to the increased intracellular resistance due to the greater number of lateral connexions per unit length than end-to-end connexions in the longitudinal axis direction. Evidence of this was seen in the experiments of Woodbury and Crill (1961), in which they noted that with intracellular application of current decay was greater perpendicular to the trabecula axis direction. Sano, Takayama and Shimamoto (1959), using dog ventricle strips, found that the conduction velocity - which is proportional to $R_i^{-\frac{1}{2}}$ (Hodgkin, 1954) and hence proportional to the

space constant - was greater in the fibre direction than perpendicular to it. Recently, Weidmann (personal communication) has estimated that the space constant in the direction perpendicular to the fibre axis in mammalian trabeculae is some three times smaller than in the direction of the fibre axes.

The present value of the space constant thus refers to the value obtained in the fibre direction and the calculation of the value perpendicular to the axis can be carried out by evaluation of the internal conductivity tensor - as given in eq. 83).

The value of 328μ obtained for the space constant is fairly low if it is compared with the results of larger-celled cardiac preparations. The space constant is proportional to $a^{\frac{1}{2}}$ (a is the fibre radius) so that the result can be directly compared to other values. Weidmann (1970) gives a value of 960μ for the 15μ diameter ungulate ventricular cells, whilst other workers give figures of 1·20 - 1·35 mms for canine preparations with a quoted diameter of 16μ (Sakamoto and Goto, 1970; Sakamoto, 1969). If Weidmann's value is used, then a figure of about 550μ can be calculated for the 5μ diameter frog ventricle cells, which is greater than the value obtained. It is interesting to note that Bonke (1973) obtained a value of 660μ for 12μ diameter rabbit atrial cells, whereas a figure of 860μ is calculated from Weidmann's work. That the relationship between space constant and fibre diameter does exist in cardiac cells is indicated in that a figure of 2·15 mms is predicted for the 75μ diameter Purkinje cells, which compares favourably with the experimental values of 1·9 mms (Weidmann, 1952) and 2·24 mms (Fozzard, 1966).

Thus, a real discrepancy could be due to a difference in the cellular parameters between the frog and mammalian preparations - i.e. r_m or r_i - or some deviation from one-dimensional cable theory with the partition method of stimulation in the frog tissue. However, it has been indicated in the results section that any serious deviation from one-dimensional cable analysis is unlikely.

The temperature difference in the determination of the space constant in the amphibian and mammalian muscles may in itself not be important. Coraboeuf and Weidmann (1954) found that in mammalian preparations R_m and R_i both had Q_{10} values of about 1.5. However, Dulhunty and Gage (1973) have observed a reduction in the membrane resistance and an increase in the internal resistance of sartorius muscles in winter frogs as compared to summer frogs. This was reflected in a decreased space constant and they suggested that keeping the frogs in cold conditions might have the effect of 'winterising' them. This could explain some of the discrepancy between the observed and expected values of the space constant because mammals, being warm-blooded, would not be subjected to such seasonal changes of condition.

It is generally considered that the hydrocarbon chains in the membrane phospholipid exist in a liquid state (Gitler, 1972), the degree of fluidity depending on the relative amounts of saturated and unsaturated fatty acids in the phospholipids. Unsaturated fatty acids

have a lower melting point than their equivalent saturated fatty acid and it has been noted (Fox, 1972) that cells at a low temperature have a greater proportion of unsaturated fatty acids. This is to maintain the fluid nature which is, presumably, important for the proper functioning of the membrane. However, with unsaturated fatty acids present, stacking of the hydrocarbon chains is not so easy and transport processes have been observed to occur some twenty times faster (Wilson, Rose and Fox, 1970). This has been verified by studies with monolayers of unsaturated fatty acids. Closer packing is possible in the trans form than in the cis form of monounsaturated fatty acids (Schneider, Holman and Burr, 1949) as cis molecules - the form usually found in membranes (Oncley, 1959) - are unable to align either with themselves or trans molecules. Thus, Glazer and Goddard (1950) found that trans-9-octadecanoic acid forms very condensed films with a low resistance to water penetration, whilst the cis forms are highly expanded. So far, these reports have been confined to studying galactose and glucose transport in micro-organisms, but it is of interest to note that Arrhenius plots of transport show a transition phase at about 13-15 ^{o}C (Wilson, Rose and Fox, 1970; Overath, Schairer and Stoffel, 1970). This is similar to the transition temperature observed for the Na^{+}-K^{+}-activated ATPase present in mammalian brain membrane preparations (Priestland and Whittam, 1972).

This enzyme - the sodium pump enzyme - is present in the cell membrane and has been shown to be closely associated with phosphatidylserine for proper functioning (Wheeler and Whittam, 1970), so that similarities could exist with the microbial systems. Thus, if the permeability to ions is increased at lower temperatures, this would become manifest in a decrease in the value of the membrane resistance.

Membrane capacity values will also alter due to the introduction of unsaturated fatty acids. Reference to table 9 shows that as the degree of unsaturation increases from stearic to linoleic acids the dielectric constant increases, so that introduction of increasing amounts of unsaturated fatty acids will increase the dielectric constant and hence the membrane capacity. This is opposite to the findings of Dulhunty and Gage (1973) - i.e. they found a decreased membrane capacity in winter sartorius muscles - so that possibly the membrane thickness also increases, which would serve to decrease the capacity.

Although the fall in the space constant during the series of experiments was not statistically significant, the fact that it was found necessary to add glucose to the Ringer to obtain normal electrical responses with some frogs indicated that some physical deterioration may have occurred. The frogs used in

Table 9. Dielectric Constants of Some Saturated and Unsaturated Fatty Acids

			ε_{70}	ε_{20}
Palmitic acid	(C_{16})	$CH_3.(CH_2)_{14}.COOH$	2·30*	
Stearic acid	(C_{18})	$CH_3.(CH_2)_{16}.COOH$	2·29*	
Oleic acid	(C_{18})	$CH_3.(CH_2)_7.CH{=}CH.(CH_2)_7.COOH$	2·45*+	2·46*
Linoleic acid	(C_{18})	$CH_3.(CH_2)_3.(CH_2.CH{=}CH)_2.(CH_2)_7.COOH$	2·70*	2·70*
Linolenic acid	(C_{18})	$CH_3.(CH_2.CH{=}CH)_3.(CH_2)_7.COOH$	2·97x+	2·76x

ε_{70}, ε_{20} = dielectric constant at 70°C and 20°C respectively.

ε_{20} (H_2O) = 80·18

ε_{vacuum} = 1

\+ dielectric constant at 60°C not 70°C

* data from Handbook of Chemistry and Physics (1971-1972)

x data from Markley (1960)

these experiments were starved and kept at 4°C, so that they were winter-conditioned. There is evidence that in winter frogs metabolism is largely fat-based (Freeman, Satchell, Chang and Gay, 1968) and it has been observed that metabolism of endogenous lipids can occur if exogenous fatty acids are absent (Shipp, Thomas and Crevasse, 1964; Crass, McCaskill, Shipp and Murthy, 1971). The observation of Shipp Thomas and Crevasse suggested that the fatty acids for oxidation were derived from phospholipids and triglycerides. Crass et al. (1971) found that although the total phospholipid content was unchanged, it seemed that the ester groups were turning over, possibly reflecting acyl transfer from other lipid esters and/or free fatty acids, so that the fatty acid composition of the membrane phospholipids could be altered.

In addition, the fact that addition of glucose eventually changed the mechanical and electrical responses suggests that the endogenous lipids were in low supply, because the heart oxidises endogenous supplies of triglycerides in preference to exogenous glucose. This suggests that just prior to the addition of glucose to the Ringer, oxidisable foodstuffs were in low supply. This could affect the membrane in a number of ways. Either some membrane lipids could be mobilised for oxidation, thus impairing the integrity of the membrane - which could include the sodium pump system - or the supply of ATP to the sodium pump enzyme would eventually become reduced.

Cable Complications in Voltage-Clamp Studies

In the light of the present results, the applicability of the sucrose-gap technique of voltage-clamping to cardiac preparations should be discussed. In the period covered by the present study, several papers have been published which have concerned themselves almost wholly with the feasibility of this technique and they suggest that a considerable re-examination is necessary.

Due to the low-resistance connexions between cells, it can be concluded that the sucrose-gap technique is applicable to frog ventricular myocardium as current is able to pass from the current pool to the central node via the intracellular pathway. Such studies with frog ventricle have already been reported (Morad and Orkand, 1971) and a large amount of work with frog auricular trabeculae has also been reported (Rougier, Vassort and Stämpfli, 1968; Haas, Kern and Einwächter, 1970; Besseau, 1971; Léoty and Raymond, 1972), so that the conclusion is not a surprising one.

However, one must be concerned with the quality of the voltage clamp within the test region and this will be determined by the cable properties of the preparation. Morad and Orkand (1971), using a single sucrose gap, reported that adequate voltage control was achieved - as measured with a microelectrode - in

the absence of any quickly changing currents over a length of 0·3 to 0·5 mms. However, with the measured space constant of 328μ, the voltage of the terminal end of a cable which has one sealed end - representing the preparation - will have decayed to 69% - 42%. Morad and Orkand (1971) and Einwächter, Haas and Kern (1972) however, conflict in their ideas of what an inadequate clamp looks like.

One explanation that has been mooted recently is as to the actual definition of the space constant. It has been found that the more stable preparations were those with a larger diameter (New and Trautwein, 1972; Harrington and Johnson, 1973; McGuigan, 1974) and it has been suggested that side-to-side connexions will increase the effective diameter of fibres and so increase the space constant, which in turn will improve the homogeneity of the clamp.

It is doubtful however, whether such an argument is completely justifiable because the space constant was measured in a similar way to which current is passed into the test region of the preparation - i.e. as a planar source perpendicular to the longitudinal axis of the preparation. It is more likely that in the larger diameter preparations, a greater proportion of the fibres will be in a more healthy condition, so

that greater overall stability is achieved. Harrington and Johnson (1973), using rabbit ventricular trabeculae 30 - 80μ in diameter, claimed that the life of a trabecula was 5 minutes or less, but rarely up to 20 minutes, whereas Morad and Orkand quote a life of 6 hours for their ventricle strips. It is more likely, using a single sucrose-gap, that voltage non-homogeneity depends upon where the control microelectrode is placed in the preparation. New and Trautwein (1972) showed that with the control microelectrode at the end of the preparation, a great deal more current is needed than if the electrode is at the sucrose/Ringer border. In the former case, an independent measuring microelectrode at the sucrose/Ringer border recorded a very large transient voltage change, which never reached a stable state. With the situation reversed, the independent microelectrode - now at the preparation terminus - reached a steady-state value before the end of the 110 msec pulse. Thus, they concluded that control at the end of the preparation makes the system more vulnerable to oscillations than control at the sucrose/Ringer border - when the preparation is out of the feedback loop - which does not produce such large voltage variations in the preparation. As previously stated, they found that not just short, but wide diameter preparations were the most stable. One must note however, that in some of the data with an independent microelectrode measuring the membrane potential, although it shows no temporal changes during the clamp pulse (cf. fig. 7 of New and Trautwein, 1972), the potential is different from that recorded extracellularly, the error increasing with increasing pulses. This means that there is a constant error, so

that the membrane will not be clamped to the potential measured by the external electrode.

During activity, of course, the situation is much more serious and it is now almost universally agreed that clamping of the membrane during the fast inward current is not feasible (cf. Kootsey and Johnson, 1972; New and Trautwein, 1972; McGuigan, 1974; Tarr and Trank, 1974). The space constant is drastically reduced due to a decrease in the membrane resistance as a result of the sodium conductance increase. There is also a decrease in reactance in parallel with the resistance due to the increasing frequency of current used to clamp the membrane. As will be noted from figure 23 the space constant is approximately halved at a measuring current frequency of 600 Hz as compared to the d.c. space constant. Whether there is a link between the two changes is an interesting problem - i.e. it is possible that charge movements due to a decrease in the membrane capacitative impedance during the foot of the action potential could control the sodium conductance increase. A similar theory has been put forward by Armstrong and Bezanilla (1973) for squid axons - the so-called gating currents.

Some attempts have however been made to measure the fast inward current. Haas and his co-workers (Haas, Kern and Einwächter, 1970; Haas, Kern, Einwächter and Tarr, 1971; Einwächter, Haas and Kern, 1972) have performed their experiments at 4-7^{o}C and consider that the reduced rate of rise of the action potential does not cause such a great fall in the space constant. They claim that the spatial variation in the 200μ node is not greater than 2mV during the fast inward current and almost zero during outward currents. With intracellular microelectrodes, they

state that a 5mV 'hump' occurs during the fast inward current, indicating some non-homogeneity - but this is not serious. However, Kootsey and Johnson (1972) among others have shown that such voltage traces are not a reliable measure of spatial control, so that when the observed potential changes show only a small peak, the true membrane potential is essentially one of an uncontrolled action potential.

One of the greatest problems that occurs with the sucrose-gap technique is the formation of an adequate sucrose-Ringer border that is sharp throughout the depth of the preparation - in a plane perpendicular to the axis of the preparation. The problem is however difficult to visualise, as some mixing of the solutions is inevitable - it being more acute in the double sucrose-gap as two sucrose-Ringer borders surround the test region. Some quantitative studies by Einwächter (1974), using dyed solutions of sucrose, have shown that incursion by the sucrose into a 200μ wide central node is not too serious, but that action potentials were reduced in size and duration as the sucrose-Ringer boundary was approached. However, it is most likely that the surface boundary may not reflect the boundary deep in the trabecula, so that the whole boundary will be a diffuse region between the two flows of sucrose and Ringer. This border region will thus be depleted in sodium and calcium, so that the activity of such cells will be different from that of the cells in the node proper. Removal of the external sodium has been shown to cause a hyper-polarisation of the membrane (Goto, Kimoto and Suetsugu, 1972; Chapman, 1974), and a reversible contracture occurs even if the external calcium concentration is less than 10^{-7} M (Chapman, 1974).

This would account for the fact that as the central gap is progressively reduced, the action potential duration, height and maximum rate of rise are reduced (de Hemptinne, 1973). In this situation, the ionic and temporal behaviour of different fibres may well vary due to the varying external ionic concentrations and different resistive pathways - such a possibility led Johnson and Lieberman (1971) to relegate the slow inward current component to artefacts due to such cells. Thus, it is likely that separation of the two inward currents is not demonstrated by adjustments of the external sodium and calcium concentrations, as the local environment of cells deep in the fibre may be different from that around superficial fibres (Johnson and Lieberman, 1971). Indeed de Hemptinne (1974) observed that with ramp functions of current, several inward components were observed - all abolished by TTX - and that no control over the inward current was possible in that interruption of the pulse during inward current flow did not stop such current flow. Thus, there is a basic dilemma between shortening the gap and so increasing the spatial homogeneity and widening the gap to decrease the proportional amount of pollution from the sucrose insulating cuffs. Bolton (1975) has observed similar results with smooth muscle preparations, so that changing the width of the central node could greatly affect the spike form and the temporal character of the observed inward currents.

One interesting experimental observation is pertinent to the discussion here. It was originally attempted to measure any changes in longitudinal impedance during activity, but the contraction of the

muscle caused a much greater impedance change, presumably by the increase in membrane area in the outer chambers. Attempts to arrest such contractions by perfusing the outer chambers with Ringer made three times hypertonic with sucrose, were found to stop the surface fibres from contracting; but frequently, an impedance change of similar form persisted - eventually disappearing - even though there was no visible contraction, which presumably came from deeper fibres. Thus, although no contraction was visible, it was evident, so that it is advisable to take strict precautions that a similar situation does not occur in a sucrose-gap chamber, where pollution of the sucrose by Ringer may well cause some of the fibres in the sucrose gap to contribute to the total tension. Due to the low extra cellular resistance under the oil gap, such longitudinal impedance measurements were thus not considered reliable.

The pollution by sucrose manifests itself in both the single and double sucrose-gaps by the series resistance. The problem was discussed by Lieberman and Johnson (1971) in their critical review and the problem experimentally realised by Beeler and Reuter (1970a) in mammalian ventricle and by Tarr and Trank (1971) in frog atrium. A similar situation would be expected in frog ventricle, due to the fact that all the membrane seems equally accessible electrically and probably to sucrose also. The resistance to cells deeper in the trabecula will, of course, be greater than more superficial cells and so a distributed value of time constants will result, so that no specific measurements are possible. Recently, several devices have been designed to compensate for the series resistance (Cheval, 1973;

Gebhardt, 1974; Léoty and Poindessault, 1974) and it has been observed that with compensation, the fast inward current is both faster and larger, indicating that the membrane potential is less inadequately controlled.

McGuigan and Tsien (McGuigan, 1974 appendix) have also studied the effects of leakage of current through the sucrose gap. They found that at short nodal distances in a double sucrose-gap arrangement, the leakage current greatly exceeded the membrane current. Thus, again a compromise has to be found as to the width of the gap between the swamping effect of leakage current and voltage non-homogeneity. Such a compromise was reached at about 0·9 space constants under most experimental conditions, so that both factors could not be ignored - both tending to underestimate the membrane resistance. At best, the resistance is underestimated by 50%. The situation deteriorates, the smaller the extracellular to intracellular resistance ratio is and it is now common practice to add Ca^{2+} to the sucrose. New and Trautwein (1972) observed no increase in resistance with addition of 10^{-5} M $CaCl_2$, but the addition has the extra advantage that it prevents an increase in the intracellular resistance by an order of magnitude - over a period of several hours (Kléber, 1973).

New and Trautwein (1972) have emphasized the importance of determining the intracellular and extracellular resistance through the sucrose-gap, in order to choose adequate preparations. Although the extracellular resistance was observed to be generally stable at about 100 kΩ over a 1mm gap, the intracellular resistance varied between

10 kohm and 10 Mohm. As it is desirable to have as large a ratio for the extracellular to intracellular resistance as possible, accurate determination of the ratio is important. The parallel sum of the two resistances was found by passing a 1 kHz signal between the two outer chambers. The individual intracellular resistance was determined by holding both outer chambers at earth potential and measuring the current flow by passing an action potential down the preparation. From these values they calculated the extracellular resistance. However, it has been shown that in frog ventricular muscle - and a similar situation may well exist in mammalian ventricular muscle also - that about half of the intracellular resistance is in parallel with a capacity that offers very little impedance at 1 kHz. Thus, the intracellular impedance will be different as measured with a high frequency signal or an action potential, thus leading to an erroneous estimation of the extracellular resistance. A similar situation has been observed by Tarr and Trank (1974) using frog atrial strips, who noted that generally, the extracellular to intracellular resistance ratio was much greater than that observed by New and Trautwein (1972).

Measurement of inward currents must then be open to some doubt and every effort should be made to choose the least undesirable preparation. One problem that requires particular attention is the state of the fibres whilst in the sucrose-gap condition. Harrington and Johnson (1973) have observed that their thin rabbit trabeculae survive only a matter of minutes, whilst some studies have

been made over a matter of hours. It would be interesting to see what the physiological state of the fibres is - especially those in the sucrose gap (even more so, when no calcium has been added). However, if the errors due to potential non-homogeneities and leakage currents can be quantified, measurement of slowly changing currents should be feasible (McGuigan, 1974; Ojeda and Rougier, 1974).

BIBLIOGRAPHY

ABE, Y. and TOMITA, T. (1968). Cable properties of smooth muscle. J. Physiol. 196, 87-100.

ABRAMOVITZ, M. and STEGUN, I.A. (1968). Handbook of mathematical functions, 5th printing. New York: Dover Publications Inc.

AMATNIEK, E. (1958). Measurement of bioelectric potentials with microelectrodes and neutralized input capacity amplifiers. I.R.E. Trans. med. Elect. (PGME) 10, 3-14.

ARMSTRONG, C.M. and BEZANILLA, F. (1973). Currents related to movement of the gating particles of the sodium channels. Nature, Lond. 242, 459-461.

ARVANITAKI, A. (1940). Temps longs et variables de transmission de l'excitation au niveau de la synapse experimentale axono-axonique. C.R. Soc. Biol. 133, 211-215.

BARR, L., DEWEY, M.M. and BERGER, W. (1965). Propagation of action potentials and the structure of the nexus in cardiac muscle. J. gen. Physiol. 48, 797-823.

BEELER, G.W.,Jr and REUTER, H. (1970a). Voltage clamp experiments on ventricular myocardial fibres. J. Physiol. 207, 165-190.

BEELER, G.W.,Jr and REUTER, H. (1970b). Membrane calcium current in ventricular myocardial fibres. J. Physiol. 207, 191-209.

BEELER, G.W.,Jr and REUTER, H. (1970c). The relation between membrane potential, membrane currents and activation of contraction in ventricular myocardial fibres. J. Physiol. 207, 211-229.

BESSEAU, A. (1971). Analyse, selon le modèle de Hodgkin et Huxley, des conductances de la membrane myocardique de grenouille (Rana esculenta). Thèse de Doctorat ès Sciences, Poitiers.

BLINKS, L.R. (1930). The direct current resistance of Nitella. J. gen. Physiol. 13, 495-508.

BOGUE, J.Y. and ROSENBURG, H. (1934). The rate of development and spread of electrotonus. J. Physiol. 82, 353-368.

BOLTON, T.B. (1975). Voltage-clamp of potential recorded intracellularly with micro-electrodes in smooth muscle. J. Physiol. 244, 25-26P.

BONKE, F.I.M. (1973). Passive electrical properties of atrial fibers of the rabbit heart. Pflügers Arch. ges. Physiol. 339, 1-15.

BROWN, H.F. and NOBLE, S.J. (1969). Membrane currents underlying delayed rectification and pace-maker activity in frog atrial muscle. J. Physiol. 204, 717-736.

CARMELIET, E.E. (1961). Chloride ions and the membrane potential of Purkinje fibres. J. Physiol. 156, 375-388.

CHAPMAN, R.A. (1966). The repetitive responses of isolated axons from the crab Carcinus maenas. J. exp. Biol. 45, 475-488.

CHAPMAN, R.A. (1971). Is there a T-system in frog cardiac muscle cells? J. Physiol. 215, 48-49P.

CHAPMAN, R.A. (1974). A study of the contractures induced in frog atrial trabeculae by a reduction of the bathing sodium concentration. J. Physiol. 237, 295-313.

CHAPMAN, R.A. and TUNSTALL, J. (1971). The dependence of the contractile force generated by frog auricular trabeculae upon the external calcium concentration. J. Physiol. 215, 139-162.

CHEVAL, J. (1973). Enregistrements simultanés du potentiel et du courant transmembrainaires à l'aide d'une seule micro-électrode intracellulaire. C.R. Acad. Sci. 277, 2521-2524.

CLARK, J. and PLONSEY, R. (1966). A mathematical evaluation of the core conductor model. Biophys. J. 6, 95-112.

COLE, K.S. (1928). Electric impedance of suspensions of Arbacia eggs. J. gen. Physiol. 12, 37-54.

COLE, K.S. (1932). Electric phase angle of cell membranes. J. gen. Physiol. 15, 641-649.

COLE, K.S. (1935). Electric impedance of Hipponôë eggs. J. gen. Physiol. 18, 877-887.

COLE, K.S. (1968). Membranes, ions and impulses. University of California Press. Berkeley, Los Angeles, London.

COLE, K.S. and BAKER, R.F. (1941). Longitudinal impedance of the squid giant axon. J. gen. Physiol. 24, 771-788.

COLE, K.S. and COLE, R.H. (1936a). Electric impedance of Asterias eggs. J. gen. Physiol. 19, 609-623.

COLE, K.S. and COLE, R.H. (1936b). Electric impedance of Arbacia eggs. J. gen. Physiol. 19, 625-632.

COLE, K.S. and CURTIS, H.J. (1936). Electric impedance of nerve and muscle. Cold Spring Harbour symposia on quantitative biology, Cold Spring Harbour, Long Island biological association. vol. 4, pp. 73-89.

COLE, K.S. and CURTIS, H.J. (1938). Electric impedance of Nitella during activity. J. gen. Physiol. 22, 37-64.

COLE, K.S. and CURTIS, H.J. (1939). Electric impedance of the squid giant axon during activity. J. gen. Physiol. 22, 649-670.

COLE, K.S. and HODGKIN, A.L. (1939). Membrane and protoplasm resistance in the squid giant axon. J. gen. Physiol. 22, 671-687.

CONWAY, E.J. (1957). Nature and significance of concentration relations of potassium and sodium ions in skeletal muscle. Physiol. Rev. 37, 84-132.

CORABOEUF, E. and WEIDMANN, S. (1949). Potentiel de repos et potentiels d'action du muscle cardiaque measurés à l'aide d'électrodes internes. C.R. Soc. Biol. 143, 1329-1331.

CORABOEUF, E. and WEIDMANN, S. (1954). Temperature effects on the electrical activity of Purkinje fibres. Helv. Physiol. Acta 12, 32-41.

CRASS, M.F.,III, McCASKILL, E.S., SHIPP, J.C. and MURTHY, V.K. (1971). Metabolism of endogenous lipids in cardiac muscle: effect of pressure development. Am. J. Physiol. 220, 428-435.

CURTIS, H.J. and COLE, K.S. (1938). Transverse electric impedance of the squid giant axon. J. gen. Physiol. 21, 757-765.

DANIELLI, J.F. and DAVSON, H. (1935). A contribution to the theory of permeability of thin films. J. cell. comp. Physiol. 5, 495-508.

DECK, K.A., KERN, R. and TRAUTWEIN, W. (1964). Voltage clamp technique in mammalian cardiac fibres. Pflügers Arch. ges. Physiol. 280, 50-62.

de HEMPTINNE, A. (1973). Electrical properties of isolated atrial fibres disposed in a perfusion chamber for double sucrose gap. Soc. Belge Physiol. Pharmacol. 81, 549-551.

de HEMPTINNE, A. (1974). Discussion on voltage-clamp techniques at Pont-à-Mousson, France. (G. Vassort, chairman).

de MELLO, W.C., MOTTA, G.E. and CHAPEAU, M. (1969). A study on the healing-over of myocardial cells of toads. Circulation Res. 24, 475-487.

DEWEY, M.M. and BARR, L. (1964). A study of the structure and distribution of the nexus. J. cell Biol. 23, 553-585.

DRAPER, M.H. and WEIDMANN, S. (1951). Cardiac resting and action potentials recorded with an intracellular electrode. J. Physiol. 115, 74-94.

DUDEL, J., PEPER, K., RUEDEL, R. and TRAUTWEIN, W. (1966). Excitatory membrane current in heart muscle (Purkinje fibers). Pflügers Arch. ges. Physiol. 292, 255-273.

DUDEL, J. and RUEDEL, R. (1970). Voltage and time dependence of excitatory sodium current in cooled sheep Purkinje fibres. Pflügers Arch. ges. Physiol. 315, 136-158.

DULHUNTY, A.F. and GAGE, P.W. (1973). Electrical properties of toad sartorius muscle fibres in summer and winter. J. Physiol. 230, 619-641.

EHARA, T. (1971). Rectifier properties of canine papillary muscle. Jap. J. Physiol. 21, 49-69.

EINWAECHTER, H.M. (1974). Discussion on voltage-clamp techniques at Pont-à-Mousson, France. (G. Vassort, chairman).

EINWAECHTER, H.M., HAAS, H.G. and KERN, R. (1972). Membrane current and contraction in frog atrial fibres. J. Physiol. 227, 141-171.

EISENBERG, R.S. and ENGEL, E. (1970). The spatial variation of membrane potential near a small source of current in a spherical cell J. gen. Physiol. 55, 736-757.

EISENBERG, R.S. and JOHNSON, E.A. (1970). Three-dimensional electrical field problems in physiology. Prog. Biophys. mol. Biol. 20, 1-65.

ENGEL, E., BARCILON, V. and EISENBERG, R.S. (1972). The interpretation of current-voltage relations recorded from a spherical cell with a single microelectrode. Biophys. J. 12, 384-403.

FABIATO, A. and FABIATO, F. (1972). Excitation-contraction coupling of isolated cardiac fibers with disrupted or closed sarcolemmas. Circulation Res. 31, 293-307.

FALK, G. and FATT, P. (1964). Linear electrical properties of striated muscle fibres observed with intracellular electrodes. Proc. R. Soc. B. 160, 69-123.

FALK, G. and FATT, P. (1973). An analysis of light-induced admittance changes in rod outer segments. J. Physiol. 229, 185-220.

FATT, P. (1964). An analysis of the transverse electrical impedance of striated muscle. Proc. R. Soc. B. 159, 606-651.

FATT, P. and KATZ, B. (1951). An analysis of the end-plate potential recorded with an intra-cellular electrode. J. Physiol. 115, 320-370.

FAWCETT, D.W. and SELBY, C.C. (1958). Observations on the fine structure of the turtle atrium. J. biophys. biochem. Cytol. 4, 63-72.

FETTIPLACE, R., ANDREWS, D.M. and HAYDON, D.A. (1971). The thickness, composition and structure of some lipid bilayers and natural membranes. J. memb. Biol. 5, 277-296.

FOX, C.F. (1972). The structure of cell membranes. Sci. Amer. 226, (2), 30-38.

FOZZARD, H.A. (1966). Membrane capacity of the cardiac Purkinje fibre. J. Physiol. 182, 255-267.

FREEMAN, S.E., SATCHELL, D.G., CHANG, C.S. and GAY, W.S. (1968). The effect of high K^+ solutions and fatty acid substrates on metabolic pathways in toad heart. Comp. Biochem. Physiol. 26, 31-44.

FREYGANG, W.H. and TRAUTWEIN, W. (1970). The structural implications of the linear electrical properties of cardiac Purkinje strands. J. gen. Physiol. 55, 524-547.

FRICKE, H. (1923). The electric capacity of cell suspensions. Physics Rev. 21, 708-709.

FRICKE, H. (1924). A mathematical treatment of the electric conductivity and capacity of disperse systems. I. The electric conductivity of a suspension of homogeneous spheroids. Physics Rev. 24, 575-587.

FRICKE, H. (1925a). A mathematical treatment of the electric conductivity and capacity of disperse systems. II. The capacity of a suspension of conducting spheroids surrounded by a non-conducting membrane for a current of low frequency. Physics Rev. 26, 678-681.

FRICKE, H. (1925b). The electric capacity of suspensions of red corpuscles of a dog. Physics Rev. 26,682-687.

FRICKE, H. (1926). The electric capacity of suspensions with special reference to blood. J. gen. Physiol. 9, 137-152.

FRICKE, H. and MORSE, S. (1926). The electric resistance and capacity of blood for frequencies between 800 and 4½ million cycles. J. gen. Physiol. 9, 153-167.

GEBHARDT, U. (1974). A fast voltage clamp with automatic compensation for changes of extracellular resistivity. Pflügers Arch. ges. Physiol. 347, 1-7.

GEORGE, E.P. (1961). Resistance values in a syncitium. Aust. J. exp. Biol. med. Sci. 39, 267-274.

GIEBISCH, G. and WEIDMANN, S. (1971). Membrane currents in mammalian ventricular heart muscle fibres using a voltage-clamp technique.. J. gen. Physiol. 57, 290-296.

GITLER, C. (1972). Plasticity of biological membranes. A. Rev. Biophys. Bioeng. 1, 51-92.

GLAZER, J. and GODDARD, E.D. (1950). Monolayer properties of elaidyl alchohol. J. chem. Soc. 4, 3406-3408.

GORTER, E. and GRENDEL, F. (1925). On bimolecular layers of lipoids on the chromocytes of the blood. J. exp. Med. 41, 439-443.

GOTO, M., KIMOTO, Y. and SUETSUGU, Y. (1972). Membrane currents responsible for contraction and relaxation of the bull frog ventricle. Jap. J. Physiol. 22, 315-331.

GRIMLEY, P.M. and EDWARDS, G.A. (1960). The ultrastructure of cardiac desmosomes in the toad and their relationship to the intercalated disc. J. biophys. biochem. Cytol. 8, 305-318.

HAAS, H.G., KERN, R. and EINWAECHTER, H.M. (1970). Electrical activity and metabolism in cardiac tissue: An experimental and theoretical study. J. memb. Biol. 3, 180-209.

HAAS, H.G., KERN, R., EINWAECHTER, H.M. and TARR, M. (1971). Kinetics of Na inactivation in frog atria. Pflügers Arch. ges. Physiol. 323, 141-157.

HAASS, A. (1975). Effects of lanthanum, calcium and barium on resting membrane resistance of guinea-pig papillary muscle. Arch. exp. Path. Pharmak. 290, 207-220.

HAGIWARA, S. and NAKAJIMA, S. (1966). Differences in Na and Ca spikes as examined by application of tetrodotoxin, procaine and manganese ions. J. gen. Physiol. 49, 793-806.

HANAI, T., HAYDON, D.A. and TAYLOR, J. (1965). The influence of lipid composition and of some adsorbed proteins on the capacitance of black hydrocarbon membranes. J. theor. Biol. 9, 422-432.

HANDBOOK of chemistry and physics, 52nd ed. (1971-1972). Publ. Chemical Rubber Co., Cleveland, Ohio. ed. WEAST, R.C.

HARRINGTON, L. and JOHNSON, E.A. (1973). Voltage clamp of cardiac muscle in a double sucrose gap: A feasibility study. Biophys. J. 13, 626-647.

HARTREE, W. and HILL, A.V. (1921). The specific electrical resistance of frog's skeletal muscle. Biochem. J. 15, 379-382.

HAUSWIRTH, O., NOBLE, D. and TSIEN, R.W. (1972a). The dependence of plateau currents in cardiac Purkinje fibres on the interval between action potentials. J. Physiol. 222, 27-49.

HAUSWIRTH, O., NOBLE, D. and TSIEN, R.W. (1972b). Separation of the pace-maker and plateau components of delayed rectification in cardiac Purkinje fibres. J. Physiol. 225, 211-235.

HEINTZEN, P. (1954). Untersuchungen über die Temperaturabhängigkeit der elektrischen Erregungsvorgänge am Froschherzen. Pflügers Arch. ges. Physiol. 259, 381-399.

HELLERSTEIN, D. (1968). Passive membrane potentials: A generalization of the theory of electrotonus. Biophrys. J. 8, 358-379.

HENN, F.A. and THOMPSON, T.E. (1969). Synthetic lipid bilayer membranes. A. Rev. Biochem. 38, 241-262.

HEPPNER, D.B. and PLONSEY, R. (1970). Simulation of electrical interaction of cardiac cells. Biophys. J. 10, 1057-1075.

HERMANN, L. (1879). Theorie des electrotonus, in Handbuch der Physiologie, Band 2, Theil 1, pp. 171-184. Leipzig: Vogel.

HERMANN, L. (1905). Beiträge zur Physiologie und Physik des Nerven. Pflügers Arch. ges Physiol. 109, 95-114.

HOEBER, R. (1910). Eine Methode, die elektrische Leitfähigkeit im Innern von Zellen zu messen. Pflügers Arch. ges. Physiol. 133, 237-255.

HOEBER, R. (1912). Ein zweites Verfahren, die Leitfähigkeit im Innern von Zellen zu messen. Pflügers Arch. ges. Physiol. 148, 189-224.

HODGKIN, A.L. (1954). A note on conduction velocity. J. Physiol. 125, 221-224.

HODGKIN, A.L. and HUXLEY, A.F. (1952a). Currents carried by sodium and potassium ions through the membrane of the giant axon of Loligo. J. Physiol. 116, 449-472.

HODGKIN, A.L. and HUXLEY, A.F. (1952b). The components of membrane conductance in the giant axon of Loligo. J. Physiol. 116, 473-496.

HODGKIN, A.L. and HUXLEY, A.F. (1952c). The dual effect of membrane potential on sodium conductance in the giant axon of Loligo. J. Physiol. 116, 497-506.

HODGKIN, A.L. and HUXLEY, A.F. (1952d). A quantitative description of membrane current and its application to conduction and excitation in nerve. J. Physiol. 117, 500-544.

HODGKIN, A.L., HUXLEY, A.F. and KATZ, B. (1952). Measurement of current-voltage relations in the membrane of the giant axon of Loligo. J. Physiol. 116, 424-448.

HODGKIN, A.L. and NAKAJIMA, S. (1972). The effect of diameter on the electrical constants of frog skeletal muscle fibres. J. Physiol. 221, 105-120.

HODGKIN, A.L. and RUSHTON, W.A.H. (1946). The electrical constants of a crustacean nerve fibre. Proc. R. Soc. B. 133, 444-479.

HOSHIKO, T., SPERELAKIS, N. and BERNE, R.M. (1959). Evidence for non-syncitial nature of cardiac muscle from impedance measurements. Proc. Soc. exp. Biol. Med. 101, 602-604.

HOWELL, J.N. (1969). A lesion of the transverse tubules of skeletal muscle. J. Physiol. 201, 515-533.

HOWELL, J.N. and JENDEN, D.J. (1967). T-tubules of skeletal muscle: morphological alterations which interrupt excitation-contraction coupling. Fedn Proc. 26, 553, abstract 1663.

IMANAGA, I. (1974). Cell-to-cell diffusion of Procion Yellow in sheep and calf Purkinje fibres. J. memb. Biol. 16, 381-388.

JAMES, T.N. and SHERF, L. (1970). Ultrastructure of the myocardium. The Heart, Arteries and Veins, ed. HURST, J.W. and LOGUE, R.B., pp. 58-73. Tokyo: McGraw-Hill and Kogakusha.

JEANS, J. (1911). Mathematical theory of electricity and magnetism. 5th ed. (1963). Cambridge: University Press.

JOHNSON, E.A. and LIEBERMAN, M. (1971). Heart: Excitation and contraction. A. Rev. Physiol. 33, 479-532.

JONGSMA, H.J. and van RIJN, H.E. (1972). Electrotonic spread of current in monolayer cultures of neonatal rat heart cells. J. memb. Biol. 9, 341-360.

JOO, F. and CSILLIK, B. (1962). Cholinesterase activity of intercalated disks (Eberth's lines) in mammalian heart muscle. Nature 193, 1192-1193.

JULIAN, F.J., MOORE, J.W. and GOLDMAN, D.E. (1962). Membrane potentials of the lobster giant axon obtained by use of the sucrose-gap technique. J. gen. Physiol. 45, 1195-1216.

KAHN, M. (1941). Der physikalische Elektrotonus des Herzmuskels. Pflügers Arch. ges. Physiol. 245, 235-264.

KAMIYAMA, A. and MATSUDA, K. (1966). Electrophysiological properties of the canine ventricular fiber. Jap. J. Physiol. 16, 407-420.

KATZ, B. (1948). The electrical properties of the muscle fibre membrane. Proc. R. Soc. B 135, 506-534.

KAVANAU, J.L. (1965). Structure and function in biological membranes. vol. 1. Holden Day Inc.

KLĖBER, A.G. (1973). Effects of sucrose solution on the longitudinal tissue resistivity of trabecular muscle from mammalian heart. Pflügers Arch. ges. Physiol. 345, 195-205.

KOOTSEY, J.M. and JOHNSON, E.A. (1972). Voltage clamp of cardiac muscle. A theoretical analysis of early currents in the single sucrose gap. Biophys. J. 12, 1496-1508.

KURIYAMA, H. and MEKATA, F. (1971). Biophysical properties of the longitudinal smooth muscle of the guinea-pig rectum. J. Physiol. 212, 667-683.

LAMB, J.F. and McGUIGAN, J.A.S. (1968). The efflux of potassium, sodium, chloride, calcium and sulphate ions and sorbitol and glycerol during the cardiac cycle in frog's ventricle. J. Physiol. 195, 283-315.

LAEUGER, P., LESSLAUER, W., MARTI, E. and RICHTER, J. (1967). Electrical properties of bimolecular phospholipid membranes. Biochim. biophys. Acta 135, 20-32.

LEOTY, C. and POINDESSAULT, J. P. (1974). Effects and compensation of the series resistance in voltage-clamp experiments using double sucrose-gap technique. J. Physiol. 239, 108-109P.

LEOTY, C. and RAYMOND, G. (1972). Mechanical activity and ionic currents in frog atrial trabeculae. Pflügers Arch. ges. Physiol. 334, 114-128.

LIEBERMAN, M., KOOTSEY, J.M., JOHNSON, E.A. and SAWANOBORI, T. (1973). Slow conduction in cardiac muscle - a biophysical model. Biophys. J. 13, 37-55.

LING, G. and GERARD, R.W. (1949). The normal membrane potential of frog sartorius fibers. J. cell. comp. Physiol. 34, 383-396.

LING, G.N. (1973). What component of the living cell is responsible for its semipermeable properties? Polarised water or lipids? Biophys. J. 13, 807-816.

LORBER, V. and BERTAUD, W.S. (1971). Cellular surfaces of amphibian atrial muscle. J. cell Sci. 9, 427-433.

MARCEAU, F. (1904). Recherches sur la structure et le développement comparés des fibres cardiaques dans la série des vertébrés. Annls Sci. nat. (Zool.) 19, 191-365.

MARKLEY, K.S. (1960). Fatty acids, pt 1, pp. 600-601, 2nd. ed. New York: Interscience Inc.

MARTIN, A.R. (1954). The effect of change in length on conduction velocity in muscle. J. Physiol. 125, 215-220.

MASCHER, D. and PEPER, K. (1969). Two components of inward current in myocardial muscle fibres. Pflügers Arch. ges. Physiol. 307, 190-203.

MATEUCCI, C. (1862). Electrophysiological researches - Eleventh series on the secondary electromotor power of nerves and its application to the explanation of certain electro-physiological phenomena. Proc. R. Soc. 11, 384-389.

MATTER, A. (1973). A morphometric study of the nexus of rat cardiac muscle. J. cell Biol. 56, 690-696.

MAXWELL, J.L. (1872). On the induction of electric currents in an infinite plane sheet of uniform conductivity. Proc. R. Soc. 20, 160-167.

McALLISTER, R.E. and NOBLE, D. (1966). The time and voltage dependence of the slow outward current in cardiac Purkinje fibres. J. Physiol. 186, 632-662.

McGUIGAN, J.A.S. (1974). Some limitations of the double sucrose gap, and its use in a study of the slow outward current in mammalian ventricular muscle. J. Physiol. 240, 775-806.

McLACHLAN, N.W. (1963). Bessel functions for engineers, 2nd edn. Oxford: Clarendon Press.

MORAD, M. and ORKAND, R.K. (1971). Excitation-contraction coupling in frog ventricle: evidence from voltage clamp studies. J. Physiol. 219, 167-189.

MORAD, M. and TRAUTWEIN, W. (1968). The effect of the duration of the action potential on contraction in the mammalian heart muscle. Pflügers Arch. ges. Physiol. 299, 66-82.

MUELLER, P., RUDIN, D.O., TIEN, H. and WESCOTT, W.C.(1962a). Reconstruction of excitable cell membrane structure in vitro. Circulation 26, 1167-1171.

MUELLER, P., RUDIN, D.O., TIEN, H. and WESCOTT,W.C.(1962b). Reconstruction of cell membrane structure in vitro and its transformation into an excitable system. Nature 194, 979-980.

NAYLER, W.G. and MERRILLEES, N.C.R. (1964). Some observations on the fine structure and metabolic activity of normal and glycerinated ventricular muscle of the toad. J. cell Biol. 22, 533-550.

NEUMANN, E. (1899). Ueber die Polarisationcapacität umkehrbarer Elektroden. Ann. Phys. 67, 500-534.

NEW, W. and TRAUTWEIN, W. (1972). Inward membrane currents in mammalian myocardium. Pflügers Arch. ges. Physiol. 334, 1-23.

NIEDERGERKE, R. (1963). Movements of Ca in frog heart ventricles at rest and during contractures. J. Physiol. 167, 515-550.

NIEMEYER, G. and FORSSMAN, W.G. (1971). Comparison of glycerol treatment in frog skeletal muscle and mammalian heart: An electrophysiological and morphological study. J. cell Biol. 50, 288-299.

NOBLE, D. and TSIEN, R.W. (1968). The kinetics and rectifier properties of the slow potassium current in cardiac Purkinje fibres. J. Physiol. 195, 185-214.

NOBLE, D. and TSIEN, R.W. (1969a). Outward membrane currents activated in the plateau range of potentials in cardiac Purkinje fibres. J. Physiol. 200, 205-231.

NOBLE, D. and TSIEN, R.W. (1969b). Reconstruction of the repolarization process in cardiac Purkinje fibres based on voltage clamp measurements of membrane current. J. Physiol. 200, 233-254.

NORMAN, R.S. (1972). Cable theory for finite length dendritic cylinders with initial and boundary conditions. Biophys. J. 12, 25-45.

NOYES, A.A. and FALK, K.G. (1912). The properties of salt solutions in relation to ionic theory. III. Electrical conductance. J. Am. chem. Soc. 34, 454-485.

OCHI, R. (1970). The slow inward current and the action of manganese ions in guinea-pig's myocardium. Pflügers Arch. ges. Physiol. 316, 81-94.

OCHI, R. and TRAUTWEIN, W. (1971). The dependence of cardiac contraction on depolarization and slow inward current. Pflügers Arch. ges. Physiol. 323, 187-203.

OJEDA, C. and ROUGIER, O. (1974). Kinetic analysis of the delayed outward currents in frog atrium. Existence of two types of preparation. J. Physiol. 239, 51-73.

ONCLEY, J.L. (1959). Chemical characterisation of proteins, carbohydrates and lipids. Rev. modern Phys. 31, 30-49.

OVERATH, P., SCHAIRER, H.H. and STOFFEL, W. (1970). Correlation of in vivo and in vitro phase transitions of membrane lipids of Escherichia coli. Proc. natn Acad. Sci. U.S.A. 67, 606-612.

PAGE, E., McCALLISTER, L.P. and POWER, B. (1971). Stereological measurements of cardiac ultrastructures implicated in excitation-contraction coupling (sarcotubules and T-system). Proc. natn Acad. Sci. U.S.A. 68, 1465-1466.

PAGE, S.G. and NIEDERGERKE, R. (1972). Structures of physiological interest in the frog heart ventricle. J. cell Sci. 11, 179-203.

PATLAK, C. (1973). An approximation diffusion equation for a long narrow channel with varying cross-sectional area. Bull. math. Biol. 35, 81-86.

PHILLIPSON, M. (1921). Les lois de la résistance électrique des tissus vivants. Bull. Acad. R. Belgique, Cl. Sc. 7, 387-403.

POISSON, S.D. (1826). From the proceedings of Mem. Acad. R. sci. Inst., France, vol.5.

PRIESTLAND, R.N. and WHITTAM, R. (1972). The temperature dependence of activation by phosphatidylserine of the sodium pump adenosine triphosphatase. J. Physiol. 220, 353-361.

RALL, W. (1969a). Time constants and electrotonic length of membrane cylinders and neurones. Biophys. J. 9, 1483-1508.

RALL, W. (1969b). Distributions of potential in cylindrical coordinates and time constants for a membrane cylinder. Biophys. J. 9, 1509-1541.

RAPPORT, D. and RAY, G.B. (1927). Changes of electrical conductivity in the beating tortoise ventricle. Am. J. Physiol. 80, 126-139.

ROSENBLEUTH, A. and del POZO, E.C. (1943). The changes of impedance of the turtle's ventricular muscle during contraction. Am. J. Physiol. 139, 514-519.

ROSENBLEUTH, A., WIENER, N., PITTS, W. and GARCIA RAMOS, J. (1948). An account of the spike potential of axons. J. cell. comp. Physiol. 32, 275-317.

ROUGIER, O., VASSORT, G., GARNIER, D., GARGOUIL, Y.M. and CORABOEUF, E. (1969). Existence and role of a slow inward current during the frog atrial action potential. Pflügers Arch. ges. Physiol. 308, 91-110.

ROUGIER, O., VASSORT, G. and STAEMPFLI, R. (1968). Voltage clamp experiments on frog atrial heart muscle fibres with the sucrose gap technique. Pflügers Arch. ges. Physiol. 301, 91-108.

SAKAMOTO, Y. (1969). Membrane characteristics of the canine papillary muscle fibre. J. gen. Physiol. 54, 765-781.

SAKAMOTO, Y. and GOTO, M. (1970). A study of the membrane constants in the dog myocardium. Jap. J Physiol. 20, 30-41.

SANO, T., TAKAYAMA, N. and SHIMAMOTO, T. (1959). Directional difference of conduction velocity in the cardiac ventricular syncitium studied by microelectrodes. Circulation Res. 7, 262-267.

SCHANNE, O. (1966). Measurement of the cytoplasmic resistivity by means of the glass microelectrode. Glass microelectrodes, ed. LAVALLEE, M., SCHANNE, O. and HEBERT, N.C., pp. 299-321. New York, London, Sydney and Toronto: J. Wiley & sons Inc.

SCHANNE, O., THOMAS, L. and CERETTI, E. (1966). The input resistance of the rat atria. Fedn Proc. 25, 635, abstract 2515.

SCHNEIDER, V.L., HOLMAN, R.T. and BURR, G.O. (1949). A monolayer study of the isomerism of unsaturated and oxy fatty acids. J. phys. Colloid Chem. 53, 1016-1029.

SCHWAN, H.P. (1963). Determination of biological impedances. In Physical Techniques in biological Research, vol. VI, electrophysiological methods, pt B, ed. NASTUK, W.L. New York and London: Acedemic Press.

SHIBA, H. (1971). Heaviside's "Bessel cable" as an electric model for flat simple epithelial cells with low resistive junctional membranes. J. theor. Biol. 30, 59-68.

SHIPP, J.C., THOMAS, J.M. and CREVASSE, L. (1964). Oxidation of carbon-14-labeled endogenous lipids by isolated perfused rat heart. Science, N.Y. 143, 371-373.

SJOESTRAND, F.S., ANDERSSON-CEDEGREN, E. and DEWEY, M.M. (1958). The ultrastructure of the intercalated discs of frog, mouse and guinea pig cardiac muscle. J. ultrastruct. Res. 1, 271-287.

SOMMER, J.R. and JOHNSON, E.A. (1968). Cardiac muscle: a comparative study of Purkinje fibres and ventricular fibers. J. cell Biol. 36, 497-526.

SOMMER, J.R. and JOHNSON, E.A. (1969). Cardiac muscle: a comparative ultrastructural study with special reference to frog and chicken hearts. Z. Zellforsch. mikrosk. Anat. 98, 437-468.

SPERELAKIS, N. (1969). Lack of electrical coupling between contiguous myocardial cells in vertebrate hearts. In Experientia supplementum, vol 15, Comparative physiology of the heart: current trends, pp. 135-165.

STALEY,N.A. and BENSON, E.S. (1968). The ultrastructure of frog ventricular cardiac muscle and its relationship to mechanisms of excitation-contraction coupling. J. cell Biol. 38, 99-114.

STAEMPFLI, R. (1954). A new method for measuring membrane potentials with external electrodes. Experientia 10, 508-509.

STEFANI, E. and STEINBACH, A.B. (1968). Resting potential and electrical properties of frog slow muscle fibres. Effect of different external solutions. J. Physiol. 203, 383-401.

STERN, O. (1924). Ueber der Theorie der elektrolytischen Doppelschicht. Z. Elektrochem. 30, 508-516.

STIBITZ, G.R. and McCANN, F.V. (1974). Studies of impedance in cardiac tissue using sucrose gap and computer techniques. II. Circuit simulation of passive electrical properties and cell-to-cell transmission. Biophys. J. 14, 75-98.

STIGTER, D. and MYSELS, K.J. (1955). Tracer electrophoresis. II. The mobility of the micelle of sodium lauryl sulphate and its interpretation in terms of zeta potential and charge. J. phys. Chem. 59, 45-51.

STROSBERG, A.M., KATZUNG, B.G. and LEE, J.C, (1972). Glycerol removal treatment of guinea pig cardiac muscle. J. mol. cell. Cardiol. 4, 39-48.

TAMASHIGE, M. (1951). Effect of potassium ions upon the electrical resistance of an isolated frog muscle fibre. Annot. zool. jap. 24, 141-149.

TANAKA, I, and SASAKI, Y. (1966). On the electrotonic spread in cardiac muscle of the mouse. J. gen. Physiol. 49, 1089-1110.

TARR, M. and SPERELAKIS, N. (1964). Weak electrotonic interaction between contiguous cardiac cells. Am. J. Physiol. 207, 691-700.

TARR, M. and TRANK, J. (1971). Equivalent circuit of frog atrial tissue as determined by voltage clamp-unclamp experiments. J. gen. Physiol. 58, 511-522.

TARR, M. and TRANK, J.W. (1974). An assesment of the double sucrose-gap voltage clamp technique as applied to frog atrial muscle. Biophys. J. 14, 627-643.

TASAKI, I. (1955). New measurements of the capacity and the resistance of the myelin sheath and the nodal membrane of the isolated frog nerve fiber. Am. J. Physiol. 181, 639-650.

TASAKI, I. and HAGIWARA, S. (1957). Capacity of muscle fiber membrane. Am. J. Physiol. 188, 423-429.

THOMPSON, W.T. (1855). On the theory of the electric telegraph. Proc. R. Soc., May, 61-76.

TILLE, J. (1966). Electrotonic interaction between muscle fibres in the rabbit ventricle. J. gen. Physiol. 50, 189-202.

TOMITA, T. (1966). The longitudinal tissue impedance of the smooth muscle of guinea-pig taenia coli. J. Physiol. 201, 145-159.

TRAUTWEIN, W., KUFFLER, S.W. and EDWARDS, C. (1956). Changes in membrane characteristics of heart muscle during inhibition. J. gen. Physiol. 40, 135-145.

TSCHIRJEW, S. (1879). Arch. Anat. Physiol. Leipzig (Physiol. Abt.), pp. 525 & 543.

U.S. NATIONAL Bureau of Standards, Department of Commerce (1952). Tables of the Bessel functions $Y_o(x)$, $Y_1(x)$, $K_o(x)$, $K_1(x)$ $0 \leq x \leq 1$. Washington: United States Government Printing Office.

van der KLOOT, W.G. and DANE, B. (1964). Conduction of the action potential in the frog ventricle. Science, N.Y. 146, 74-75.

WEIDMANN, S. (1952). The electrical constants of Purkinje fibres. J. Physiol. 118, 348-360.

WEIDMANN, S. (1955). Effects of calcium ions and local anaesthetics on electrical properties of Purkinje fibres. J. Physiol. 129, 568-582.

WEIDMANN, S. (1966). The diffusion of radiopotassium across intercalated disks of mammalian cardiac muscle. J. Physiol. 187, 323-342.

WEIDMANN, S. (1969). Electrical coupling between myocardial cells. In Progress in Brain Research, vol.31, ed. AKERT, K. and WASER, P.G. pp.275-281. Amsterdam: Elsevier Publishing Company.

WEIDMANN, S. (1970). Electrical constants of trabecular muscle from mammalian heart. J. Physiol. 210, 1041-1054.

WEINGART, R. (1974). The permeability to tetraethylammonium ions of the surface membrane and the intercalated disks of sheep and calf myocardium. J. Physiol. 240, 741-762.

WEISS, O. and GILDEMEISTER, M. (1903). Ueber die Fortpflanzungsgeschwindigkeit des Elektrotonus. Pflügers Arch. ges. Physiol. 94, 509-532.

WHEELER, K.P. and WHITTAM, R. (1970). The involvment of phosphatidylserine in adenosine triphosphatase activity of the sodium pump. J. Physiol. 207, 303-328.

WHITE, S.H. (1970). A study of lipid bilayer membrane stability using precise measurements of membrane specific capacitance. Biophys. J. 10, 1127-1148.

WHITE, S.H. and THOMPSON, T.E. (1973). Capacitance, area and thickness variations in thin lipid films. Biochim. biophys. Acta. 323, 7-22.

WILSON, G., ROSE, S.P. and FOX, C.F. (1970). The effect of membrane lipid unsaturation on glycoside transport. Biochem. biophys. Res. Commun. 38, 617-623.

WOO, B.Y. and WEI, L.Y. (1973). Electrical capacitances of thin lipid films. J. biol. Phys. 1, 36-49.

WOODBURY, J.W. and CRILL, W.E. (1961). On the problem of impulse conduction in the atrium. Nervous Inhibition, ed. FLOREY, E., pp. 124-135. Oxford: Pergamom Press.

WOODBURY, J.W. and CRILL, W.E. (1970). The potential in the gap between two abutting cardiac muscle cells: A closed solution. Biophys. J. 10, 1076-1083.

WOODBURY, L.A., HECHT, H.H. and CHRISTOPHERSON, A.R. (1951). Membrane resting and action potentials of single cardiac muscle fibres of the frog ventricle. Am. J. Physiol. 164, 307-318.

WOODBURY, L.A., WOODBURY, J.W. and HECHT, H.H. (1950). Membrane resting and action potentials of single cardiac muscle fibres. Circulation 1, 264-266.

YOUNG, J.Z. (1936). Structure of nerve fibres and synapses in some invertebrates. Cold Spring Harbour symposia on quantitative biology, Cold Spring Harbour, Long Island biological association. vol. 4, pp. 1-6.